MASTER IN BIOCHEMISTRY AND MOLECULAR AND CELLULAR BIOLOGY

Characterization of the bifunctional kinase/phosphatase PleC regulating cell cycle progression and development in Caulobacter crescentus

Brochier, Thomas

Award date:
2018

Awarding institution:
University of Namur

Faculté des Sciences

Characterization of the bifunctional kinase/phosphatase PleC regulating cell cycle progression and development in *Caulobacter crescentus*

Mémoire présenté pour l'obtention

du grade académique de master 120 en biochimie et biologie moléculaire et cellulaire

BROCHIER Thomas

Janvier 2018

Université de Namur
FACULTE DES SCIENCES
Secrétariat du Département de Biologie
Rue de Bruxelles 61 - 5000 NAMUR
Téléphone: + 32(0)81.72.44.18 - Téléfax: + 32(0)81.72.44.20
E-mail: joelle.jonet@unamur.be - http://www.unamur.be

Caractérisation de l'histidine kinase bifonctionnelle PleC régulant la progression du cycle cellulaire et le développement chez *Caulobacter crescentus*

BROCHIER Thomas

Résumé

La division asymétrique est une stratégie exploitée par les bactéries afin de produire une descendance parfaitement adaptée aux conditions environnementales dans lesquelles elles vivent. Cette diversification apporte un avantage indiscutable à la population bactérienne quand celle-ci vit dans un environnement précaire. L'alphaprotéobactérie *Caulobacter crescentus* est devenu un modèle pour l'étude de la régulation du cycle cellulaire et développement bactérien par son potentiel de division asymétrique et l'adoption d'un cycle de vie dimorphique composé d'une cellule mobile incapable de répliquer son génome, la cellule flagellée et d'une cellule sessile capable d'initier la réplication de son génome, la cellule pédonculée. De plus, l'entrée de la cellule flagellée dans le cycle cellulaire se fait en parallèle d'une différentiation de celle-ci en cellule pédonculée. La régulation du cycle cellulaire et développement de *C. crescentus* est orchestré par un réseau composé de différents modules interconnectés dont les acteurs protéiques appartiennent à la famille des systèmes à deux composantes (TCS). Une des actions cruciales de ce réseau est la régulation de l'activité de CtrA, le régulateur de réponse impliqué dans l'inhibition de la réplication de l'ADN. En effet, l'activité de CtrA est critique pour réprimer la réplication de l'ADN dans les cellules G1/flagellées ainsi que de permettre l'expression d'un panel de gènes nécessaire à ce moment. L'inactivation du régulateur de réponse est ensuite nécessaire pour permettre l'avancement du cycle cellulaire et initier la transition G1-S et la différentiation en cellule pédonculée. L'état d'activation de CtrA dans les cellule flagellées et pédonculées est dépendant de l'histidine kinase (HK) bifonctionnelle PleC, pouvant agir comme phosphatase ou kinase. Cette protéine fonctionne comme un interrupteur moléculaire en alternant son activité de phosphatase à kinase (P-K), activant et inhibant l'activité de CtrA de manière respective.
Durant ce travail, nous avons caractérisé différents mutants catalytiques de PleC afin d'évaluer l'implication de chaque activité sur la physiologie de *C. crescentus*. De Plus, nous avons étudié la dégradation protéolytique que PleC afin d'identifier les acteurs responsables de sa disparition temporaire à la transition G1-S. Finalement, nous avons utilisé des approches à grande échelle afin d'identifier des nouveaux acteurs impliqués dans la régulation de PleC et CtrA.

Mémoire de master 120 en biochimie et biologie moléculaire et cellulaire
Janvier 2018
Promoteur: HALLEZ Régis

Université de Namur
FACULTE DES SCIENCES
Secrétariat du Département de Biologie
Rue de Bruxelles 61 - 5000 NAMUR
Téléphone: + 32(0)81.72.44.18 - Téléfax: + 32(0)81.72.44.20
E-mail: joelle.jonet@unamur.be - http://www.unamur.be

Characterization of the bifunctional kinase/phosphatase PleC regulating cell cycle progression and development in *Caulobacter crescentus*

BROCHIER Thomas

Abstract

Asymmetric cell division is a strategy used by bacteria to produce a specialized offspring perfectly adapted to environmental conditions. Diversification provides an indisputable advantage to the whole population when living in challenging environments. The alphaproteobacterium *Caulobacter crescentus* became a model organism for studying of cell cycle regulation and development because it divides asymmetrically to adopt a dimorphic life cycle composed of the motile - non-replicative - swarmer cell and the sessile stalked cell competent for replication. In addition, the entry of the swarmer cell into the cell cycle is concomitant with its differentiation into a stalked cell. *C. crescentus* cell cycle and development are regulated by a complex regulatory pathway, composed of multiple interconnected regulators belonging to the two-component signal transduction system (TCS). The major output of this regulatory pathway is the tight control of the master cell cycle regulator CtrA. Indeed, its activity is rigorously regulated to be optimal in the G1/swarmer cells to inhibit initiation of DNA replication, and annihilated at the G1-S transition to allow this process to happen. This dichotomy between high and low CtrA activity respectively in the swarmer and stalked cells relies on the bifunctional histidine kinase (HK) PleC, which harbors both kinase and phosphatase activities. Indeed, PleC works as a bistable switch by alternating its activity from phosphatase to kinase (P-K), turning the activity of CtrA ON and OFF respectively.
In this work, we first characterized catalytic mutants of PleC to evaluate the implication of each activity on the physiology of *C. crescentus*. In addition, we investigated the proteolytic degradation of PleC and tried to uncover actors responsible for its transient disappearance at the G1-S transition of the cell cycle. Finally, we performed genome-wide approaches to identify potential new actors involved in the regulation of PleC and CtrA.

Mémoire de master 120 en biochimie et biologie moléculaire et cellulaire
Janvier 2018
Promoteur: HALLEZ Régis

Acknowledgments

I would like to thank my promoter, Régis Hallez, to have given me the opportunity to work and learn in his group. I thank him for the many constructive and inspiring conversations we had together and for the time and effort he devoted to improve my scientific knowledge and curiosity.

I would also like to thank my tutor, Jérôme Coppine. He participated, if not entirely on his own, to the training of my scientific skills as an experimenter. His dedication, as an assistant, towards the students he mentors has to be regarded with the utmost respect. I would also like to thank him for the heart-warming atmosphere he created enabling the proper development of his students along their years at the University of Namur.

My thanks also go to the rest of the BCcD unit, Kenny, Elie, Aurélie and Aravind for the discussions, help and entertaining moments we shared together. I would like to thank especially Kenny for his help on the Tn-Seq analysis.
Elie has been my fellow bench mate during this whole year and I would like to thank him for the time he shared with me.

I thank also all the technicians who help to keep this place up and running. Thank you, Patricia, for making the laboratory a perfectly clean place even with messy people like me.

I would also like to thank my family who have always provided for me, encouraged me in my decisions and provided me with emotional support when needed.

Furthermore, I would like to thank all the persons who helped me get to my master thesis: Mr. Hermand, Pr. Arnould, Pr. Raes and Pr. Michiels. Mr. Hermand kindly accepted me into his laboratory (Gémo) and gave me the opportunity to work with Julie Candiracci who I also thank for her contribution to my development as a scientist.
Mr. Hermand, Pr. Arnould, Pr. Raes and Pr. Michiels were critical during my years at the University of Namur for their advice and help during difficult times.

Finally, I would like to thank the members of my jury for their time and I hope that you will enjoy my work.

Yours sincerely,

Thomas Brochier

"The complexity of a given developmental system arises from the integration of multiple processes. Much of the research on development is spent not only teasing out the specifics of an individual process but also finding out how that process is integrated into the overall program of the organism. By metaphor, a given process is a thread, but multiple threads may be twined together to form a string, and the string itself is woven into a tapestry. It is the purpose of the prokaryotic development researcher to simultaneously see the thread individually and the tapestry as a whole."

(Curtis & Brun, 2010)

Table of content

Abbreviation list

Δ	Deletion mutant
ATP	Adenosine Triphosphate
c-di-GMP	Cyclic-di-GMP
DNA	Deoxyribonucleic Acid
HK	Histidine Kinase
HPt	Histidine Phosphotransferase
LB	Luria Bertani
-P	Phosphorylated
PCR	Polymerase Chain Reaction
PleC^{K}	PleC Kinase
PleC^{P}	PleC Phosphatase
PST	Phosphate Specific Transport
PTS^{NTR}	Nitrogen-related Phosphotransferase system
PYE	Peptone Yeast Extract
RR	Response Regulator
Tn	Transposon
WT	Wild-type

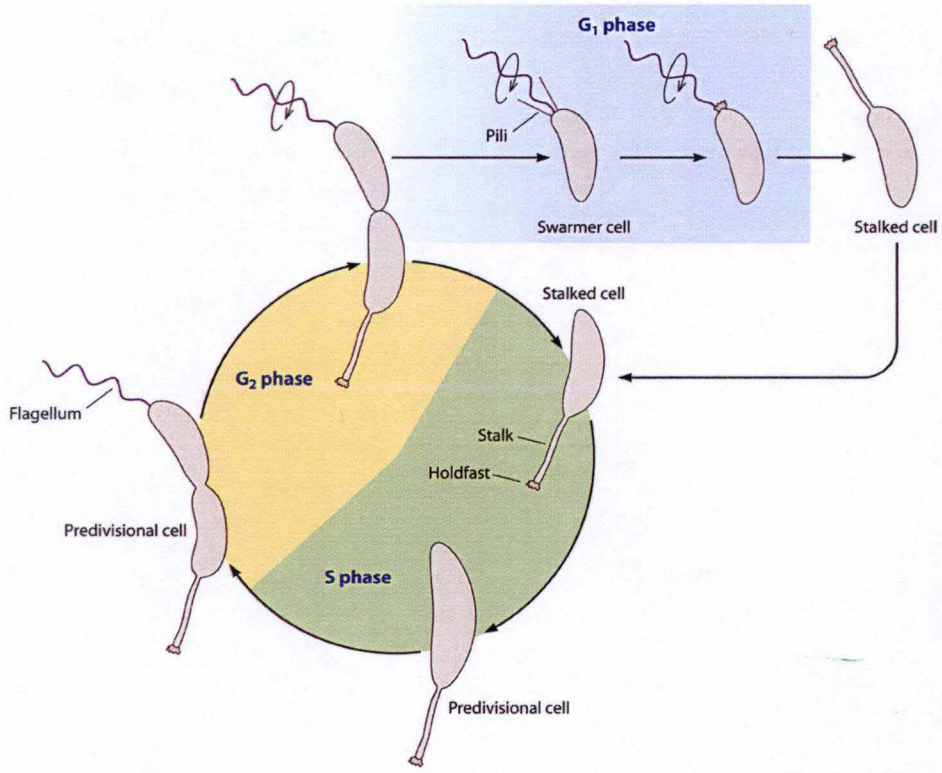

Figure 1: Cell cycle and development of Caulobacter crescentus, adapted from (Curtis & Brun, 2010). The life cycle of C. crescentus begins with the motile swarmer cell, which is unable to replicate its DNA and is referred to as the G1 phase of the bacterium. When the conditions are favorable, the bacterium will enter into a differentiation process, implying ejection of the flagellum, retraction of pili, synthesis of holdfast and biogenesis of a stalk at the flagellated pole. The bacterium will then undergo a single phase of DNA replication (S phase) to give rise to a predivisional cell, referred to as the G2 phase of the cell cycle. At the new swarmer cell pole, a flagellum will be synthesized and the predivisional cell will begin to divide giving birth to a similar stalked cell, which will be able to directly undergo a new round of DNA replication, and a swarmer cell that will swim to a permissive site.

Regulatory pathway governing cell cycle and development

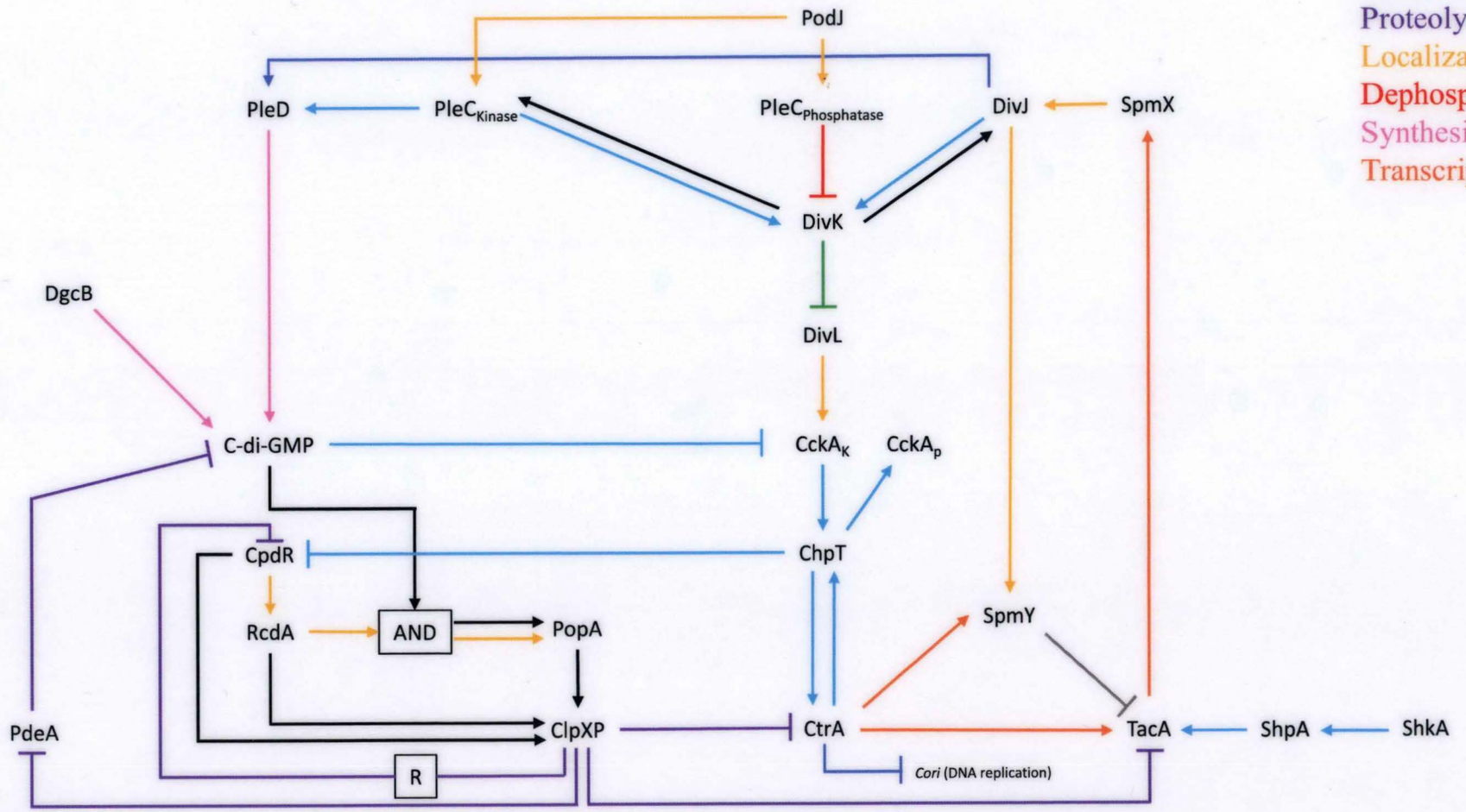

Phosphorylation
Allosteric regulation
Interaction
Proteolysis
Localization (aid)
Dephosphorylation
Synthesis
Transcription

1. Introduction

1.1. *Caulobacter crescentus*, model for prokaryotic development and asymmetrical division

Caulobacter crescentus is an aquatic and oligotrophic bacterium belonging to the alphaproteobacteria. It evolved a strategy to face recurrent nutritional stresses by adopting a dimorphic life cycle based on asymmetric cell division. The asymmetric cell division generates two morphologically and functionally distinct daughter cells that will help the bacterial population to face starving conditions. The two morphotypes of *Caulobacter* are the motile, chemotactic and non-replicative swarmer cell and the sessile, replication potent stalked cell (**Figure 1**). The swarmer cell is able to swim away from harsh conditions whereas the stalked cell adheres to the surface by a glue-type structure called the holdfast and colonizes favorable biotopes.
The alphaproteobacteria is a heterogeneous class of Gram-negative bacteria harboring very different lifestyles, such as free living aquatic bacteria like *Caulobacter* but also plant and animal pathogens (*Agrobacterium* and *Brucella,* respectively) or symbionts (*Rhizobium*). Asymmetric cell division seems to have been inherited from a common ancestor because it constitutes one of the conserved features of this bacterial class (Hallez, Bellefontaine, Letesson, & De Bolle, 2004).
The ability to synchronize a *Caulobacter* population and to easily follow cell differentiation under microscope makes of *Caulobacter* a powerful model for studying the transcriptional programs of the two daughter cells determining their cell fate. In addition, the availability of molecular tools helps to decipher regulatory networks underlying cell cycle progression and differentiation.

1.1.1. Cell cycle and development

The swarmer cell is unable to replicate its DNA and is referred to as the G1 phase (**Figure 1**). This morphotype is characterized by its unique polar flagellum and multiple Type IV pili. In a favorable environment, the swarmer cell exits G1 phase to enter S phase, a step is called G1-S transition. The entry into the cell cycle is also accompanied by an irreversible differentiation into a stalked cell, called the swarmer-to-stalked transition. This differentiation process is characterized by ejection of the flagellum, retraction of the pili, biosynthesis of the holdfast and biogenesis of the stalk at the pole previously occupied by the flagellum. The stalk is a thin polar extension of the cell membrane harboring the holdfast at its extremity. Initiation of DNA replication will take place during this morphological transition. In contrast to rapidly growing *Escherichia coli*, a complex regulatory network controlling the cell cycle allows one and only one round of DNA replication initiation per cell cycle. At the same time, the stalked cell starts to elongate into a predivisional cell, building up a single flagellum at the pole opposite to the stalk, commonly referred to as the new pole. Constriction of the predivisional cell then occurs concomitantly to the rotation of the flagellum, allowing the newborn swarmer cell whereas the newborn stalked cell is able to directly initiate a new round of DNA replication (**Figure 1**). A very interesting feature of *Caulobacter* is that the two processes of cell cycle and development are coordinated. This coordination is possible because they are both regulated by the same underlying network.

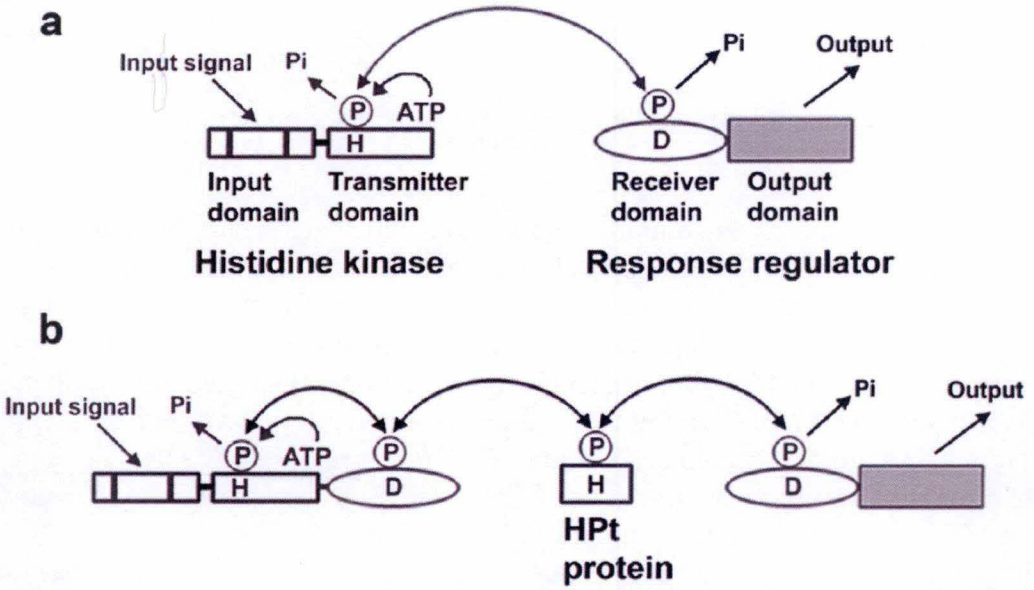

Figure 2: General features of (A) a two-component system and (B) a phosphorelay, adapted from (Mähönen, 2005). (A) The histidine kinase (HK) is composed of an input/sensing domain and a transmitter/kinase domain. Upon receiving a signal, the sensing domain of the HK will activate the kinase domain and stimulate autophosphorylation of the conserved His residue by hydrolyzing ATP. The phosphoryl group will then be transferred onto the conserved Asp residue of the receiver domain of the response regulator (RR). This will activate the output domain of the RR resulting in the generation of an output response. (B) In a phosphorelay, the HK contains both transmitter and receiver domain with respectively a conserved His and Asp residue. Upon perception of a signal, the kinase domain will autophoshorylate and transfer the phosphoryl group onto its own receiver domain. An additional protein is therefore required for the transfer of the phosphoryl group to the Asp residue of the RR. This protein is called the Histidine phosphotransferase (Hpt) and contains a conserved His residue.

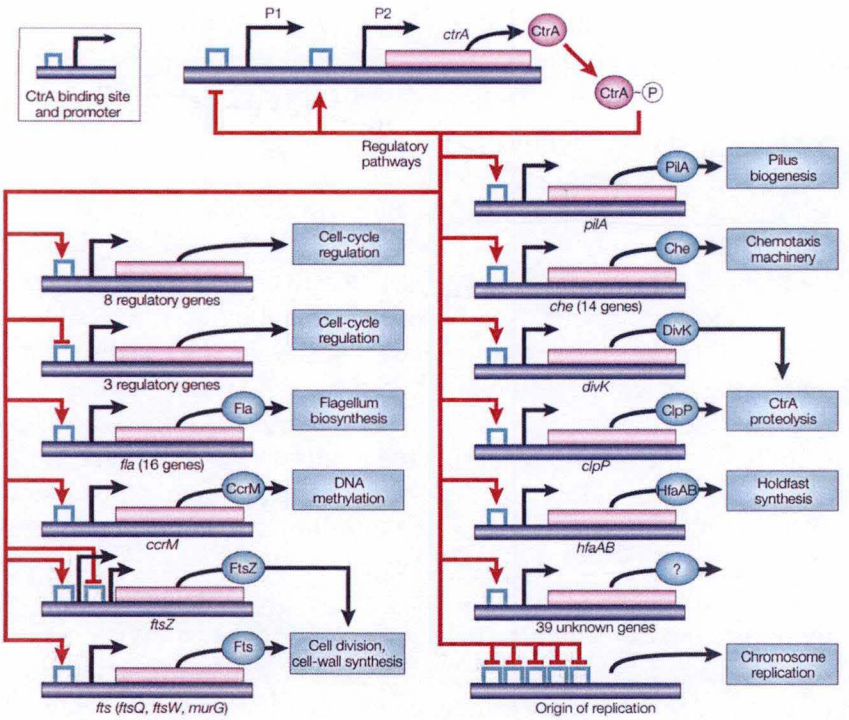

Figure 3: Schematic representation of the CtrA regulon from (Skerker & Laub, 2004).
Phosphorylated CtrA regulates expression of many genes involved in cell-cycle processes like cell division, DNA methylation and polar morphogenesis. It is also able to bind the origin of chromosomal replication (Cori).

1.2. Two component systems regulating cell cycle and development

The regulatory network regulating cell cycle and development in *Caulobacter* is composed of proteins belonging to the large family of two-component signal transduction systems (TCS). These regulatory proteins are capable of signal transduction by transferring a phosphoryl group from ATP to a conserved histidine of the first protein, the histidine kinase (HK). This process is called autophosphorylation. The HK then transfers this phosphoryl group from its His residue to another protein harboring a conserved aspartate residue, the response regulator (RR). The HK often features a sensing domain allowing it to be activated in response to a specific stimulus. The RR often harbors a regulatory domain, such as a DNA binding domain allowing the activation of the TCS by a stimulus to implement a specific response/ transcriptional program (**Figure 2**).
A more complex form of the TCS, called "phosphorelay", is composed of a hybrid HK harboring both conserved His and Asp residues. Because the phosphoryl group can only be transferred between His and Asp, another protein is required to make the link between the hybrid HK and the final RR. This protein is called a histidine phosphotransferase (Hpt), which is able to accept the phosphoryl group from the Asp residue of the hybrid HK on its conserved His residue to finally transfer it onto the RR (**Figure 2**).
The regulatory pathway regulating development and cell cycle in *Caulobacter* is composed of various interconnected TCS, allowing integration of a large panel of intracellular and extracellular stimuli and respond in an appropriate way.

1.2.1. CtrA

A major decision that the bacteria has to make is to whether or not initiate the replication of DNA. Indeed, if this process takes place, the cell has to commit to finish the whole cell cycle. Regulation of the G1-S transition is therefore a crucial step and the major actor involved in this decision is CtrA. CtrA (Cell transcriptional regulator A) is a response regulator able, when phosphorylated, to positively or negatively regulate expression of several hundreds of cell cycle regulated genes (Fumeaux et al., 2014; Laub, Chen, Shapiro, & McAdams, 2002). These genes are involved in polar morphogenesis, DNA replication initiation, cell division, DNA methylation and cell wall metabolism (Laub et al., 2002) (**Figure 3**). CtrA is also able to bind to the origin of chromosomal replication (also known as *Cori*) in order to inhibit the initiation of DNA replication.
In the swarmer cell, CtrA is present and active to inhibit DNA replication initiation. At the G1-S transition, CtrA is degraded to allow initiation of DNA replication before being resynthetized during S-phase. This transient disappearance avoids overinitiation of DNA replication and allows temporal and spatial regulation of transcription (Tsokos & Laub, 2012) (**Figure 4**). Having such impact on the decision made in the cell throughout the cell cycle, the bacterium has developed two strategies for the fine-tuning of CtrA activity. The first is the control of its activity by phosphorylation/dephosphorylation whereas the second acts on its abundance by controlling its proteolytic degradation. These mechanisms are redundant so that the inactivation of one of these mechanisms is compensated by the other one (Domian, Quon, & Shapiro, 1997). However, inactivating both mechanisms at the same time leads to an uncontrolled CtrA that is lethal for the cell (Domian et al., 1997).

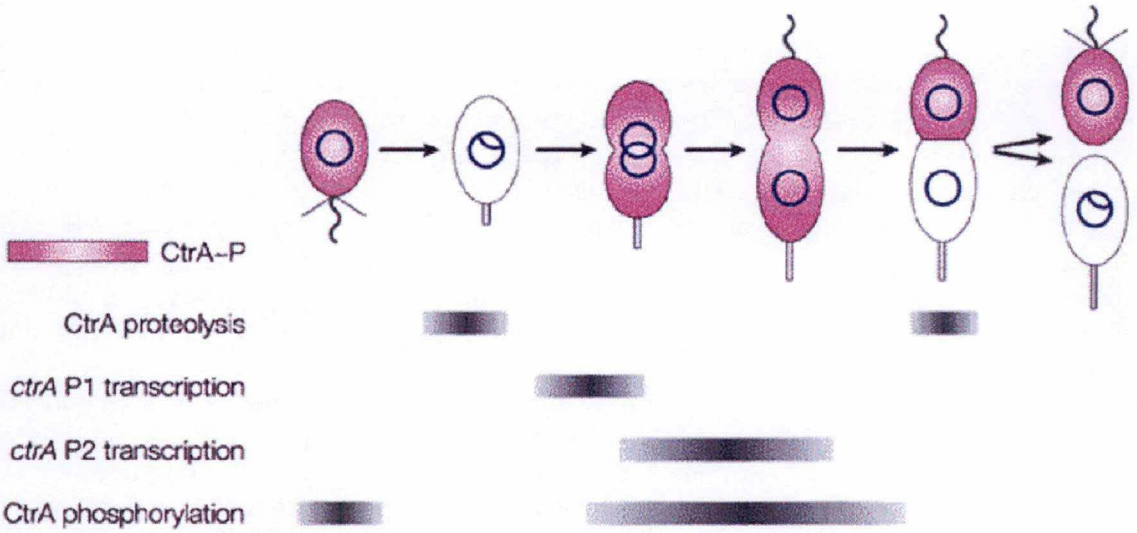

Figure 4: Regulation of the CtrA response regulator along the cell cycle from (Skerker & Laub, 2004). CtrA is present and phosphorylated in the swarmer/G1 cell. At the G1-S transition, CtrA will be dephosphorylated and degraded and will not be present in the stalked cell anymore. Following this degradation, *ctrA* transcription will be activated and CtrA will be phosphorylated again. Upon separation of the two daughter cells, CtrA will only be present and phosphorylated in the swarmer compartment and cleared from the stalked compartment.

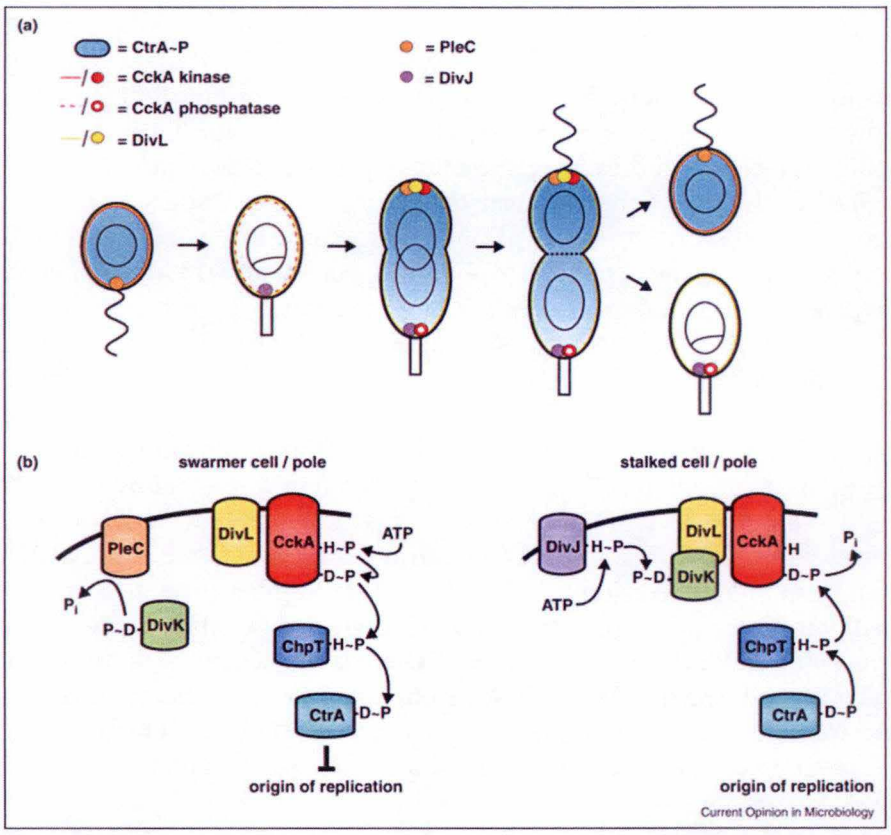

Figure 5: Regulation of CtrA activity and implementation of asymmetry in *C. crescentus* from (Tsokos & Laub, 2012). (A) The differential localization of the two HK PleC and DivJ will implement a CtrA-P gradient in the predivisional cell. (B) Molecular organization of cell fate determinants at the flagellated and stalked poles. In the swarmer cell, PleC will dephosphorylate DivK thereby inhibiting its inhibitory action on DivL-CckA and allowing the phosphorylation of CtrA. In the stalked cell, DivJ will increase the DivK-P concentration, resulting in the inhibition of DivL-CckA and the subsequent inversion of the phosphate flow.

1.2.2. Regulation of CtrA activity

1.2.2.1. The CtrA phosphorelay

The phosphorylation of CtrA is the final step of a signaling circuit known as the CckA-ChpT-CtrA phosphorelay. CckA (cell cycle kinase A) is a transmembrane hybrid HK harboring a conserved Aspartate residue in addition to a Histidine residue required to accept the phosphoryl group from ATP. CckA is the only kinase described to phosphorylate ChpT (Cell cycle Histidine Phosphotransferase), a Hpt relaying phosphorylation between CckA and CtrA (Biondi, Reisinger, et al., 2006). In addition to CtrA, ChpT can also phosphorylate another RR, namely CpdR, involved in the coordination of the *Caulobacter* cell cycle by regulating CtrA proteolysis (see below) (Iniesta, McGrath, Reisenauer, McAdams, & Shapiro, 2006). In fact, phosphorylation of CpdR inhibits its activity as a stimulator of CtrA degradation (Biondi, Reisinger, et al., 2006). In conclusion, this phosphorelay activates CtrA in two ways, by direct phosphorylation of CtrA and by preventing its proteolytic degradation.
As many HK, CckA is bifunctional with both kinase and phosphatase activities. Importantly, when not stimulated as a kinase, CckA is able to reverse the phosphate flow thereby decreasing the phosphorylation levels of CtrA and CpdR, and thereby triggering CtrA inactivation (Y. E. Chen, Tsokos, Biondi, Perchuk, & Laub, 2009). In predivisional cells, CckA is bipolarly localized but displays antagonistic activity at each pole, kinase at the swarmer pole and phosphatase at the stalked pol). This leads to a gradient of phosphorylated CtrA along the predivisional cell and the inheritance of different CtrA activity in two daughter cells (**Figure 4**).

1.2.2.2. DivL, the link between two regulatory modules

The polar localization of CckA is mediated by its interaction with the unorthodox HK DivL (Tsokos & Laub, 2012). Firstly, DivL has a Tyrosine residue instead of a Histidine as the phosphorylation site (Wu, Ohta, Zhao, & Newton, 1999). Secondly, the ATPase domain is dispensable whereas the rest of the protein is essential for cell cycle (Childers et al., 2014; Christen et al., 2011). Instead of being phosphorylated as other HK, DivL serves as an allosteric regulator of CckA activating its kinase activity at the new pole in the swarmer compartment of the predivisional cell (Tsokos, Perchuk, & Laub, 2011). DivL also plays a role as a docking interface to mediate protein-protein interaction necessary to regulate the activity of CckA (Childers et al., 2014; Tsokos & Laub, 2012). DivL is therefore considered as a repurposed HK.

1.2.2.3. The DivK-DivJ-PleC multicomponent system

Another regulatory module is superimposed DivL/CckA-ChpT-CtrA, namely the DivK-DivJ-PleC multicomponent system. The HK DivJ and PleC both modulate the activity of the RR DivK. When DivK is phosphorylated, it is able to interact with DivL and prevent activation of the kinase activity of CckA (Childers et al., 2014). The phosphorylation state of DivK therefore determines the phosphorylation state of CtrA. Thanks to the antagonistic activities of PleC and DivJ, DivK is unphosphorylated and inactive in the swarmer cell whereas in the stalked cell, it is activated by phosphorylation. Indeed, DivJ is the major kinase of DivK and PleC its major phosphatase. PleC is present at the flagellated pole in its phosphatase form in the swarmer cell, participating to the low DivK activity. At the G1-S transition, DivJ is recruited at the differentiating pole thereby increasing phosphorylation levels of DivK and resulting in CtrA inactivation (**Figure 5 b**).

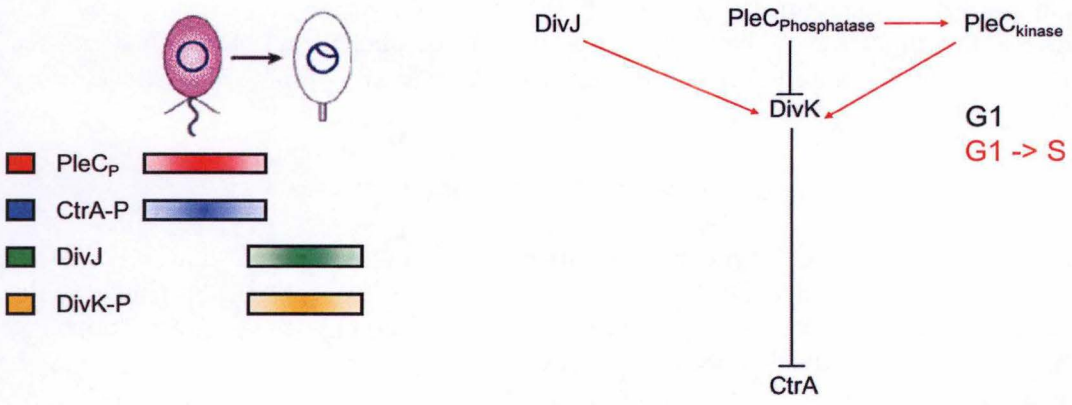

Figure 6: Model for the G1-S and swarmer-to-stalked cell transitions. In G1/swarmer cells, PleC is in its phosphatase form ($PleC^P$) protecting CtrA from inactivation. At the G1-S transition, PleC will experience an activity shift from phosphatase to kinase and, with the DivJ, will promote accumulation of DivK-P. This will lead to the inactivation of CtrA and allow the cell to initiate DNA replication.

The relation between DivK and CtrA is more complicated in the predivisional cell where both are phosphorylated but at different poles. This is due to the opposite distribution of their kinase, respectively DivJ at the stalked pole (Wheeler & Shapiro, 1999) and CckA at the flagellated pole (Iniesta, Hillson, & Shapiro, 2010). Importantly, PleC co-localizes with CckA at the new pole to protect DivL/CckA^{K} from inhibition by DivK-P. Thus, the asymmetric localization of kinases and phosphatase allows implementation of the CtrA-P gradient (high in the swarmer compartment and low in stalked one) and therefore the distinct cell fate of the future daughter cells (Y. E. Chen et al., 2011) (**Figure 5 a**).
In addition, a transition from one state to the other takes place at the G1-S transition. Indeed, upon differentiation, DivJ is recruited at the differentiating pole and co-localizes with PleC (Paul et al., 2008). This co-localization coincides with the increase of DivK phosphorylation at that pole. Above a certain threshold, DivK-P works as an allosteric regulator by stimulating the autokinase activity of DivJ and PleC (Paul et al., 2008). This mechanism results in a shift of PleC activity, from a phosphatase (PleC^{P}) to a kinase (PleC^{K}). This shift is particularly important to stimulate the phosphorylation of another RR, PleD (see below). Soon after the shift, PleC quickly delocalizes from the pole before being degraded by proteolysis (J. C. Chen, Viollier, & Shapiro, 2005; Wheeler & Shapiro, 1999).
This inhibition of CtrA at the G1-S transition enables the initiation of DNA replication and the differentiation of a swarmer into a stalked cell (**Figure 6**).
In conclusion, PleC is an important determinant in cell fate and cell cycle regulation because of its capacity to work as a switch that governs the complex regulatory network underlying these events.

1.2.3. Regulation of DivK & CtrA modules

Additional actors are involved in this regulatory network and have effects both upstream and downstream of CtrA.

1.2.3.1. PleD and the c-di-GMP: inactivation of CtrA and initiation of differentiation

PleD is another target of the HK PleC and DivJ (Aldridge, Paul, Goymer, Rainey, & Jenal, 2003). It is a response regulator with a diguanylate cyclase (DGC) activity responsible for the production of the second messenger cyclic di-GMP (c-di-GMP). Phosphorylation of PleD results in its dimerization and activation of the DGC domain. PleD is activated at the G1-S transition, where it is sequestrated at the differentiating pole, which results in a burst of c-di-GMP synthesis. This is required to direct flagellar ejection, holdfast synthesis and stalk biogenesis (Levi & Jenal, 2006; Paul et al., 2007). PleD is therefore an important developmental regulator, critical for the attachment of the stalked cell.
The c-di-GMP is also involved in the entry into S-phase by promoting inactivation of CtrA (Lori et al., 2015). Indeed, c-di-GMP triggers the activity shift of CckA from kinase to phosphatase, promoting the dephosphorylation of CtrA. This activity shift of CckA also reduces the phosphorylation state of CpdR, which promotes the proteolytic degradation of CtrA. A mutation in CckA (CckA$_{Y514D}$) was found to be insensitive to c-di-GMP (Lori et al., 2015). In addition, c-di-GMP also promotes directly CtrA degradation by binding another protein required for CtrA degradation, namely PopA. Even PleD is responsible for the burst of c-di-GMP at the G1-S transition, other DGC participate to the overall synthesis of the second messenger (Abel et al., 2013; Abel et al., 2011). For example, DcgB is responsible for the basal rate synthesis of c-di-GMP (Abel et al., 2011). On the other hand, c-di-GMP is degraded by phosphodiesterase (PDE) and PdeA has been shown to maintain c-di-GMP levels low in

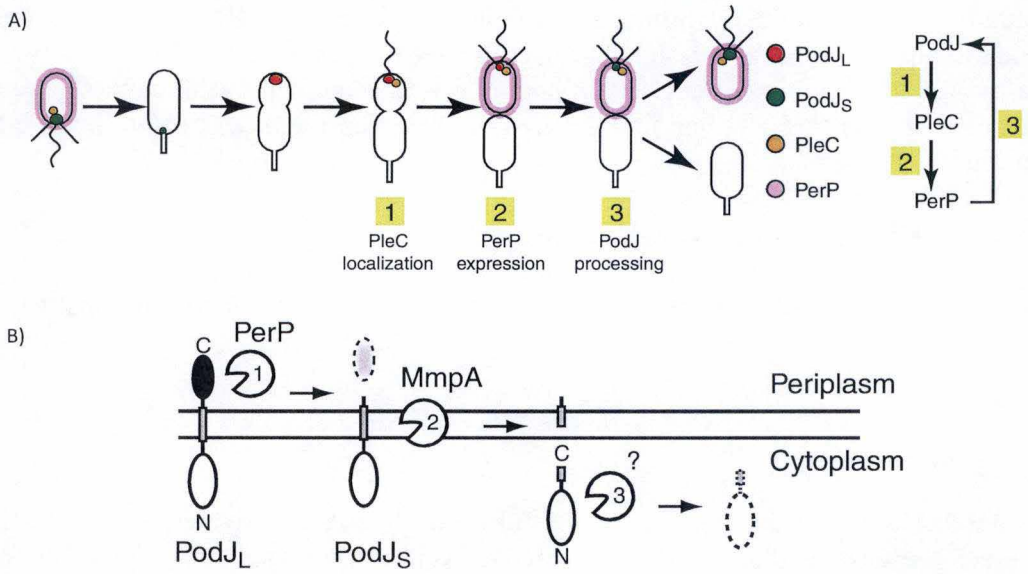

Figure 7: Processing of PodJ along the cell cycle (Chen et al., 2006). (A) Processing of PodJ along the cell cycle. (B) Actors implicated in the processing and degradation of PodJ. PodJ is synthesized in its long form ($PodJ_L$) and is composed of a cytoplasmic N-terminal domain, a single transmembrane segment and a periplasmic C-terminal region. Following cytokinesis, PerP will degrade the periplasmic C-terminal region leaving PodJ in its short form ($PodJ_S$). At the G1-S transition, the N-terminal domain of PodJ is cleaved off by the metalloprotease MmpA, releasing PodJ from the membrane into the cytoplasm where an unknown protease will degrade it.

G1/swarmer cells (Abel et al., 2011). At the G1-S transition, PdeA is also degraded by proteolysis, which allows c-di-GMP to accumulate.

1.2.3.2. PodJ: localization of PleC and DivL

PodJ is a polarity determinant composed of a cytoplasmic N-terminal domain, a single transmembrane segment and a periplasmic C-terminal region. It is implicated in the polar morphogenesis by recruiting PleC and DivL as well as actors required for the pili biogenesis (J. C. Chen et al., 2006; Curtis et al., 2012; Hinz, Larson, Smith, & Brun, 2003).
PodJ exists under two forms in the cell, the long ($PodJ_L$) and the short forms ($PodJ_S$). Synthesized in the early predivisional cell, $PodJ_L$ localizes to the swarmer pole to recruit PleC, DivL and components of the pili assembly machinery (Hinz et al., 2003) (**Figure 7 a**). Following cytokinesis, $PodJ_L$ is then processed by the periplasmic protease PerP into the truncated $PodJ_S$ form (J. C. Chen et al., 2006). Finally, at the G1-S transition, PodJ will be cleared from the cell by its release from the membrane thanks to the membrane metalloprotease MmpA and followed by its proteolysis in the cytosol by an unknown protease (J. C. Chen et al., 2005) (**Figure 7 b**). The processing and membrane dissociation of PodJ determines to its asymmetric distribution since inhibition of one of these steps (in Δ*perP* or Δ*mmpA* cells) leads to a permanent bipolar localization. This regulation of localization explains also the pattern that PleC adopts along the cell cycle.

1.2.3.3. TacA

TacA is a response regulator involved in the stalk biogenesis by regulating gene expression of factors required for stalk (Biondi, Skerker, et al., 2006). As a σ-54-dependent RR, the expression of TacA-dependent genes requires σ-54 encoded by *rpoN* (Biondi, Skerker, et al., 2006; Brun & Shapiro, 1992). As a RR, TacA is activated by a phosphorelay comprising two proteins, the hybrid HK ShkA and the Hpt ShpA (Biondi, Skerker, et al., 2006). Once phosphorylated, TacA-P binds to more than 125 putative target promoters (Janakiraman, Mignolet, Narayanan, Viollier, & Radhakrishnan, 2016). Interestingly, CtrA-P regulates the transcription factor of *tacA* and *rpoN* (Laub et al., 2002). In addition, TacA impacts the activity of CtrA by stimulating the expression of *spmX*, which encodes a protein stimulating DivJ localization and activity (Radhakrishnan, Thanbichler, & Viollier, 2008). Finally, TacA abundance oscillates along the cell cycle in phase with CtrA, by being present in the swarmer cell, disappearing at the G1-S transition and reappearing in the predivisional cell (Joshi, Bergé, Radhakrishnan, Viollier, & Chien, 2015).

1.2.3.4. SpmX and SpmY

SpmX is a lysozyme homolog required for the polar localization of DivJ (Radhakrishnan et al., 2008). This protein is therefore important for DivK phosphorylation. As previously said, *spmX* expression depends on TacA. In the G1 phase, *tacA* transcription is stimulated by active CtrA. Then, TacA activates transcription of *spmX*, which initiates CtrA inactivation (Radhakrishnan et al., 2008). This negative feedback loop enables the cyclic activation CtrA regulating the cell cycle and development of *Caulobacter*. Interestingly, SpmX also negatively impacts TacA activity by regulating SpmY (Janakiraman et al., 2016). SpmY is an inhibitor of TacA localized at the differentiating pole in a SpmX- and DivJ-dependent way (Janakiraman et al., 2016) .

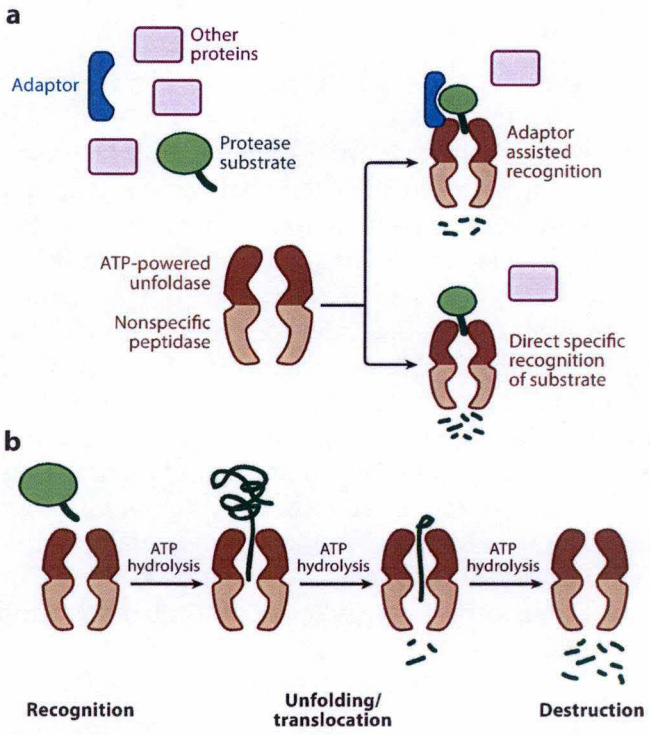

Figure 8: Functioning of AAA^+ proteases (Joshi & Chien, 2016). AAA^+ (ATPases associated with cellular activities) proteases are composed of an ATP-dependent unfoldase domain and a non-specific peptidase domain. (A) The specificity of the proteases comes from the recognition between the ATPase domain and the substrate. This interaction requires sometimes the help of adaptor proteins. (B) The unfoldase domain is required to allow efficient degradation of the protein by the peptidase by disassembling the structure of the protein and translocating the unfolded polypeptide into the peptidase chamber for its proteolytic degradation.

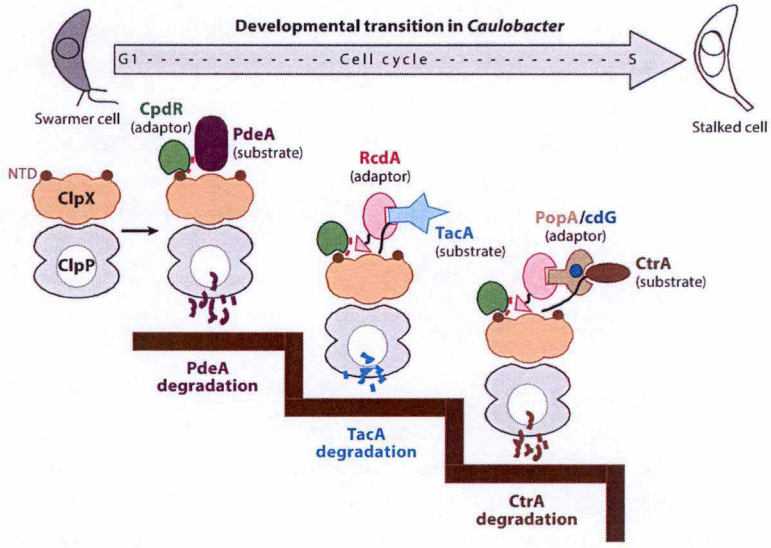

Figure 9: The coordinated proteolysis of key components regulating the cell cycle at the G1-to-S transition depends on an adaptor hierarchy in C. crescentus (Joshi & Chien, 2016). The ClpXP protease will interact with CpdR, the first adaptor, to degrade a first set of substrates. Afterwards, RcdA will bind to CpdR, inhibiting the degradation of CpdR-dependent substrates but also allowing proteolysis of a second set of substrates by ClpXP. Finally, PopA will be recruited and, in presence of c-di-GMP, will be able to initiate ClpXP-dependent proteolysis of a third subset of cell cycle regulators, among which CtrA is. This will de-repress the chromosomal origin of replication and enable the initiation of DNA replication.

1.3. Proteolysis regulating the cell cycle and development

Proteolytic degradation is an essential process used to limit the effect of proteins at a specific time during the cell cycle. Therefore, timely proteolysis of key regulators during eukaryotic or bacterial cell cycle is required for an efficient replication. Additionally, malfunctioning proteins have to be degraded to avoid undesired effects. Rapid proteolytic degradation is also required to respond to environmental stresses. The proteolytic degradation of time-specific actors results their oscillatory profile along the cell cycle of *C. crescentus*.
AAA^+ (ATPase associated with cellular activities) proteases use the energy released from the hydrolysis of ATP to allow recognition, unfolding and degradation of target proteins (Joshi & Chien, 2016) (**Figure 8**). They are composed of an ATP-dependent unfoldase domain that allows the peptidase domain to degrade the unfolded polypeptide. Both domains can be encoded on a single gene or on two separate genes (Joshi & Chien, 2016). Interaction between the protease and its substrate relies on the unfoldase domain. Each unfoldase domain interacts with a specific set of proteins enabling substrate specific degradation by each protease. Sometimes, adaptor proteins mediate or stabilize the interaction between the protease and its substrate thereby expanding the panel of substrates for the protease.

1.3.1. Regulation of CtrA abundance

In *C. crescentus*, the degradation of CtrA is necessary not only fluctuate gene expression of CtrA-dependent targets along the cell cycle, ensuring the proper gene expression at the right time, but also to relieve the inhibition of the *Cori* and allow initiation of DNA replication. The proteolysis of CtrA is mediated by the ClpXP protease (Joshi et al., 2015). This protease is composed of two separated proteins, the ATP-dependent unfoldase ClpX and the ClpP peptidase. This protease also degrades many other key cell cycle and developmental regulators (PdeA, GdhZ, TacA, ...) (Abel et al., 2011; Beaufay et al., 2015; Joshi & Chien, 2016).
The proteolysis of CtrA at the G1-S transition requires three adaptor proteins: CpdR, RcdA and PopA (Joshi & Chien, 2016) (**Figure 9**). CpdR is a single domain response regulator phosphorylated by the CckA-ChpT phosphorelay. In contrast to CtrA, this phosphorylation inhibits the activity of CpdR. Unphosphorylated CpdR localizes at the differentiating pole where it recruits ClpXP (Iniesta et al., 2006). When bound to ClpXP, CpdR also plays a role of adaptor protein for a set of ClpXP-dependent substrates. This is the case of the phosphodiesterase PdeA which is delivered to ClpXP by CpdR (Abel et al., 2011).
RcdA constitutes a second adaptor protein for ClpXP, especially required for TacA degradation. It binds to another set of substrates, which are directed to ClpXP already primed by CpdR (Joshi et al., 2015). Interestingly, RcdA will also inhibit the degradation of CpdR-dependent substrates (Joshi et al., 2015). This role as anti-adaptor has been proposed to regulate the timing of degradation of substrates by ClpXP.
The last adaptor protein required for CtrA degradation is PopA. It binds to ClpXP already primed by CpdR and RcdA. PopA has also an anti-adaptor role, inhibiting the degradation of RcdA-dependent substrates (Joshi et al., 2015). Interestingly, PopA binds to CtrA only in the presence of c-di-GMP. Indeed, PopA is a c-di-GMP effector protein, which dimerizes upon c-di-GMP binding (Duerig et al., 2009).
This mechanism of hierarchical proteolysis events enables substrate specific degradation in a specific order with the integration of second messenger cues to drive the cell cycle progression and development of *Caulobacter* (**Figure 9**).

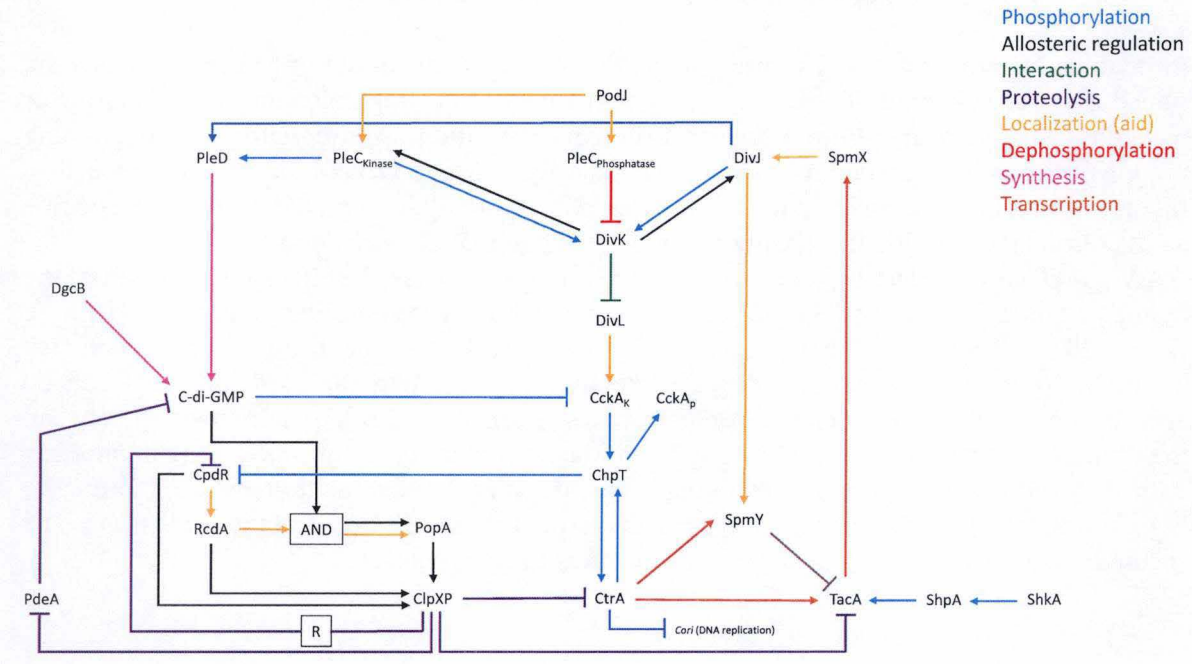

Figure 10: Regulatory network implicated in the modulation of activity and abundance of CtrA.

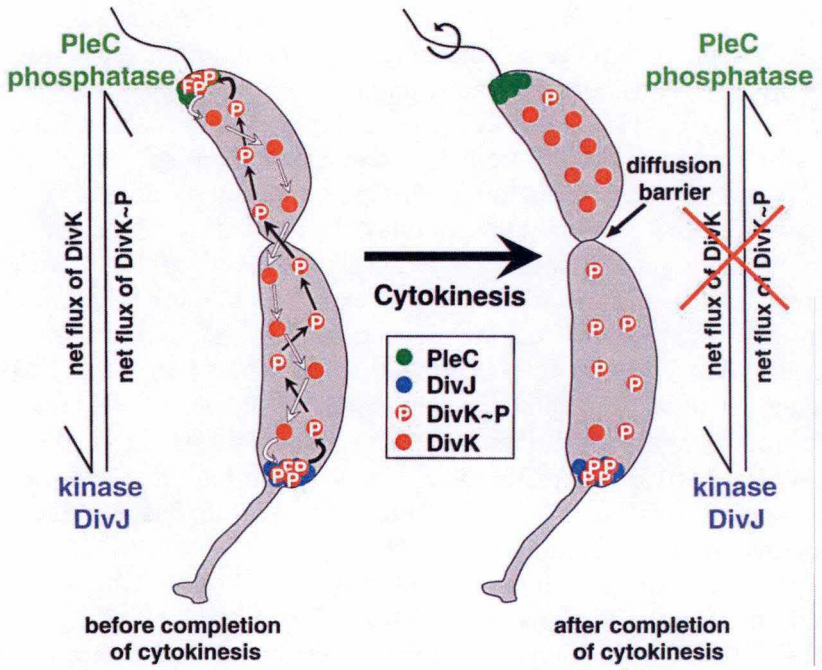

Figure 11: The ping pong mechanism regulating the activity of DivK at the poles (Matroule, Lam, Burnette, & Jacobs-Wagner, 2004). PleC and DivJ localize at opposite poles in the predivisional cell. PleC acts as a phosphatase at the flagellated pole and DivJ as a kinase at the stalked pole. Antagonistic activities lead to a pole-to-pole shuttling of DivK phosphorylating and dephosphorylating it continuously. Once the two compartments are separated, DivK-P levels decrease in the swarmer cell.

1.4. Spatiotemporal model integrating the cell cycle and development

The information from the literature allows us to build up a model integrating the signals that governs cell cycle progression and development in *C. crescentus*.

At the G1/swarmer phase, PleC acts as a phosphatase ($PleC^P$) at the swarmer pole thereby dephosphorylating DivK-P, and protecting CtrA-P from premature inactivation (**Figure 10**). At the same time, PdeA degrades the c-di-GMP and the TacA regulon is transcribed with the help of σ-54. On the other hand, CpdR is phosphorylated and thus unable to stimulate ClpXP-dependent degradation of PdeA, TacA and CtrA. PodJ is present in its short form ($PodJ_S$) by being previously processed by PerP. Once SpmX is translated, DivJ is recruited at the swarmer pole where the concentration of DivK-P increases. This DivK-P burst will trigger the activity shift of PleC from phosphatase to kinase ($PleC^K$), initiating the G1-S and swarmer-to-stalked cell transitions. Indeed, the $PleC^P$-$PleC^K$ shift rapidly increases the phosphorylation state of PleD. At the same time, DivK-P inhibits the stimulatory effect of DivL on the kinase activity of CckA and the PleD-dependent c-di-GMP burst stimulates the phosphatase activity of CckA, thereby reversing the phosphate flow and decreasing the phosphorylation of CtrA and CpdR. Unphosphorylated CpdR recruits ClpXP at the pole and allows degradation of PdeA, which contributes to the increase of c-di-GMP levels. Then RcdA is recruited to ClpXP-CpdR to allow proteolysis of TacA. Finally, PopA::c-di-GMP binds to ClpXP-CpdR-RcdA, which allows CtrA degradation. As CtrA is dephosphorylated and proteolyzed, initiation of DNA replication can start. At that time, PodJ is released from the membrane by MmpA, which triggers PleC delocalization and subsequent degradation. Meanwhile, the concomitant action of the TacA regulon and c-di-GMP allows ejection of the flagellum, retraction of the pili, biogenesis of the holdfast and biogenesis if the stalk. The stalked cell can now replicate its DNA and grow as a predivisional cell. Then, CtrA starts to reaccumulate, which allows transcription of $podJ_L$ whose product localizes at the new flagellated pole and recruits neo-synthesized PleC, whereas DivJ is maintained at the old stalked pole. This opposite localization creates a gradient of CtrA-P with high levels at the flagellated pole and lower levels at the stalked pole. The high CtrA-P content at the flagellated pole results in the synthesis if the flagellum and pili. Finally, cytokinesis, which coincides with the rotation of the flagellum, takes place, allowing subsequent separation of the two daughter cells. At the same time, PerP starts the processing of $PodJ_L$ into $PodJ_S$. Whereas the stalked cell will be able to immediately reinitiate DNA replication and restart a cell cycle, the chemotactic swarmer cell will swim enter into G1 phase.

A "ping pong mechanism" proposed by Matroule and colleague implies that PleC is a phosphatase at the flagellated pole (Matroule, Lam, Burnette, & Jacobs-Wagner, 2004). In this model, PleC and DivJ will both have antagonistic effects on DivK at opposite poles. At the stalked pole, DivK phosphorylated by DivJ diffuses in the cell to reach the flagellated pole. There, PleC dephosphorylates DivK-P and DivK diffuses back to the stalked pole to be phosphorylated again by DivJ. This process is called the ping pong model because DivK-P/DivK molecules are shuttled from one pole to another (**Figure 11**). After cytokinesis, this exchange is blocked and DivK-P levels rapidly dropped in the swarmer cells, which coincides with the rotation of the flagellum.

An alternative mechanism, based on the "inhibitor sequestration" model, has been proposed by Subramanian and colleagues (Subramanian, Paul, & Tyson, 2015). This mathematical model predicts that PleC is in its kinase mode at the flagellated pole of the predivisional cell. They proposed that PleC binds to DivK-P in its kinase form to sequester it and protect DivL-CckA interaction at the new pole. This hypothesis relies on the fact that DivK-P levels are high at the flagellated pole, and can thereby sustain the phosphatase-kinase switch of PleC. After

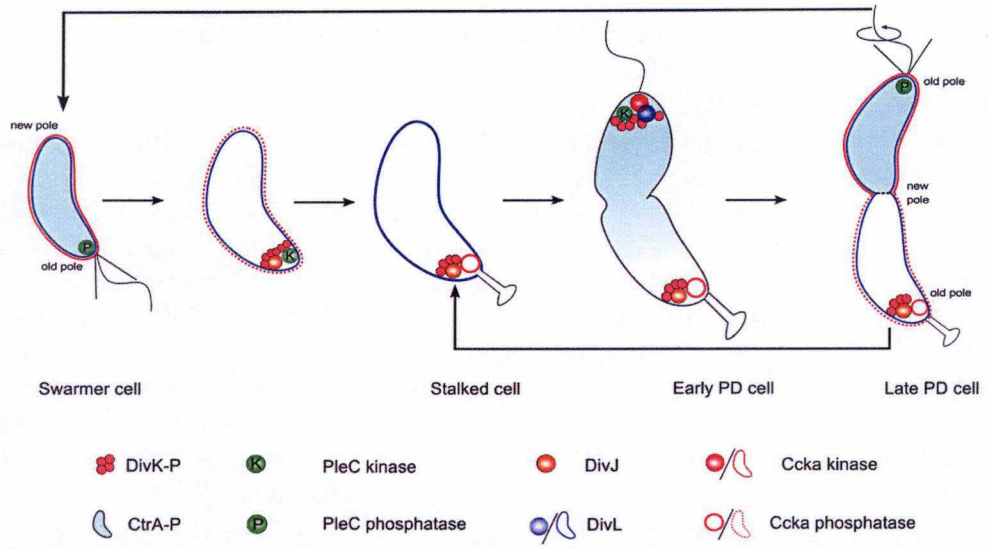

Figure 12: The "inhibitor sequestration" model regulating the activity of DivK (Subramanian, Paul, & Tyson, 2013). In the swarmer cell, PleC acts as a phosphatase on DivK-P protecting DivL from interaction with DivK-P. At the G1-S transition, PleC shifts its activity from phosphatase to kinase and with the help if DivJ phosphorylates DivK, which enables inhibition of CtrA. Soon after, PleC disappears from the pole and is cleared from the cell by proteolysis. PleC is then resynthesized and localizes to the opposite flagellated pole of the predivisional cell in its kinase conformation, thus able to interact with DivK-P originating from the stalked pole. The interaction between $PleC^{K}$ and DivK-P protects DivL from DivK-P at the flagellated pole. This sequestration therefore results in the phosphorylation of CtrA at this pole. Upon cytokinesis, PleC will shift back its activity from kinase to phosphatase and dephosphorylate DivK-P to ensure that CtrA-P can accumulate in the swarmer cell.

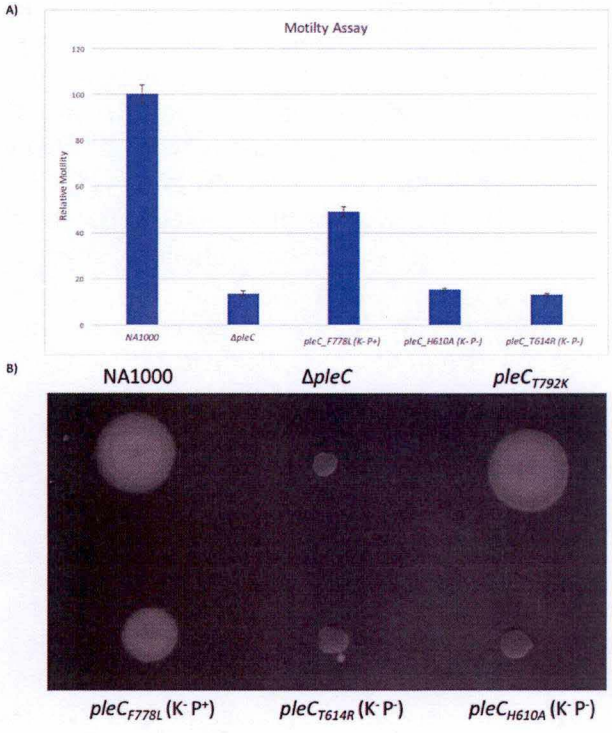

Figure 13: Characterization of *pleC* mutants.
Motility assays for the *pleC* mutants at the *pleC* locus. The strains NA1000, Δ*pleC*, $pleC_{F778L}$, $pleC_{H610A}$ and $pleC_{T614R}$ were tested and normalized to the wild-type (NA1000). (A) Quantification of the motility for represented in (B) by measurement of the colony area, error bars = s.d.(n=6).

cytokinesis, PleC could switch back into phosphatase and dephosphorylate DivK-P in the newborn swarmer cell (**Figure 12**).
Whatever PleC is doing exactly at the flagellated pole, it is a central regulator of the cell cycle and development. Not only it sustains optimal activity of CtrA-P, but also auto-determines its fate by activating transcription of *spmX* and *perP* in the predivisional cell. Indeed, SpmX will initiate a cascade of events culminating in the $PleC^{P}$-$PleC^{K}$ switch and the PerP-dependent processing of $PodJ_L$ into $PodJ_S$ is a pre-requisite to the delocalization of PleC from the pole.

1.5. Conservation of the regulation of CtrA in other alphaproteobacteria

Like stated before, the alphaproteobacteria contains a very heterogeneous group of bacteria with very different lifestyles. It has been demonstrated that asymmetric division takes place in several alphaproteobacteria, such as *Agrobacterium tumefasciens*, *Sinorhizobium meliloti* and *Brucella abortus* (Hallez et al., 2004). Interestingly orthologs of CtrA, DivJ, DivK, PleC, DivL and CckA were found in the genomes of the same alphaproteobacteria (Brilli et al., 2010; Hallez et al., 2004), suggesting that asymmetric cell division and CtrA regulatory network were both inherited from a common ancestor of alphaproteobacteria.

2. Objectives

We have three objectives for this master thesis. Firstly, we would like to carefully characterize at the molecular levels *pleC* point mutants described to have lost either one or both catalytic activities, *i.e.* kinase and phosphatase. The second objective of this master thesis is to characterize the proteolytic degradation of PleC especially by identifying factors involved in this process. Lastly, we plan to identify potential new regulators of the CtrA pathway thanks to genetic screens: a suppressor screen and a Tn-Seq experiment.

3. Results

3.1. Characterization of PleC activities

The inactivation of CtrA-P is a critical step during the cell cycle and development of *C. crescentus*, especially at the G1-S transition to allow the DNA replication to initiate (Wortinger, Sackett, & Brun, 2000). This is achieved by two different but complementary processes, namely ClpXP-dependent proteolysis and CckA-dependent dephosphorylation. Concomitantly, PleC will experience a shift in activity from phosphatase to kinase (P -> K) participating to the burst of DivK-P (Paul et al., 2008). To evaluate the contribution of each activity of PleC on cell cycle progression and development in *C. crescentus*, single point mutants harboring different activities have been generated (Matroule et al., 2004; Viollier, Sternheim, & Shapiro, 2002). $PleC_{H610A}$ (K^- P^-), where the conserved phosphorylation site (His610) has been mutated into an alanine residue; $PleC_{T614R}$ (K^- P^-), which still harbors His610 but is catalytically inactive; and the kinase dead mutant $PleC_{F778L}$, (K^- P^+). Unfortunately, a specific phosphatase dead mutant (K^+ P^-) was not isolated. In addition, all these mutant alleles were expressed on multi-copy plasmids in a Δ*pleC* background (Matroule et al., 2004; Paul et al., 2008), which could have masked a potential role of PleC kinase activity on DivK and/or of PleC phosphatase activity on PleD.
During this work, we will first characterize the phenotypes displayed by *Caulobacter* strains expressing these *pleC* mutant alleles (*pleC*$_{H610A}$ (K- P-), *pleC*$_{T614R}$ (K- P-) and *pleC*$_{F778L}$ (K-

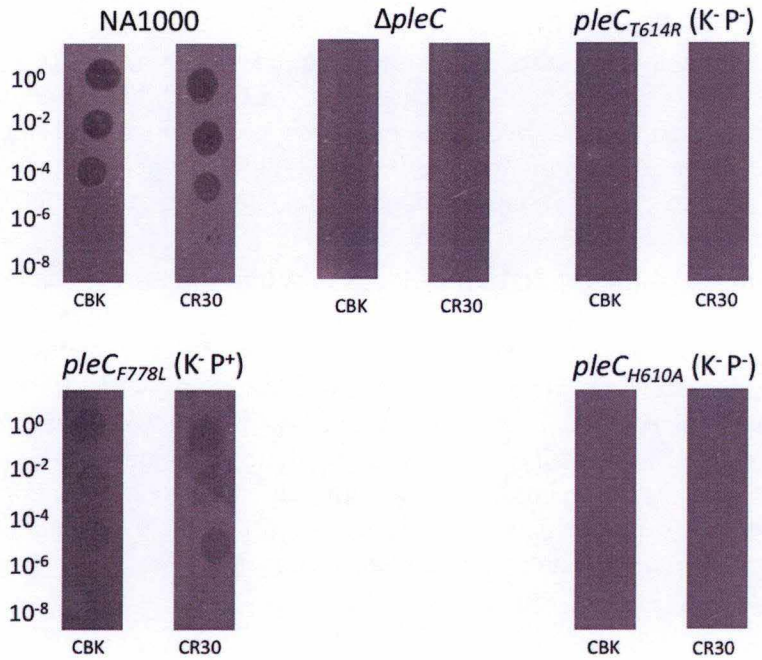

Figure 14: Characterization of *pleC* mutants.
Phage resistance assays for the *pleC* mutants at the *pleC* locus. The strains NA1000, Δ*pleC*, *pleC*$_{F778L}$, *pleC*$_{H610A}$ and *pleC*$_{T614R}$ were tested and normalized to the wild-type (NA1000).

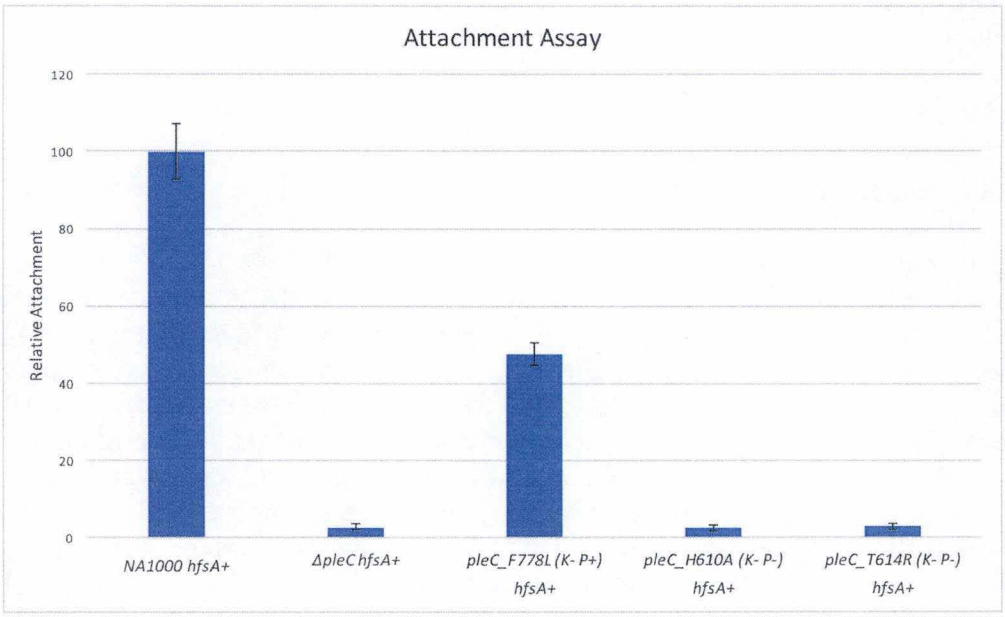

Figure 15: Characterization of *pleC* mutants.
Attachment assays for the known *pleC* mutants at the *pleC* locus. The strains NA1000 *hfsA*$^{+}$, Δ*pleC hfsA*$^{+}$, *pleC*$_{F778L}$ *hfsA*$^{+}$, *pleC*$_{H610A}$ *hfsA*$^{+}$ and *pleC*$_{T614R}$ *hfsA*$^{+}$ were tested and normalized to the wild-type (NA1000 *hfsA*$^{+}$), error bars = s.d. (n=6).

P+)) as the only copy of *pleC*. All the mutants described above were constructed at the *pleC* locus (CCNA_02567) by homologous recombination in the NA1000 wild-type strain expressing a functional copy of the *hfsA* gene required for attachment. The three phenotypes analyzed were motility, phage resistance and attachment to abiotic surface.

3.1.1. Motility

It is known that an optimal activity of CtrA is required for *C. crescentus* to be motile (Sciochetti, Lane, Ohta, & Newton, 2002). By dephosphorylating DivK-P, $PleC_P$ contributes to protect CtrA-P from inactivation in swarmer cells so that a Δ*pleC* strain is non-motile even though the flagellum is present. To evaluate the motility behavior of each mutant, motility assays were performed in a soft agar medium (PYE swarmer agar) and the results were normalized to the WT. As expected and in agreement with the literature, both $PleC_{H610A}$ and $PleC_{T614R}$ mutants were non-motile with a motility halo equivalent to the one displayed by Δ*pleC* (**Figure 13**). Unexpectedly, $pleC_{F778L}$ cells showed a motility efficiency of about 50 % of the WT even though $PleC_{F778L}$ was shown to have *in vitro* phosphatase activity similar to the WT (Matroule et al., 2004).

3.1.2. Phage resistance

C. crescentus is naturally sensitive to the CbK and Cr30 bacteriophages, CbK infecting through the polar pili composed of pilin subunits encoded by *pilA* (Guerrero-Ferreira et al., 2011) and Cr30 using the S layer as a receptor (Edwards & Smit, 1991). Recently, it was shown that capsule protects *Caulobacter* from infection by Cr30, and that decreasing expression of a transglutaminase encoded by that inhibits capsule formation and therefore leads to Cr30 resistance (Ardissone et al., 2014). Since both *pilA* and *hvyA* genes are positively regulated by CtrA-P, a fully functional PleC protein is required for phages to infect *C. crescentus*.
To evaluate the resistance to phage infection of each *pleC* mutant, dilutions of CbK and Cr30 were spotted onto PYE Top Agar containing *Caulobacter* cells and the efficiency of infection was assessed by analysis of the lysis plaques. As for the motility assay, mutants having lost PleC activities ($pleC_{H610A}$, $pleC_{T614R}$ and Δ*pleC*) were fully resistant to both phages (**Figure 14**). The $pleC_{F778L}$ mutant had an intermediate sensitivity to both phages in comparison the WT.

3.1.3. Attachment

The attachment of *C. crescentus* to an abiotic surface is achieved by a multistep process resulting in the synthesis of the holdfast that leads to the irreversible anchoring of the cells to the surface (Levi & Jenal, 2006; Smith, Hinz, Bodenmiller, Larson, & Brun, 2003). The production of the holdfast in the swarmer cell is stimulated at the post-translational level by the second messenger c-di-GMP and depends on the activity of the diguanylate cyclase PleD (Levi & Jenal, 2006; Sprecher et al., 2017). Attachment assays were therefore carried out with the different *pleC* mutants. Unsurprisingly, the loss-of-function mutants of *pleC* ($pleC_{H610A}$, $pleC_{T614R}$ and Δ*pleC*) did not attach (**Figure 15**). Again, the $pleC_{F778L}$ mutant had an intermediate phenotype as it attached less than the WT.

From these results, we can conclude that the two $K^- P^-$ mutants ($pleC_{H610A}$ and $pleC_{T614R}$) behave like the Δ*pleC* mutant whereas the $K^- P^+$ mutant ($pleC_{F778L}$) did not fully support motility, phage resistance and attachment although it was shown to have phosphatase activity *in vitro* similar to the WT. This led us to investigate the impact of the $pleC_{F778L}$ mutation on the activity of CtrA. A ß-galactosidase assay was performed on two well-described CtrA-dependent

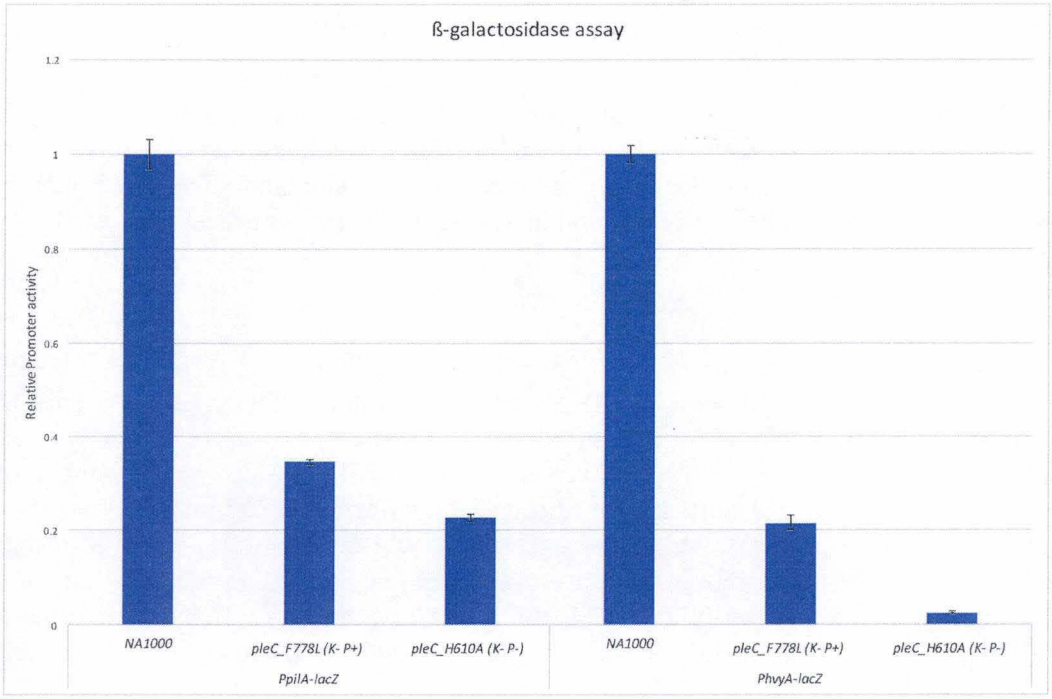

Figure 16: Measurement of CtrA-dependent promoter activity.
ß-Galactosidase assay on P_{hvyA}-*lacZ* and P_{pilA}-*lacZ* in $pleC_{F778L}$ mutant and normalized to the wild-type (NA1000). The NA1000 and $pleC_{H610A}$ strains were used as controls. Error bars = s.d. (n=6).

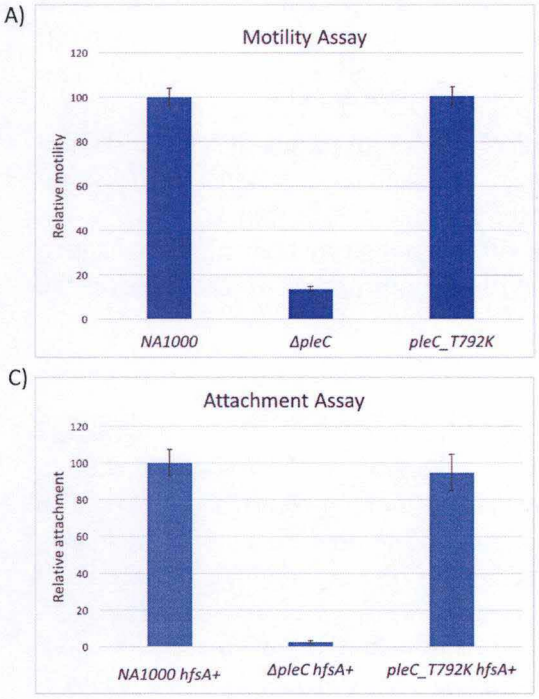

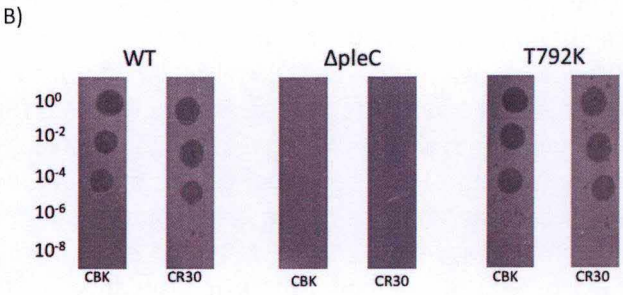

Figure 17: Characterization of the $pleC_{T792K}$ mutant.

Motility (A), phage resistance (B), and attachment assays (C) performed on the $pleC_{T792K}$ mutant. The strains NA1000, Δ*pleC* and $pleC_{T792K}$ were tested and normalized to the wild-type (NA1000) for motility and phage resistance assays. The strains NA1000 $hfsA^+$, Δ*pleC* $hfsA^+$ and $pleC_{T792K}$ $hfsA^+$ were tested and normalized to the wild-type (NA1000 $hfsA^+$) for the attachment assay. For motility (A) and attachment assay (C) the error bars = s.d. (n=6).

promoters P_{pilA} and P_{hvyA} involved in phage sensitivity to CbK and CR30, respectively. As shown in **Figure 16**, both promoters displayed a decreased activity in $pleC_{H610A}$ and $pleC_{F778L}$, although to a lesser extent for $pleC_{F778L}$. This result suggests that, *in vivo*, the phosphatase activity of $PleC_{F778L}$ is lower than the WT. Alternatively, the kinase activity of $PleC_{F778L}$ could be not entirely inactivated *in vivo*, suggesting that the kinase activity of PleC would be required for fully protecting CtrA-P activity. A K^+ P^- mutant of *pleC* would allow to discriminate between these hypotheses.

3.2. Screen for a K^+ P^- mutant

One of the aims of this study was to identify a phosphatase dead mutant (K^+ P^-) of PleC and characterize its effects on the cell physiology. Our first approach consisted to test a potential K^+ P^- mutant of PleC, namely $PleC_{T792K}$. The corresponding mutation in the HK EnvZ of *E. coli* ($EnvZ_{T402K}$) was indeed described as a K^+ P^- variant (Hsing, Russo, Bernd, & Silhavy, 1998). Therefore, a $pleC_{T792K}$ mutant allele was constructed at the *pleC* locus by homologous recombination. Unfortunately, the characterization of the $pleC_{T792K}$ strain revealed no difference in attachment, phage sensitivity and motility in comparison to the WT (**Figure 17**). Thus, we sought to use another approach to isolate a K^+ P^- mutant of PleC, based on a genetic screen. The rationale behind this screen was to isolate gain-of-attachment mutants of $pleC_{T614R}$ cells. Although this $PleC_{T614R}$ variant did not display kinase and phosphatase (K^+ P^-) activities (Matroule et al., 2004), it still harbors the conserved phosphorylated histidine at position 610 in contrast to the other catalytically inactive variant, $PleC_{H610A}$. Since His_{610} is required for both kinase and phosphatase activities, we reasoned that an intragenic compensatory mutation could reactivate the kinase activity of $PleC_{T614R}$. For this, the XL-1 Red *E. coli* strain was used randomly mutagenize on a medium copy number plasmid containing $pleC_{T614R}$ under control of its endogenous promoter. Different rounds of mutagenesis were performed before extracting the plasmids library and incorporating them into a *C. crescentus* $\Delta pleC$ $hfsA^+$ strain inefficient for attachment. After that, bacteria were pooled and allowed to attach to abiotic surfaces. Since it has been shown that overexpressing WT *pleC* in a $\Delta pleC$ background strongly stimulated attachment whereas overexpression of $pleC_{F778L}$ (K^- P^+) did not stimulate the attachment (Paul et al., 2008), mutations reactivating the kinase activity (K^+) of $PleC_{T614R}$ could thereby be selected. Then bacteria able to attach in the first round of selection were treated with bacteriophages (CbK and Cr30) to counteract $PleC_{T614R}$ variants displaying phosphatase (P^+) activity since phase sensitivity primarily relies on the PleC phosphatase activity.

Unfortunately, no candidates were selected with this approach. After sequencing analysis of different mutagenized plasmids, we concluded that the mutation rate generated by XL-1 Red was not sufficient.

To solve this problem and increase the mutation rate on $pleC_{T614R}$, a mutagenic PCR based approach will be performed. The idea would be to create a mutant library of $pleC_{T614R}$ amplicons before clone them in a high copy plasmid harboring an inducible promoter (P_{vanA} or P_{xylX} respectively induced with vanillate or xylose). Afterwards, the plasmid library would be transferred into the $\Delta pleC$ $hfsA^+$ strain by electroporation and candidates selected as described above, that is proficient for attachment but resistant to bacteriophages. Preliminary data for the attachment selection done a $\Delta pleC$ $hfsA^+$ strain expressing WT *pleC* under the control of P_{vanA} (NA1000 $\Delta pleC$ $hfsA^+$ P_{vanA}::*pleC*) showed a reduced attachment efficiency compared to the WT, despite the addition of vanillate (**Figure 18 a**). A western blot analysis showed that PleC levels were lower in NA1000 $\Delta pleC$ $hfsA^+$ P_{vanA}::*pleC* after induction with vanillate than in WT (**Figure 18 b**). This lower abundance of PleC could account for the reduced attachment efficiency. In order to get higher protein levels after induction, the experiment should be done with the xylose inducible promoter (P_{xylX}), which is known to be stronger.

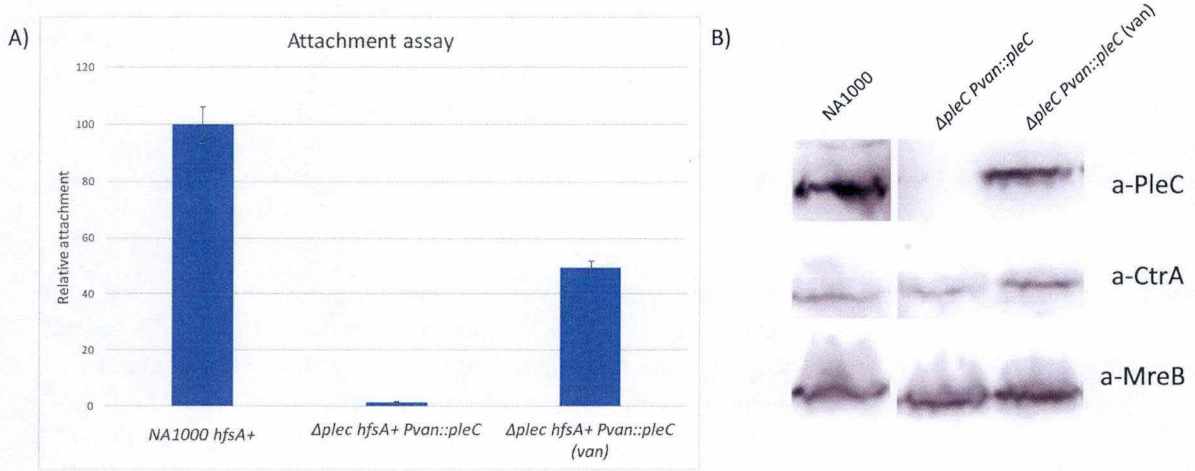

Figure 18: Characterization of the *pleC* induction strain at the *vanA* locus. (A) Attachment assay performed on the Δ*pleC* pVC-6 *pleC hfsA*$^{+}$ strain with or without vanillate induction and normalized to the wild-type (NA1000 *hfsA*$^{+}$). (B) Western blot analysis on the protein abundance of PleC and CtrA in the Δ*pleC* pVC-6 *pleC* strain with or without vanillate induction compared to the wild-type (NA1000). MreB was used as loading control.

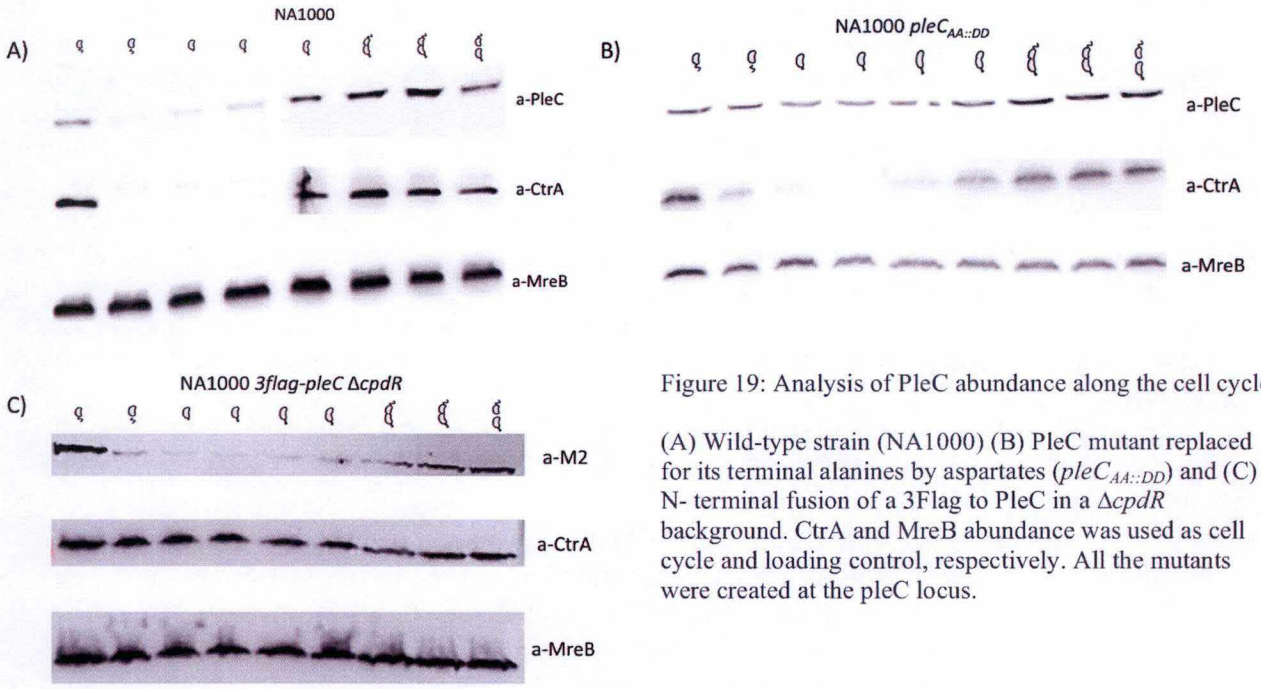

Figure 19: Analysis of PleC abundance along the cell cycle.

(A) Wild-type strain (NA1000) (B) PleC mutant replaced for its terminal alanines by aspartates (*pleC*$_{AA::DD}$) and (C) N- terminal fusion of a 3Flag to PleC in a Δ*cpdR* background. CtrA and MreB abundance was used as cell cycle and loading control, respectively. All the mutants were created at the pleC locus.

3.3. Protein abundance and degradation

Like CtrA, the abundance of PleC oscillates along the cell cycle (J. C. Chen et al., 2005; Viollier et al., 2002). However, the protease(s) responsible for this oscillation remains unknown. We first wanted to confirm the data from the literature by analyzing the abundance of PleC along the cell cycle. For this experiment, we collected WT G1/swarmer cells in a density gradient centrifugation, re-inoculated them in a fresh medium and withdrawed protein samples throughout the cell cycle. In agreement with the literature, PleC was present during the G1 phase before disappearing at the G1-S transition and reappearing in predivisional cells (**Figure 19 a**). CtrA, which is protected from degradation during the G1 phase, thanks to the phosphatase activity of PleC ($PleC^{P}$) that inactivates DivK-P, follows the same pattern (**Figure 19 a**). The oscillation of CtrA is mediated by specific proteolysis at the G1-S transition (Domian et al., 1997). In addition, PleC also harbors two C-terminal hydrophobic residues (Ala-Ala) shown in CtrA to allow specific recognition by the ClpXP protease (Bhat, Vass, Stoddard, Shin, & Chien, 2013; Domian et al., 1997; Joshi et al., 2015). Thus, to test the implication of proteolysis in the oscillation of PleC along the cell cycle, the abundance of a PleC variant, in which the two terminal alanine residues were replaced by two aspartate residues ($PleC_{AA::DD}$), was followed throughout the cell cycle. As illustrated in **Figure 19 b**, $PleC_{AA::DD}$ was essentially stabilized along the cell cycle whereas CtrA still fluctuated. This result indicates that a protease is involved in the disappearance of PleC at the G1-S transition.
To further characterize the proteolysis of PleC, we evaluated the steady state levels of PleC in different mutants of proteases and proteolytic adaptors. Five ATP-dependent proteases have been characterized in *C. crescentus*, two harboring the ATPase and peptidase domains on the same protein (FtsH and Lon) and three with separate ATPase and peptidase sub-units (HslUV, ClpAP and ClpXP). It is noteworthy that *clpP* and *clpX* genes are essential except in a Δ*socAB* background. This lethality comes from the fact that the toxin component (SocB) of the SocAB toxin-antitoxin system is degraded by ClpXP (Aakre, Phung, Huang, & Laub, 2013). Thus, the Δ*clpX* or Δ*clpP* allele were constructed in a Δ*socAB* background whereas Δ*ftsH,* Δ*lon*, Δ*hslV* and Δ*clpA* were created in a $socAB^{+}$ background. Because PleC and CtrA oscillate in-phase and share common proteolytic motifs (Ala-Ala), we focused on the 3 adaptor proteins described for ClpXP protease: CpdR, RcdA and PopA. Thus, the WT and mutant strains were grown in PYE complex medium and proteins extracts were withdrawn during mid-exponential phase of growth before being separated on SDS-PAGE. The levels of CtrA, PleC and MreB (the actin-like protein used as a loading control) were determined by western blotting. The PleC/MreB and CtrA/MreB ratios (average of 3 independent experiments) are represented in **Figure 20**. In agreement with the literature, we found (i) an accumulation of CtrA in the mutants of adaptors (Δ*cpdR*, Δ*rcdA* and Δ*popA*) as well as in $clpX^{-}$ and $clpP^{-}$ cells, and (ii) a reduction of CtrA levels in a $cpdR_{D51A}$ strain known to increase the degradation rate of CtrA. We also found a slight reduction of CtrA levels in Δ*ftsH,* Δ*lon* and Δ*hslV* strains.
Interestingly, we discovered that the PleC protein levels strongly increased in Δ*clpX* cells and to a lesser extent in a Δ*lon* background, but neither in the adaptor mutants (Δ*cpdR*, Δ*rcdA* and Δ*popA*) nor in the other protease mutants (Δ*ftsH,* Δ*hslV* and Δ*clpA*). More surprisingly, PleC abundance did not substantially increase in Δ*clpP* cells (**Figure 20**). Thus, it seems that the proteolytic degradation of PleC depends on ClpX but not on ClpP. On the other hand, the weak accumulation of PleC in Δ*lon* in comparison to the one observed in Δ*clpX* might come from a transcriptional effect (see Discussion). Likewise, the slight increase of PleC levels detected in $cpdR_{D51A}$ cells (**Figure 20**) might also come from a transcriptional effect, since CtrA represses transcription of *gcrA*, which codes for a direct transcriptional activator of *pleC*.
To confirm the results regarding the involvement of ClpX but not of ClpP in the proteolysis of PleC, the corresponding knock-out mutants (Δ*socAB*Δ*clpX* and Δ*socAB*Δ*clpP*) were

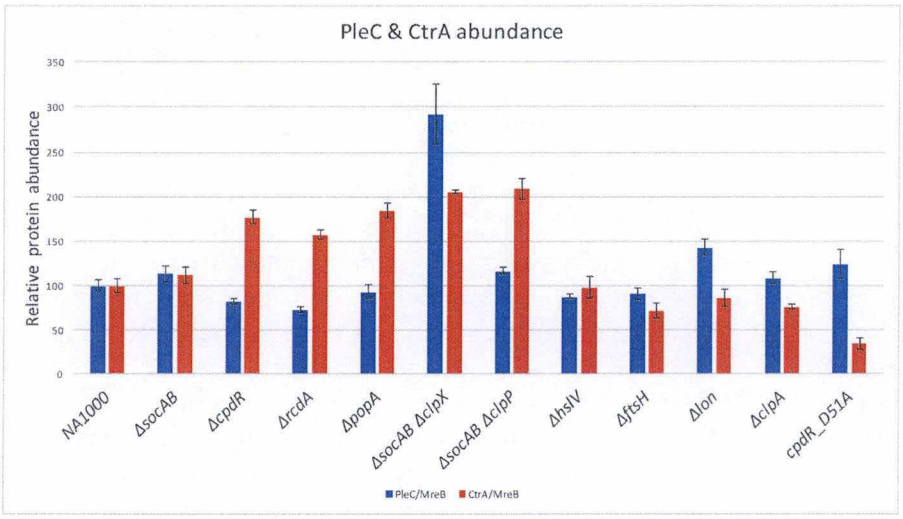

Figure 20: PleC and CtrA abundance in different proteases and adaptor proteins mutants. Quantification by ImageJ of the abundance of PleC and CtrA normalized to MreB. Abundance in the different backgrounds is expressed relative to the wild-type (NA1000). Error bars = s.d. (n=3)

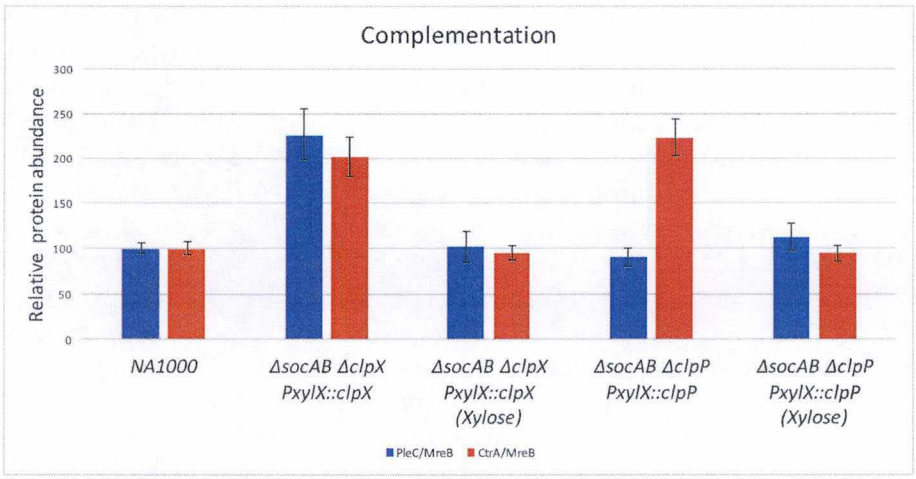

Figure 21: PleC and CtrA abundance in the complementation strains for *clpX* and *clpP*. Quantification by ImageJ of the abundance of PleC and CtrA normalized to MreB in the complementation strains for *clpX* and *clpP* with or without induction. Abundance in the different backgrounds is expressed relative to the wild-type (NA1000). Error bars = s.d. (n=3)

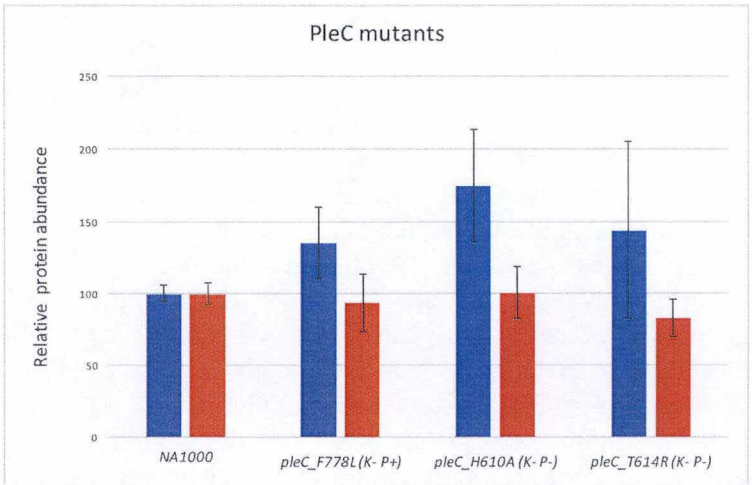

Figure 22: PleC and CtrA abundance for the different *pleC* mutants. Quantification by ImageJ of the abundance of PleC and CtrA normalized to MreB. Abundance in the different backgrounds is expressed relative to the wild-type (NA1000). Error bars = s.d. (n=3)

complemented with inducible copy of *clpX* and *clpP* (P_{xylX}::*clpX* and P_{xylX}::*clpP*), respectively. Western blot analysis was performed on extracts from exponential phase cultures with or without xylose inducer. As expected, both strains had, upon induction, wild-type levels of CtrA and PleC (**Figure 21**). Finally, we confirmed PleC is proteolyzed independently of adaptors by following PleC abundance throughout the cell cycle of a Δ*cpdR* mutant. In contrast to CtrA whose oscillation was annihilated in the absence of CpdR, we showed that PleC still oscillates during the cell cycle (**Figure 19 c**). Since CpdR is the first adaptor protein required for the two other ones (RcdA and PopA) to be functional as well as for ClpXP-dependent degradation (Joshi et al., 2015), we can conclude that PleC does not require these adaptors to be proteolyzed.

The protein levels of PleC and CtrA were also measured in strains expressing PleC variants, the K^- P^- (*pleC*$_{H610A}$ and *pleC*$_{T614R}$) and the K^- P^+, (*pleC*$_{F778L}$) mutants. All the three mutant strains had increased levels of PleC (**Figure 22**). Since the activity of CtrA is decreased in these backgrounds, it is likely that PleC increase comes from a GcrA-dependent transcriptional effect.

3.4. Identification of novel regulators of the CtrA pathway

In *C. crescentus*, the development and the cell cycle progression is strongly influenced by the CtrA pathway. It is therefore particularly important to fully understand the complex regulation it is subjected to. In order, to identify new actors of the CtrA pathway we sought to develop large scales genetic approaches based suppression of growth defects or synthetic lethality.
CtrA-P is negatively regulated by c-di-GMP and DivK-P. Both will inhibit the kinase activity of CckA, and thus the phosphorylation of CtrA (**Figure 23 a**). Since CckA$_{Y514D}$ is insensitive to c-di-GMP (Lori et al., 2015), this will lead to a slight overactivation of CtrA-P but without affecting the growth and the viability of the cell (**Figure 23 b**). In contrast, this allele becomes highly toxic when DivK-P activity is reduced (e.g. in the absence of *divJ*) (Lori et al., 2015) (**Figure 23 c**). This synthetic lethality could be due to the strong increase of CtrA-P activity experienced in this background, which would constitutively inhibit DNA replication initiation.

3.4.1. A transpositional screen in the Δ*pleC* Δ*divJ cckA*$_{Y514D}$ strain

Our first idea was to engineer a *cckA*$_{Y514D}$ strain expressing an inducible copy of *divJ* (Δ*divJ cckA*$_{Y514D}$ P_{xylX}::*divJ*), since the combination of Δ*divJ* and *cckA*$_{Y514D}$ was non-viable. Unfortunately, we were not able to find a right condition to delete *divJ* in a *cckA*$_{Y514D}$ P_{xylX}::*divJ* background. The close proximity between *cckA* and *divJ* loci (~16 kB) did not help since we could not use transduction to combine mutations. Therefore, we used the viable but slow growing Δ*divJ* Δ*pleC cckA*$_{Y514D}$ strain (**Figure 23 d, 24**) to look for transposons (Tn) that improved growth on PYE agar plates.
As a preliminary experiment, about 50 transpositional insertions were selected for faster growth. To check whether the faster growth was due to the Tn, phage lysates were prepared on five candidates and used to transduce Tn into the parental Δ*divJ* Δ*pleC cckA*$_{Y514D}$ strain. Then a growth assay was performed on transductants to check the ability of the Tn to improve growth. One of the five candidates (#3) fully restored optimal growth (**Figure 25**). To identify the insertion site of the transposon, a semi-arbitrary PCR was performed on candidate #3 and the resulting amplicon was sequenced. The transposon disrupted *rpoN*, a gene encoding the alternative sigma factor σ54. Interestingly, *rpoN* is known to be directly regulated by CtrA-P (Laub et al., 2002) and is involved in the biogenesis of polar structures like the stalk and flagellum (Brun & Shapiro, 1992). More specifically, σ54 was shown to directly control the

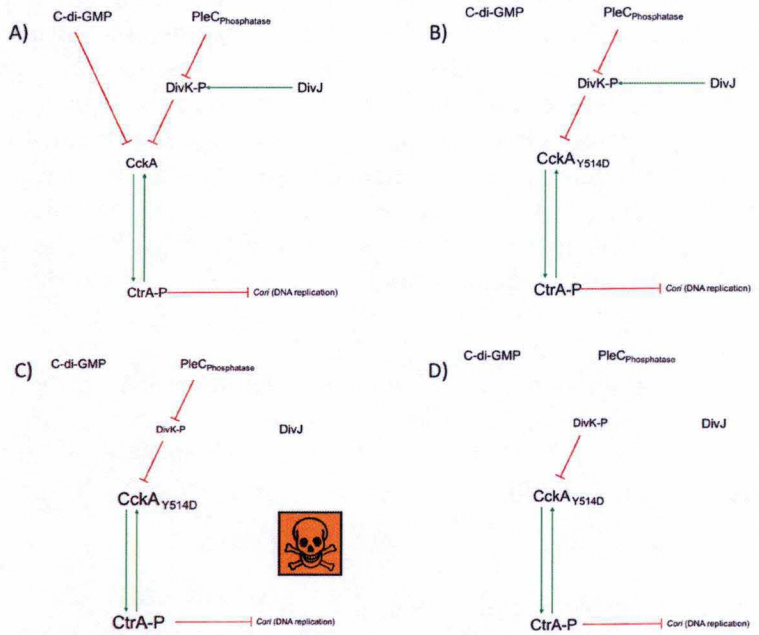

Figure 23: Regulatory network explaining the implication of different actors in the regulation of CtrA-P activity. (A) Wild-type situation: CtrA-P levels are negatively regulated by DivK-P and c-di-GMP because of their inhibitory action of CckA. DivK-P is itself regulated positively by DivJ and negatively by PleCP. CtrA-P is responsible for the repression of DNA replication initiation by binding the origin of chromosomal replication. (B) A mutation in CckA (CckAY514D) renders the protein insensitive to c-di-GMP, CtrA being therefore overactivated. (C) Combination of the CckAY514D mutation with the deletion of divJ is synthetically lethal for the cell by strong overactivation of CtrA-P. (D) A deletion of pleC in the double mutant ΔdivJ cckAY514D lowers the inhibition of DivK-P and enables a sufficient repression of CtrA-P to allow viability.

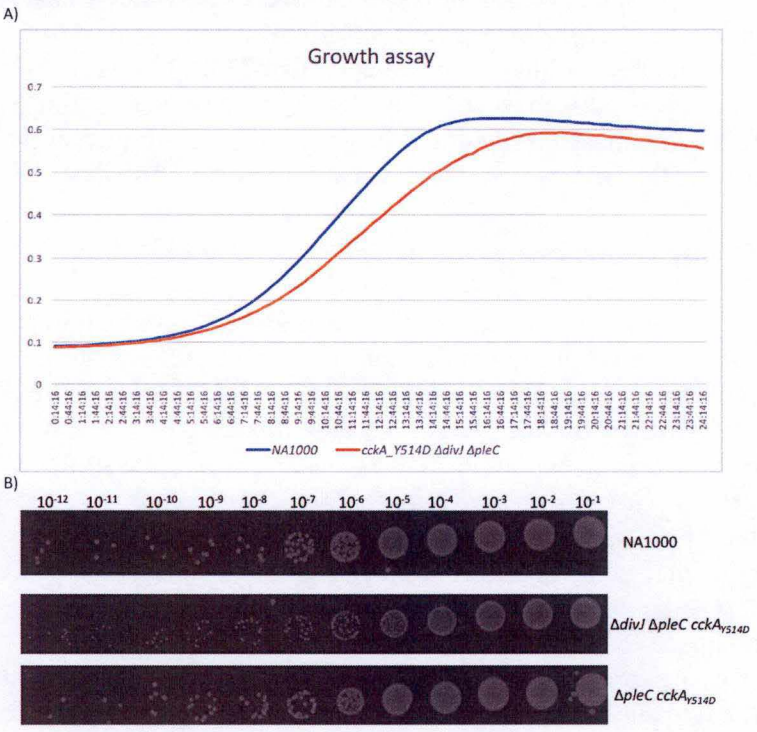

Figure 24: Growth and viability of the Δ*divJ* Δ*pleC cckA*$_{Y514D}$ strain. (A) Growth assay in PYE media for the wild-type (NA1000) and the Δ*divJ* Δ*pleC cckA*$_{Y514D}$ strain. The optical density at 660 nm was measured for each strain on an interval of 15 minutes during 24 hrs. (B) Different dilutions of an overnight culture were spotted on PYE agar plate to visualize the viability of the Δ*divJ* Δ*pleC cckA*$_{Y514D}$ strain. The NA1000 and Δ*pleC cckA*$_{Y514D}$ mutant were used as control.

expression of *tacA* and to be required for transcription of the TacA regulon (Biondi, Skerker, et al., 2006).
These findings suggest that the growth defect of the Δ*divJ* Δ*pleC cckA*$_{Y514D}$ strain and therefore of the overactivation of CtrA-P is linked to overexpression of *rpoN* and the subsequent overexpression of the σ54 regulon. More importantly, our results show that looking for growth suppressors in the Δ*divJ* Δ*pleC cckA*$_{Y514D}$ strain allows the identification of candidates linked to hyperactivation of CtrA-P. We can thus expect to find new regulators of the CtrA pathway with this approach.

3.4.2. Tn-Seq

A genome-wide hyper-saturated transposon (Tn) mutagenesis followed by deep-sequencing (Tn-Seq) was the second broad approach we used for identifying novel regulators implicated in the CtrA pathway. Large pools of single mini-Tn5 transposon insertions were generated in three strains: the wild-type (NA1000), Δ*divJ* and *cckA*$_{Y514D}$. Genomic DNA was then extracted from each library and Illumina single reads sequencing was performed to identify every transposon insertion sites. The concept behind this approach is to highlight differences of transposons density between strains in each open reading frame of *C. crescentus*. For example, if more transposon insertions into a gene "*x*" are found in one background compared to the WT, it suggests that disrupting this gene in this specific background could be beneficial for the survival and/or growth of the parental strain. Indeed, if Tn insertions into "*x*" is beneficial, they will be enriched in the library. In contrast, Tn insertions into gene "*y*" can be detrimental in a specific background by reducing the fitness of the cells. In such cases, Tn insertions into "*y*" will be impoverished in the library. Therefore, if you compare the density of Tn insertions in each gene between a condition and a reference, you can identify combination of alleles that interact negatively or positively. The *cckA*$_{Y514D}$ mutant is a great tool to investigate the regulation of CtrA by the DivK branch because of its high sensitivity to any decrease in DivK activity (Lori et al., 2015) (**Figure 23**). Likewise, Δ*divJ* is useful to identify regulators of CtrA since it is known to have over-activated CtrA-P.
First, a qualitative analysis of the sequencing data was performed using the FasQC software (Andrews, 2010). After that, truncation of the first and last five bases of each read was done since the beginning and end of sequencing data are often of poor quality.
All the reads were then mapped on the reference genome of *C. crescentus* (NA1000, NC_011916.1) strain using the Burrows-Wheeler Aligner algorithm (Li & Durbin, 2010) and for each strain, a sum of all the reads was calculated for each gene. Since Tn insertions in the 5' and 3' end of a gene often does not disturb function, we removed the first and last ten percent of each gene from the calculation. In addition, we also used a sliding window (R200) approach (Solaimanpour, Sarmiento, & Mrázek, 2015) to identify essential or sensitive protein domain encoding regions. Briefly, the number of insertions found in a window of a particular size, 200 bases in our case, were determined and this window was slided on the whole genome by a forward move of 5 bases. This enabled us to know where the transposon insertions took place in a certain gene with a resolution equal to the size of the window.
Finally, to facilitate identification of enriched or impoverished Tn insertions between Δ*divJ* or *cckA*$_{Y514D}$ and the WT reference, we calculated the ratio of transposon insertions per gene between the mutants and the WT. An increase or a decrease of 1.5-fold was listed as potential candidates for a new CtrA regulators. Using ± 1.5-fold as a threshold, lists of 889 and 474 potential candidates were created for the Δ*divJ* and *cckA*$_{Y514D}$ mutants, respectively.

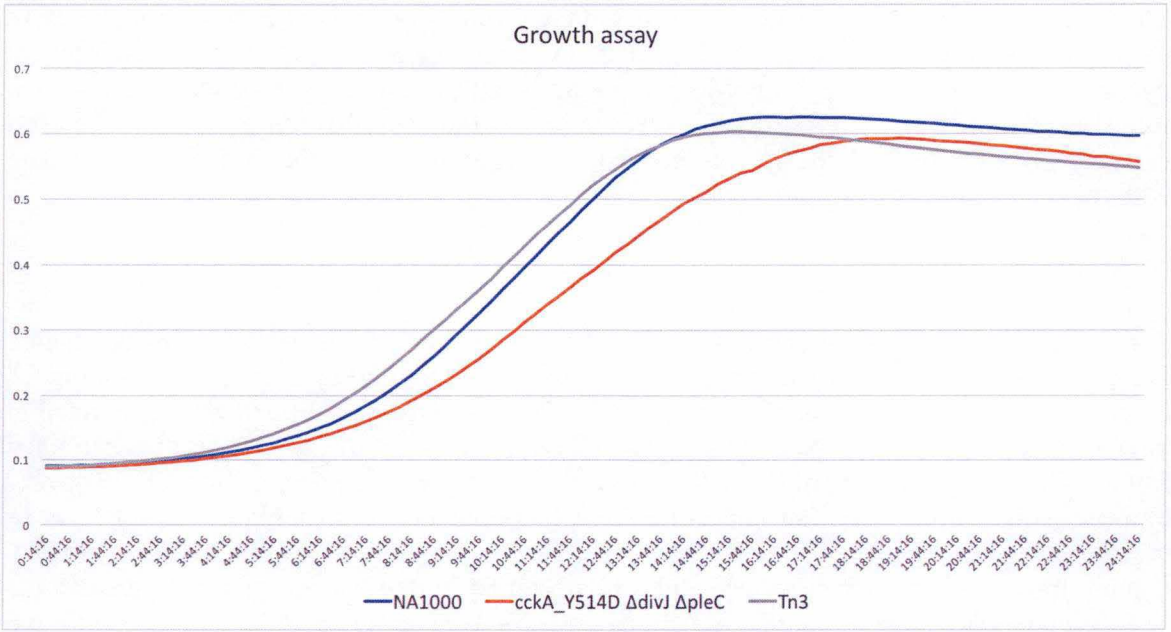

Figure 25: Identification of a suppressor restoring growth to the ΔdivJ ΔpleC cckAY514D strain. Growth assay in PYE media for the WT, *ΔdivJ ΔpleC cckA$_{Y514D}$* and the candidate #3 (identified as *rpoN*::tn5) of the suppressor screen. The optical density at 660 nm was measured for each strain on an interval of 15 minutes during 24 hrs.

Table 1: Table representing the usual suspects found in the Tn-Seq. The data in the "Essential genome" column is extracted from the analysis done by Christen and colleagues on the essential genome of Caulobacter crescentus (Christen et al., 2011).

	CCNA	Function	Essential genome	WT	*ΔdivJ*	Ratio		*cckA_Y514D*	Ratio
CtrA	CCNA_02567	sensory transduction histidine kinase pleC	Nonessential	5858	52608	8,98		5814	0,99
	CCNA_03598	two-component sensor histidine kinase divL	essential	60	4441	72,82		0	0
	CCNA_01116	histidine protein kinase DivJ	essential	230	0	0		51	0,22
	CCNA_00781	two-component receiver protein cpdR	Nonessential	3488	134	0,04		3174	0,91
	CCNA_03404	regulator of CtrA degradation rcdA	Nonessential	868	0	0,00		796	0,92
	CCNA_01918	two-component response regulator PopA	Nonessential	2869	185	0,06		3669	1,28
	CCNA_02546	GGDEF/response regulator protein pleD	Nonessential	4756	2834	0,60		4135	0,87
PodJ	CCNA_01993	membrane endopeptidase MmpA	Nonessential	1292	284	0,22		1478	1,14
TacA	CCNA_03424	AAA-family response regulator tacA	High_Fitness_Costs	1901	18071	9,50		832	0,44
	CCNA_03713	RNA polymerase sigma-54 factor rpoN	High_Fitness_Costs	754	8430	11,17		350	0,46
	CCNA_01280	SpmY	High_Fitness_Costs	2237	4260	1,90		801	0,36
	CCNA_02255	lysozyme-family localization factor spmX	High_Fitness_Costs	1523	5070	3,33		1349	0,89

3.4.2.1. Validation of the Tn-Seq results

First, we compared our Tn-Seq results obtained for the WT strain to the one published by Christen and colleagues (Christen et al., 2011) and found that out of the 480 essential genes published, 389 didn't harbor any single transposon. The 91 other genes were divided into 3 distinct categories: (i) 38 had an average Tn insertion of at most 1 every 10 bp, (ii) 47 harbored Tn insertions at a maximum of 1.5 per bp and (iii) the last category was composed of 6 genes with more than 1.5 Tn insertion per bp. Since the entire genome harbored an average Tn insertions of 2.96/bp, the 38 genes belonging to the first category can still be considered as critical if not essential for growth. On the other hand, 35 other genes did not harbor any transposon insertions at all. In (Christen et al., 2011), 17 of these genes belonged to the "High Fitness[1]" category whereas 18 were considered as "Nonessential". Altogether, our Tn-Seq data confirmed 89% (424/480) of essential genes identified by Christen and colleagues. Only 51 genes are no longer considered as essential in our experiment, but 82% (47/52) can be considered as "High Fitness" and 18 genes are considered as essential whereas they were labeled as "High Fitness". This slight discrepancy comes from the criteria used to consider a gene as essential. Indeed, Christen and colleagues considered a gene as essential when they observed no transposition events in first (5') 60% of gene length (Christen et al., 2011). Finally, false negatives are known to arise from such high throughput experiments because criteria have to be set up to define the essentiality of a gene. *divJ* and *ftsE* are examples of genes annotated as essential in the Tn-Seq analysis of Christen and colleagues but KO mutants of these genes have been published (Meier et al., 2017; Wheeler & Shapiro, 1999). However, it is noteworthy that *divJ* should be defined as "High Fitness" in our analysis given the low number of Tn insertions observed in the WT strain (**Figure 26 a**) and Δ*ftsE* cells were described to grow poorly (Meier et al., 2017), explaining why these two genes might have been categorized as essential.

Based on the literature, we were also able to recover several candidates known to suppress Δ*divJ* growth defects or to be synthetic with $cckA_{Y514D}$. For instance, inactivating *pleC* will result in the loss of the main phosphatase of DivK thereby increasing DivK-P levels, which ultimately would to a decrease of CtrA-P activity in a Δ*divJ* background. Here we observed an increase of Tn insertions (8-fold) in this gene (**Table 1**). Likewise, mutations in *divL* activity also decreases CtrA-P activity in a Δ*divJ* background (Pierce et al., 2006). Although *divL* is an essential gene, it can tolerate Tn insertions in its 3' region coding for a dispensable C-terminal ATPase domain (Christen et al., 2011; Iniesta et al., 2010; Reisinger, Huntwork, Viollier, & Ryan, 2007). In the Δ*divJ* strain, we observed a considerable increase (72-fold) in Tn insertions into *divL,* most of them covering the region coding for the kinase domain adjacent to the ATPase domain (**Figure 26 b, c**). In agreement with the findings of Christen and colleagues (Christen et al., 2011), Tn insertions into the WT were found only in C-terminal ATPase domain region. In contrast, Tn insertions into *divL* gene in the $cckA_{Y514D}$ strain were strongly counterselected since no single Tn insertions were recovered (**Table 1**) even in the dispensable 3' region (**Figure 27 b**). These results suggest that insertions in the C-terminal ATPase domain of *divL* partially disrupt the DivK-P/DivL interaction (and thereby enhance DivL/CckA/CtrA functions) whereas insertions into the adjacent kinase domain partially inactivate DivL/CckA/CtrA functions. In the same way, we observed a 4-fold decrease in Tn insertions into the *divJ* gene in $cckA_{Y514D}$ strain (**Figure 27 a**). From these few controls, we can conclude that our Tn-Seq results are reliable.

---

[1] The high fitness category gathers Tn insertions into genes required for optimal growth without being essential *per se*.

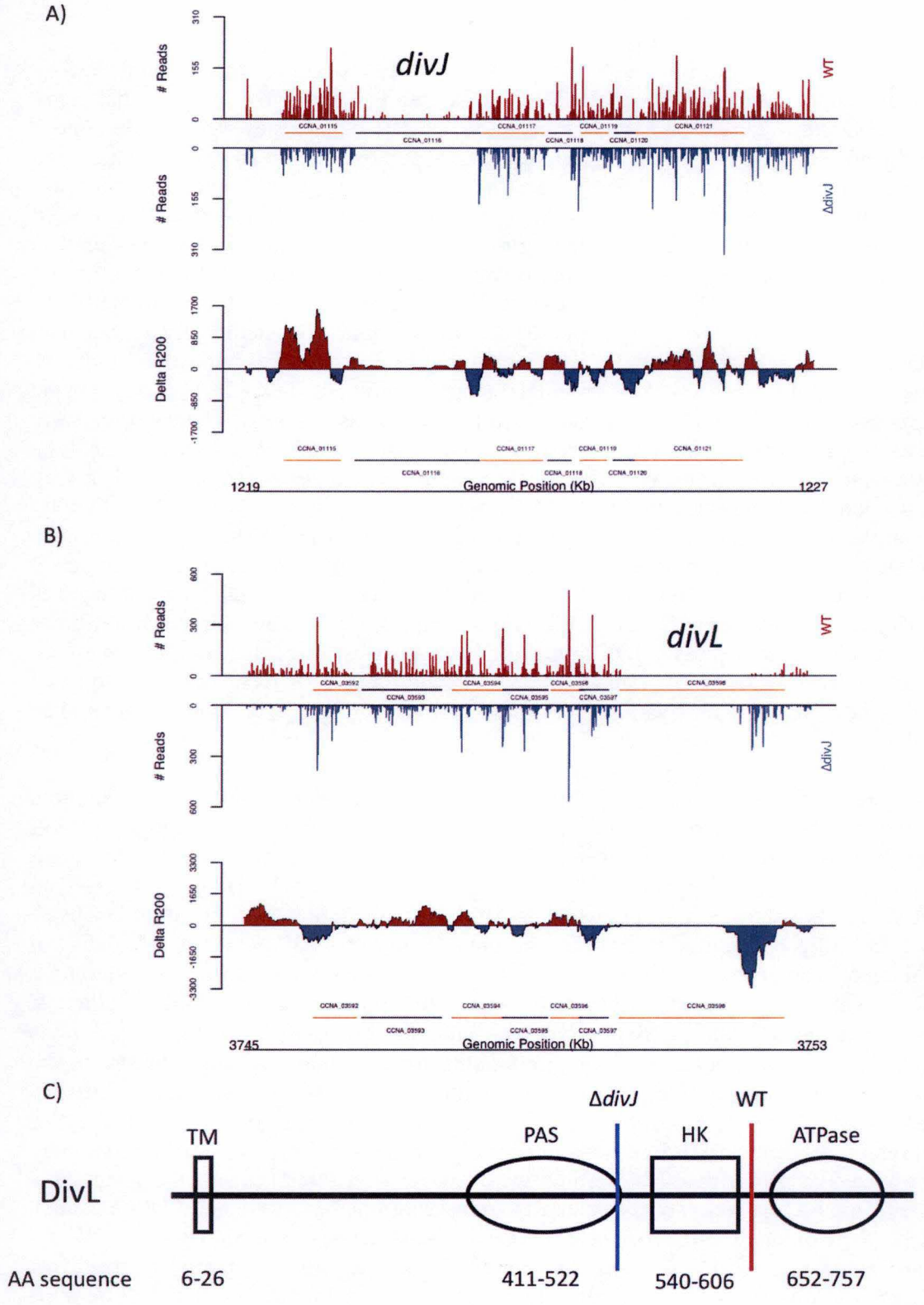

Figure 26: Transposon insertions profile in the NA1000 (WT) and Δ*divJ* strain for (A) *divJ* (CCNA_01116) and (B) *divL* (CCNA_03598). The upper graphs represent the number of reads obtained relative to their location. The bottom graphs represent the ΔR200 visualizing the difference in insertions along the gene between both strains. (C) Diagram of the DivL Protein representing its domains. The red and blue lines represent the first transposon insertion found the wild-type and Δ*divJ* strain respectively.

3.4.2.2. The usual suspects in ΔdivJ

- *pleC*

As previously stated, an increase in transposon insertions (8-fold) was observed in *pleC* for the Δ*divJ* strain (**Table 1**). Interestingly, an analysis of the location of the insertions revealed an uneven distribution along the gene. Indeed, insertions were found along the whole gene except in the last 389 nucleotides of the coding sequence corresponding to the HATPase_c domain of PleC responsible for the binding and cleavage of ATP (**Figure 28**). More interestingly, this type of distribution was not found in the WT strain. Whereas the average Tn insertions per base for the region coding for the HATPase_c domain of PleC in the WT strain (3.47) is very close to values for the whole *pleC* gene (3.50), these values are completely different in the Δ*divJ* strain, with 20.91 for the full *pleC* gene and only 0.2 for the HATPase_c coding region. This suggests that expressing a truncated version of PleC without ATPase domain is very deleterious in a Δ*divJ* background.

- *podJ*

MmpA is the metalloprotease responsible for shedding PodJ from the pole (J. C. Chen et al., 2005; Curtis et al., 2012). Interestingly, Tn insertions into *mmpA* was 4-fold lower in Δ*divJ* that in WT (**Table 1**). Since PodJ is the localization factor of PleC and DivL, inactivation of *mmpA* should lead to a permanent polar localization of these proteins. Thus, this result suggests that the phosphatase activity of PleC might be enhanced at the pole resulting in a further decrease of DivK-P that would be deleterious in a Δ*divJ* background. Alternatively, the synthetic relationship between Δ*divJ* and *mmpA* could come from an increase of CckA activity due to the constant polar localization of DivL.

- *tacA & rpoN*

Two other candidates with an increased amount of Tn insertions (9.5-fold and 11.1-fold) were *tacA* and *rpoN*, respectively (**Table 1, Figure 29**). As transcription of both genes is positively regulated by CtrA-P and both gene products are required for expressing the TacA regulon, this suggests growth defects in Δ*divJ* could be due to over-activation of TacA regulon. However, the number of Tn insertions into *spmX* and *spmY*, whose products have been described to inhibit TacA activity (Janakiraman et al., 2016), were also increased in Δ*divJ vs* WT (3.3- and 1.9-fold, respectively) (**Table 1**). Since transcription of *spmX* and *spmY* is positively regulated by TacA-P/ σ54 and CtrA-P respectively, both genes are overexpressed in Δ*divJ* cells (Radhakrishnan et al., 2008). Therefore, the problem could rather come from over-expression of these two genes, suggesting that SpmX and SpmY might control another (unknown) factor than TacA. Alternatively, the higher proportion of Tn insertions into *spmX* in Δ*divJ* could be neutral instead of deleterious in the WT, since DivJ cannot be anymore negatively impacted by *spmX* inactivation. In the same way, Tn insertions into *spmY* would not decrease the fitness of Δ*divJ* cells because SpmY has been proposed to be inactive in a Δ*divJ* background (Janakiraman et al., 2016).

The three adaptor proteins of the ClpXP protease CpdR, RcdA and PopA (the three being required for CtrA proteolysis and the two first for TacA degradation) were found to have a drastic reduction of Tn insertions in Δ*divJ* compared to the WT (**Table 1**). In particular RcdA, the adaptor protein required for TacA degradation, having no Tn insertion at all in Δ*divJ* while 868 Tn insertions were counted in the WT. This suggests that the proteolytic degradation of CtrA and TacA becomes essential in this background.

In conclusion, these results suggest that the slower growth/viability of a Δ*divJ* mutant relies essentially on hyperactivated CtrA and TacA.

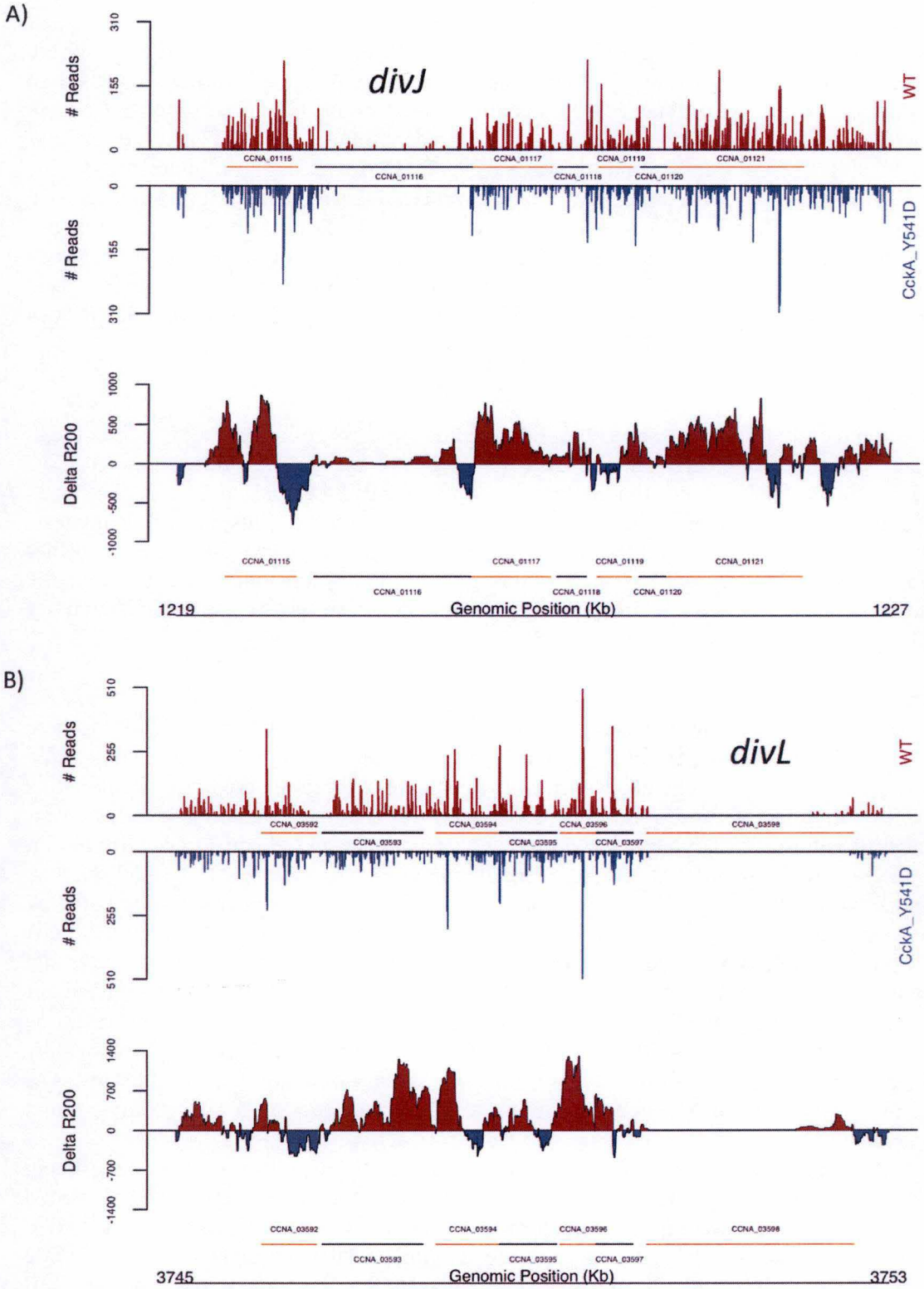

Figure 27: Transposon insertions profile in the NA1000 (WT) and $cckA_{Y514D}$ strain for (A) *divJ* (CCNA_01116) and (B) *divL* (CCNA_03598). The upper graphs represent the number of reads obtained relative to their location. The bottom graphs represent the ΔR200 visualizing the difference in insertions along the gene between both strains.

3.4.2.3. *The usual suspects in $cckA_{Y514D}$*

As stated previously, the $CckA_{Y514D}$ mutation does not induce a growth or viability defect in the cell meaning that only the synthetic lethal combinations with $cckA_{Y514D}$ can be detected by Tn-Seq analysis. Interestingly, *divJ* and *divL* had a decreased number of Tn insertions in $cckA_{Y514D}$ (**Table 1**). This result was expected since $cckA_{Y514D}$ cells hypersensitive to any increase of CtrA activity.

3.4.2.4. *Identification of New actors*

One of the aims of this master thesis was to uncover the peptidase responsible for the proteolytic degradation of PleC. Interestingly, an uncharacterized ATP-dependent protease subunit (CCNA_02072) had a 2.5-fold decrease in Tn insertions (**Table 2**). Because stabilizing PleC should overall increase its phosphatase activity, this could be deleterious in a Δ*divJ* background by lowering even more the amount of phosphorylated DivK. Given this result, this gene could potentially encode the protease responsible for the proteolysis of PleC.
The Tn-Seq also revealed that certain groups of genes belonging to the same pathway displayed a highly altered profile compared to the WT (**Table 2**). These genes belong, the PTS^{NTR} (Nitrogen-related PhosphoTransferase System) and the PST (Phosphate-Specific Transport).

- PTS^{NTR}

The PTS^{NTR} is a set of 3 proteins (EI^{NTR}, HPr and $EIIA^{NTR}$) constituting a phosphorelay (**Figure 30**) involved in the response to nitrogen starvation in *C. crescentus* (Ronneau, Petit, De Bolle, & Hallez, 2016). As glutamine inhibits EI^{NTR} autophosphorylation, phosphorylation levels of PTS^{NTR} will be enhanced upon glutamine deprivation (Ronneau et al., 2016). Once phosphorylated on a His residue $HPr_{H18\text{-}P}$ and $EIIA^{NTR}_{H66\text{-}P}$ will stimulate (p)ppGpp accumulation by modulating the bifunctional (p)ppGpp synthetase/hydrolase SpoT (Ronneau et al., 2016). The serine kinase/phosphatase HprK constitutes a fourth PTS component that is believed to catalyze the phosphorylation of HPr on Ser49 residue (Petit, 2017). And according to what is known in the literature, phosphorylating the Ser49 residue by HprK likely inhibits HPr phosphorylation on His18 by EI^{NTR} (Petit, 2017).
The four genes of PTS^{NTR} were found in our Tn-Seq analysis of the Δ*divJ* strain, with a decreased Tn insertion number into the gene coding for EI^{NTR}, HPr and $EIIA^{NTR}$, whereas *hprK* contained more Tn insertions (2.2-fold) (**Table 2**). Surprisingly we also detected a 2.3-fold increase in Tn insertions in *spoT*. This result suggests that PTS^{NTR} and (p)ppGpp influenced the survival of Δ*divJ* independently of each other.
The results found for *spoT* indicate that (p)ppGpp accumulation in a Δ*divJ* cells could be deleterious. This effect might be due to overexpression of *mopJ,* since Tn insertions into *mopJ* were decreased of 1.9-fold. Indeed, MopJ is known to be positively regulated by (p)ppGpp and required to sustain optimal CtrA activity, especially in stationary phase (Sanselicio, Bergé, Théraulaz, Radhakrishnan, & Viollier, 2015).

- PST

The PST system is a high affinity phosphate transport system and is composed of 4 Pst proteins (PstS, PstA, PstB and PstC) (Gonin, Quardokus, O'Donnol, Maddock, & Brun, 2000). The expression of the corresponding genes requires the transcriptional regulator PhoB (Lubin, Henry, Fiebig, Crosson, & Laub, 2016). We don't how phosphate starvation could improve the growth and/or the viability of Δ*divJ* cells.

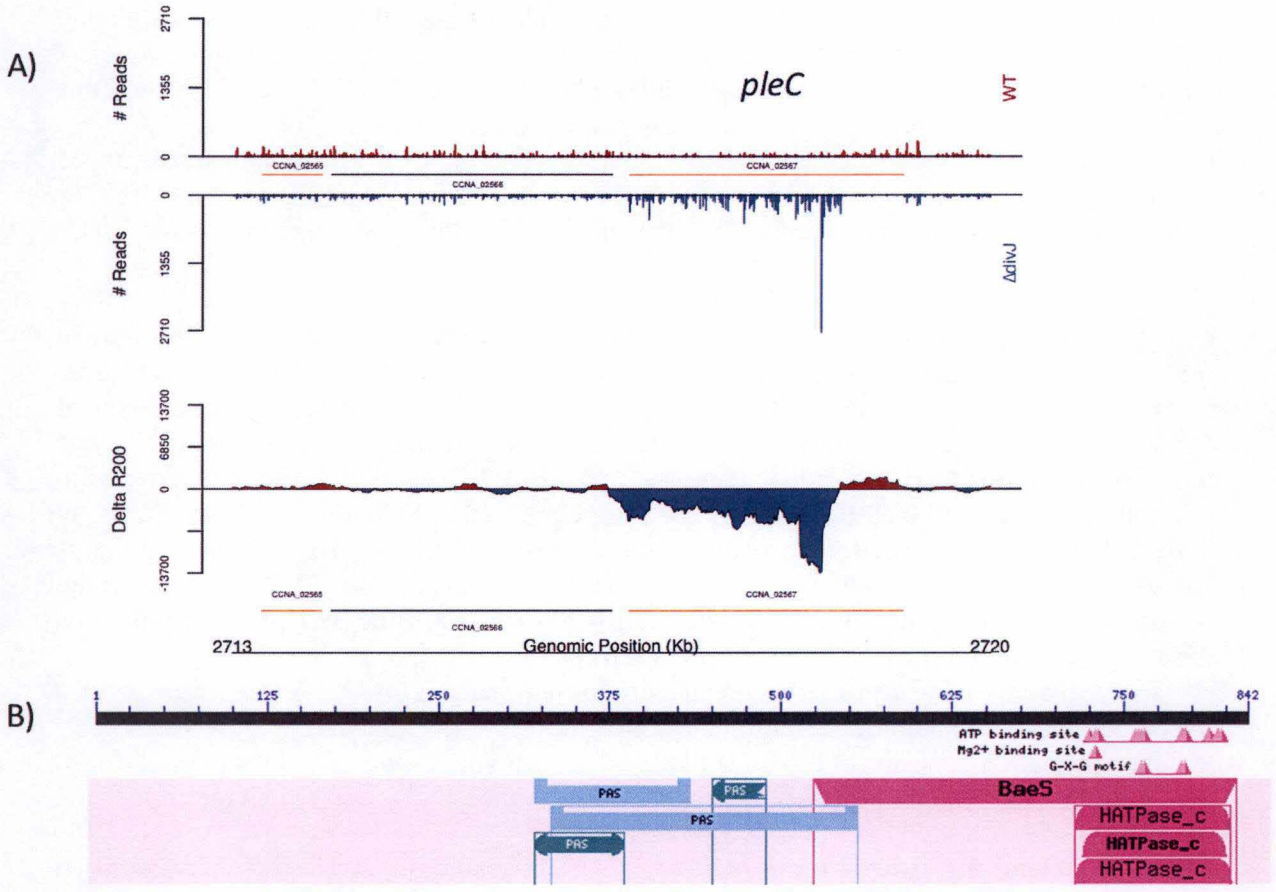

Figure 28: (A) Transposon insertions profile in the NA1000 (WT) and Δ*divJ* strain for *pleC* (CCNA_02567). The upper graph represents the number of reads obtained relative to their location. The bottom graph represents the ΔR200 visualizing the difference in insertions along the gene between both strains. (B) Prediction of protein domains for PleC showing its terminal HATPase_C domain.

3.4.2.5. *Creation of a putative candidate list*

To create a list of putative candidates regulating CtrA, Tn-Seq analysis had to be reiterated with more stringent criteria to only leave the most extreme ratios. The ratio threshold was risen to a minimum of 10 for the increase of decrease in Tn insertions for the Δ*divJ* strain. With those criteria, a list of 80 actors potentially involved in the CtrA and/or TacA pathways was generated (**Supplementary table 1**).
For the $cckA_{Y514D}$ mutant, only the candidates showing synthetic lethality were selected with a threshold value for the ratio of maximum 0.5 (2-fold decrease in Tn insertions), allowing to list 47 putative candidates involved in the CtrA and/or TacA pathways (**Supplementary table 2**).

4. Discussion & perspectives

The regulation of the cell cycle and development in *C. crescentus* has been studied for the past 40 years. PleC, as one of the first actors identified, has enabled scientist to uncover a complex spatiotemporally regulated molecular machinery underlying the life cycle of this bacterium.

4.1. Characterization of PleC activities

One of the aims of this master thesis is to understand the contribution of each activity of PleC in the regulation its substrates, namely DivK and PleD. The analysis of physiological consequences of expressing the point mutants with altered enzymatic activity as the only copy of *pleC* from its native genomic locus enabled us to better characterize this protein.
We showed that the $pleC_{H610A}$ and $pleC_{T614R}$ mutants behaved like the Δ*pleC* strain confirming the lack of both activities in these point mutants (**Figure 13,14,15**). Indeed, in the absence of $PleC^{P}$, the activity of CtrA-P is strongly reduced (Sciochetti et al., 2002). As a consequence, Δ*pleC*, $pleC_{H610A}$ and $pleC_{T614R}$ strains are non-motile and resistant to infection by bacteriophage CbK & Cr30.
The attachment assay, performed to investigate the impact of PleC on PleD, whose involvement in the holdfast formation is well known (Levi & Jenal, 2006; Paul et al., 2008), showed also similar results between the Δ*pleC* strain and the two mutants indicating the absence of their respective kinase activity.
On the other hand, the $pleC_{F778L}$ mutant showed intermediate phenotype between the WT and the Δ*pleC* strains for motility, phage resistance and attachment assay (**Figure 13,14,15**). The study of CtrA-P dependent promoters showed a reduction of activity in the $pleC_{F778L}$ cells compared to the WT (**Figure 16**), which most likely reflects a reduction of phosphotransfer from CckA to CtrA. We can therefore speculate that the $PleC_{F778L}$ mutant has, *in vivo*, a reduced phosphatase activity that would lead to an increase of DivK-P that inhibits DivL-dependent activation of CckA. This decrease in CckA activity will negatively impact the phosphorylation state of CtrA (Childers et al., 2014; Tsokos et al., 2011).
Quantification of *in vivo* phosphorylation levels of DivK can also be performed on the $pleC_{F778L}$ mutant to highlight a potential reduction of the phosphatase activity of $PleC_{F778L}$.
This phosphatase activity reduction of the $PleC_{F778L}$ mutant could be due to a decreased affinity between PleC and DivK-P. Therefore, measurements of the respective K_D of the WT and different mutant versions of PleC for DivK-P or a phosphomimetic variant of DivK by Isothermal Titration Calorimetry (ITC) could be performed.

The intermediate attachment efficiency can be explained by the fact that, even though attachment of *Caulobacter* has been shown to be PleD-dependent, other diguanylate cyclase

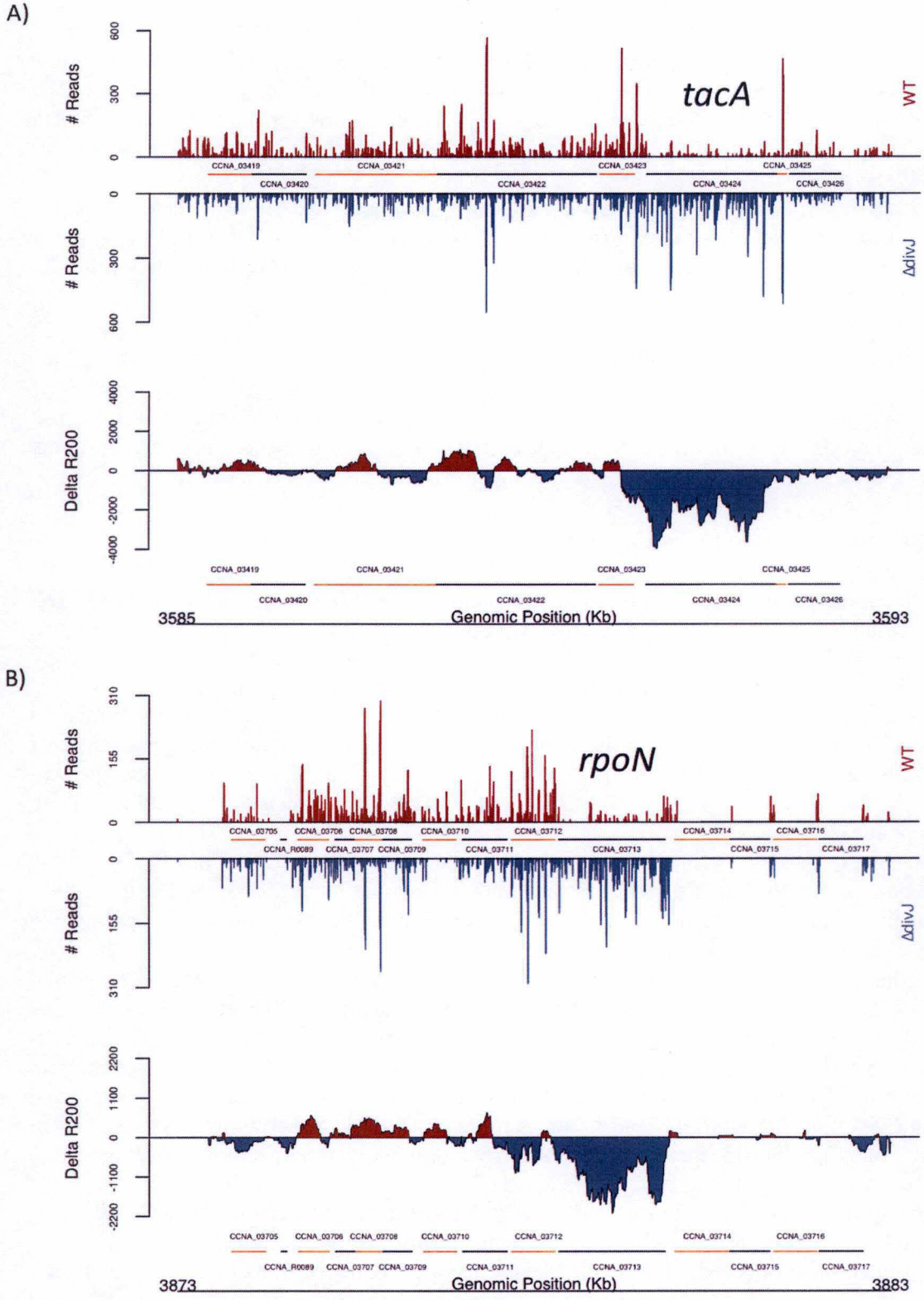

Figure 29: Transposon insertions profile in the NA1000 (WT) and Δ*divJ* strain for (A) *tacA* (CCNA_03424) and (B) *rpoN* (CCNA_03713). The upper graphs represent the number of reads obtained relative to their location. The bottom graphs represent the ΔR200 visualizing the difference in insertions along the gene between both strains.

(DGC) might be involved. For instance, DgcB is another DGC contributing to the holdfast biogenesis and surface attachment (Abel et al., 2013). Furthermore, a Δ*pleD* strain is still able to attach but with reduced efficiency (Paul et al., 2008). Finally, it has also been shown that efficient attachment requires more than just c-di-GMP effectors. Namely, the pili and flagellum are described as participating in the overall attachment process (Bodenmiller, Toh, & Brun, 2004; Levi & Jenal, 2006). Since these polar structures are not fully functional in $pleC_{F778L}$ mutant (decrease of CbK sensitivity and motility), very likely because CtrA-P activity is reduced, attachment could be sub-optimal.
Moreover, it is possible that the $PleC_{F778L}$ mutant could show *in vivo* a residual kinase activity that could not have been detected *in vitro* (Matroule et al., 2004).
It is known that the kinase activity of PleC is strongly stimulated by DivK (Paul et al., 2008)and that PleC has a tenfold increased affinity towards DivK-P compared to DivK (Childers et al., 2014). A kinase assay measuring the phosphotransfer from PleC to PleD should therefore be performed on the different PleC mutants in the presence of a phosphomimetic version of DivK (Paul et al., 2008).

4.2. Screening for a K^+ P^- mutant

Various approaches were explored to identify the missing activity mutant of PleC. Unfortunately, none of them allowed identification K^+ P^- mutant. The mutagenic PCR approach has already been shown to be an effective way to insert random mutations in a specific DNA fragment (Shi et al., 2017). In comparison to the XL1-Red based mutagenesis protocol, it has the advantage to avoid mutations leading to the alteration of expression of the gene analyzed by only mutagenizing the DNA region of interest and not the entire plasmid. The mutated amplicons should then be cloned in a high copy number plasmid allowing expression of *pleC* variants under the control of the vanillate or xylose promoter.
Our preliminary results showed that the reduced attachment of the strain expressing wild-type *pleC* at the *vanA* locus (**Figure 18 a**) in comparison to the WT strain is likely due to the reduced amount of PleC produced in this strain. The test should therefore be done on a similar high copy plasmid with the xylose promoter, known to be stronger.
The adequate tools were designed and created to allow us to mutagenize the whole gene (2529 bp) or solely the region coding for the catalytic domain of *pleC* (± 750 bp).
Since mutations inactivating the kinase or phosphatase activity have been described in EnvZ to be located in the catalytic domain (Hsing et al., 1998), it likely that mutations inactivating PleC phosphatase activity would be also located in the same domain.

The identification of the K^+ P^- mutant would be of great importance because it could bring strong evidence on the implication of the Kinase activity in regard to the development and cell cycle. Namely in the predivisional cell, different models have been proposed discussing the state of PleC at the new pole (Matroule et al., 2004; Subramanian, Paul, & Tyson, 2013). In the model described by Matroule and colleagues, proposing that PleC is a phosphatase at the new pole, the PleC K^+ P^- mutant should have an overall reduced CtrA-P activity and could maybe also increase its degradation due to an increased stimulation of PleD. With all this, it would be possible that this mutant should show severe growth and development defects or could even be lethal. If this is the case, the identification of the K^+ P^- mutant could only be possible in a background that tolerates this type of mutation, like a strain with overactivated CtrA, e.g. Δ*divJ*.
If we take the model based on mathematical predictions done by Subramanian and colleagues, in which PleC is in its kinase conformation at the new pole and traps DivK-P to avoid DivL dependent CckA inhibition (Childers et al., 2014), the PleC K^+ P^- mutant should work as the

Table 2: Candidates of the Tn-Seq experiment for the ΔdivJ strain. The genes are classified following their related to a certain group: PTS^{NTR} (Nitrogen-related phosphotransferase system), PST (Phosphate Specific Transport) or potentially related to PleC. The data in the "Essential genome" column is extracted from the analysis done by Christen and colleagues on the essential genome of Caulobacter crescentus (Christen et al., 2011).

	CCNA	Function	Essential genome	WT	*ΔdivJ*	Ratio
PleC	CCNA_02072	ATP-dependent protease subunit	Nonessential	1371	563,2205642	0,41123948
PTS	CCNA_00892	phosphoenolpyruvate-protein phosphotransferase (EI_NTR)	High_Fitness_Costs	1112	155,83	0,14
	CCNA_00241	phosphocarrier protein HPr	Nonessential	134	0,00	0,01
	CCNA_03710	nitrogen regulatory IIA protein (EIIA_NTR)	Nonessential	476	54,54	0,12
	CCNA_00239	HPR(SER) kinase/phosphatase (HprK)	Nonessential	37	81,26	2,16
	CCNA_01622	ppGpp hydrolase-synthetase relA/spoT (SpoT)	Nonessential	3531	8276,89	2,34
	CCNA_00999	MopJ	Nonessential	864	1452	1,87
PST	CCNA_00296	phosphate regulon response regulator PhoB	Nonessential	622	2855,06	4,58
	CCNA_00293	phosphate transport system permease protein pstA	Nonessential	18	483,08	25,48
	CCNA_00294	phosphate transport ATP-binding protein pstB	Nonessential	28	601,07	20,76
	CCNA_00292	phosphate transport system permease protein pstC	Nonessential	15	569,90	35,68
	CCNA_01583	phosphate-binding protein (pstS)	Nonessential	150	1383,56	9,17

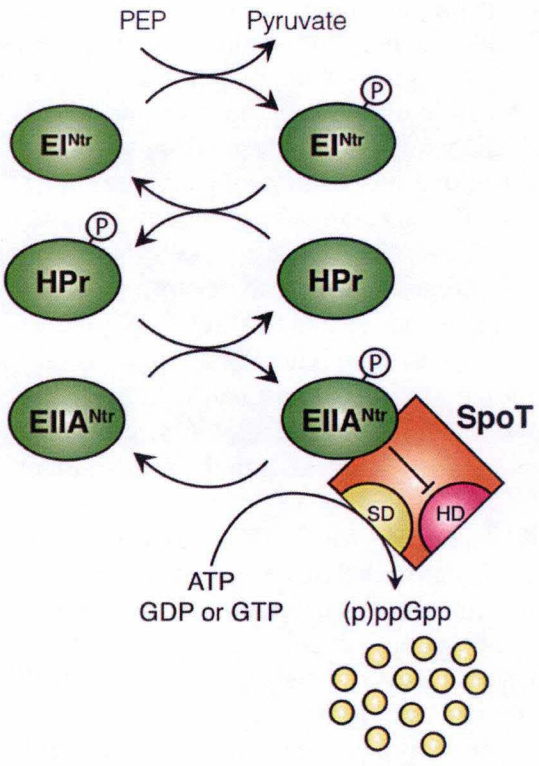

Figure 30: Control of the PTS^{Ntr} on the (p)ppGpp synthesis adapted from (Ronneau, Petit, De Bolle, & Hallez, 2016). EI^{NTR} phosphorylates HPr, which in turn phosphorylates $EIIA^{Ntr}$. $EIIA^{Ntr}$-P will lead to an accumulation of (p)ppGpp by inhibition of the hydrolase activity of SpoT.

WT. This prediction is solely based on the actors present in a normal condition at the new pole and does not include the possible effect of a PleC K^+ P^- mutant on the abundance of these actors and the respective state in which they are. Given the pleiotropic effects that PleC has by controlling a major response regulator, it is difficult to predict a clear phenotype for a hypothetical mutant.
This mutant would therefore be informative on the specific roles attributed to each activity of PleC. A more accurate characterization of this protein would therefore be feasible.

4.3. Protein abundance and degradation

As a bifunctional histidine kinase, PleC has both kinase and phosphatase activity (Matroule et al., 2004; Paul et al., 2008). With those activities, PleC is going to affect the phosphorylation state of two response regulators: In the G1 phase, PleC will act as a phosphatase dephosphorylating DivK-P whereas at the G1-S transition, PleC undergoes a phosphatase to kinase shift enabling it to rapidly phosphorylate PleD (Paul et al., 2008).
We showed that following this transition, PleC is going to be cleared from the cell in a ClpX-dependent way but independently of the usual peptidase subunit associated with ClpX, that is ClpP, or the known adaptor proteins described to mediate the ClpXP-dependent substrate proteolysis (**Figure 20**). This led us to the search for the peptidase responsible for its degradation. Unfortunately, no other single mutant for known peptidases or proteases showed a similar accumulation of PleC compared to the *clpX* mutant. The double mutant Δ*clpP* Δ*hslV* was also tested to investigate the possibility of a peptidase redundancy interacting with ClpX to degrade PleC. HslV is namely described as working with an ATPase subunit called HslU, which shows significant similarity to the ClpX ATPase subunit (Bogyo et al., 1997). Unfortunately, PleC abundance did not increase in this mutant and remains far from the one observed in the Δ*clpX* mutant (data not shown).
The slight increase of PleC abundance in a Δ*lon* mutant is thought to be indirect, rather caused by a transcriptional effect. Indeed, Lon is known to degrade the DNA methyltransferase CcrM (Wright, Stephens, Zweiger, Shapiro, & Alley, 1996). DNA methylation has been shown to be required for transcription of *pleC* and *dnaA* (Collier, Murray, & Shapiro, 2006; Fioravanti et al., 2013). In addition, DnaA was shown to positively regulate the transcription of *gcrA* (Collier, McAdams, & Shapiro, 2007; Collier et al., 2006) and GcrA directly stimulate the transcription of *pleC* (Fioravanti et al., 2013). Thus, stabilizing CcrM in Δ*lon* cells could up-regulate *pleC* expression directly but also indirectly through DnaA-GcrA.
The promoter activity of *pleC* and the abundance of *pleC* transcripts should be measured in the Δ*lon* mutant with respectively a ß-galactosidase and a qRT-PCR assays.

A potential candidate for the peptidase degrading PleC, a candidate emerged from the Tn-Seq analysis. Indeed, we reasoned that the stabilization of PleC in a Δ*divJ* background, following for example the inactivation of its specific peptidase, could lead to a hyper-activation of CtrA to a toxic level. This gene, CCNA_02072, encodes a putative ATP-dependent protease subunit. The ΔCCNA_02072 strain is currently under construction. A western blot analysis on exponential phase cultures will be done to observe a potential increase of PleC abundance in this mutant compared to the WT. The profile of PleC along the cell cycle should also be performed on this mutant to visualize a potential stabilization of the protein.

On the other hand, it has been shown that the $CpdR_{D51A}$ is permanently localized at the differentiating pole (Iniesta et al., 2006). Beside its role as an adaptor protein for ClpXP (Joshi et al., 2015), CpdR also determines the localization of ClpXP (Iniesta et al., 2006; Iniesta & Shapiro, 2008). This mutation results thus in a constitutive polar localization of ClpXP and

stimulates degradation of ClpXP substrates known to be degraded at the differentiating pole, e.g. CtrA (**Figure 20**). Interestingly, instead decreasing PleC abundance, PleC levels were slightly higher in $cpdR_{D51A}$. Several hypotheses can be stated based on this observation.
First, the proteolytic degradation of PleC does not occur at the pole. Therefore, if one of the two subunits implicated in the degradation of PleC (*i.e.* ClpX) is constitutively localized at the pole, it cannot degrade properly substrates that are not polarly degraded. Another possibility could be that both ClpX and the peptidase subunits can localize at the pole but that PleC is protected from its proteolytic degradation at this location. In both cases, this would lead to an increase of the abundance of PleC and a decrease of ClpXP substrates like CtrA. However, this hypothesis is unlikely because a Δ*podJ* mutant does not have a reduced PleC content (Viollier et al., 2002), although PleC is no longer localized in Δ*podJ cells*. Indeed, the constitutive delocalization of PleC should affect its abundance because it would be more in contact with its protease.
Another hypothesis is that the increase of the PleC content in the cells would be due to a transcriptional effect. Fioravanti and colleagues demonstrated that *pleC* was transcriptionally regulated by GcrA and *gcrA* is known to be repressed by CtrA-P (Collier et al., 2007; Fioravanti et al., 2013). This could also explain the increased abundance in the $cpdR_{D51A}$ mutant. By reducing the abundance of CtrA and therefore its activity as a transcriptional repressor on the *gcrA* promoter, an increase in PleC abundance should be observed. The transcriptional effect could be highlighted by performing a ß-galactosidase assay on the promotor of *pleC* in the $cpdR_{D51A}$ strain.

The previously characterized mutants of PleC ($PleC_{H610A}$, $PleC_{T614R}$ and $PleC_{F778L}$) were also tested for their relative abundance by western blot and a higher level of PleC was observed. Again, this effect could also be explained by transcription, since we showed that CtrA activity was reduced in *pleC* point mutants. Indeed, it was shown that, for the $PleC_{F778L}$ and $PleC_{H610A}$ mutant, the activity of CtrA-P dependent promoters is strongly reduced in comparison to $PleC_{WT}$ (**Figure 16**). This reduction is not due to a reduction of the amount of CtrA because its abundance is not changed compared to the wild-type (**Figure 22**).

PleC is also known to be localized at the flagellated pole (Matroule et al., 2004; Wheeler & Shapiro, 1999). During the G1-S transition, PleC will shift its activity from phosphatase to kinase (Paul et al., 2008). This transition coincides with its transient delocalization (Wheeler & Shapiro, 1999) and its proteolytic degradation (**Figure 19 a**). Interestingly, $PleC_{H610A}$ has been shown to not delocalize from the flagellated (Lam, Matroule, & Jacobs-Wagner, 2003; Viollier et al., 2002). Note that the localization was determined by fluorescence microscopy on cells expressing a $PleC_{H610A}$-GFP fusion that cannot be degraded at the G1-S transition. However, although $PleC_{WT}$-GFP are not degraded, it correctly delocalizes from the differentiating pole, showing that both delocalization is independent of proteolytic degradation. The reduction of CtrA activity observed $pleC_{H610A}$ could also explain the impact that PleC has on its own delocalization. Indeed, the gene *perP* is not properly expressed in strains with lower CtrA-P activity (J. C. Chen et al., 2006). This will affect the processing of PodJ, the localization factor of PleC, and unprocessed PodJ is not anymore degraded and remains at the pole (J. C. Chen et al., 2006). As a consequence, the constant polar localization of PodJ could permanently localize PleC at the same location. If this is true, $PleC_{F778L}$ should also be constantly localized at the pole. This hypothesis can be verified as well by analyzing the localization of the $PleC_{F778L}$ mutant

The literature brings additional information supporting this hypothesis. In a Δ*podJ* mutant, a reduction of activity is observed for CtrA-dependent promoters (J. C. Chen et al., 2006; Curtis

et al., 2012). This has been explained by the fact that PleC cannot be localized in this strain and will therefore be less efficient to dephosphorylate DivK-P and sustain an optimal CtrA activity (J. C. Chen et al., 2006). On the contrary, the constitutive polar localization of PleC has no effect on the CtrA activity, shown by the Δ*perP* mutant (J. C. Chen et al., 2006). This would imply that the delocalization of PleC is not required for an optimal regulation of CtrA activity and that therefore, its non-delocalization would have no effect on the on the cell cycle progression and the development of the bacteria. Secondly, the expression of a stabilized version of PleC and therefore its non-degradation along the cell cycle does not induce a particular phenotype reflecting a proper regulation of the cell cycle and development of the bacteria.
Together, these informations could mean that the two inactivation mechanisms (delocalization and proteolytic degradation) are redundant. To test this hypothesis, the effect of the *perP* deletion (no delocalization of PleC) should be investigated in a *pleC-GFP* strain, which stabilizes PleC.

4.4. Identification of new actors of the CtrA pathway

4.4.1. A transpositional screen in the Δ*pleC* Δ*divJ* $cckA_{Y514D}$ mutant

The suppressor screen enabled us to identify *rpoN*, a downstream actor of the CtrA pathway, as potentially responsible for the growth defects in Δ*divJ*.
The triple mutant is unstable and acquires spontaneous suppressor mutations rendering the strain difficult to use. As a consequence, only 1 out of the 5 suppressors we tested was linked to the Tn. Nevertheless, we were able to identify a candidate involved in growth defect of Δ*divJ* Δ*pleC* $cckA_{Y514D}$. To further validate our candidate, we could test whether deletion of *rpoN* is able to suppress lethality of the double mutant Δ*divJ* $cckA_{Y514}$.
To identify PleC regulators, we could insert Tn in the Δ*divJ* Δ*pleC* $cckA_{Y514D}$ strain and then transform the mutant library with a plasmid expressing *pleC* under the control of its endogenous promoter. The clones able to grow with a functional copy of *pleC* should harbor a Tn insertion into a positive regulator of PleC.

4.4.2. Tn-Seq

Given the reliability of our Tn-Seq data according to the literature, we can expect to identify novel regulators of the CtrA and/or TacA pathways. Note that there were some discrepancies between the genes that were defined as essential between our experiment and the one made by Christen and colleagues. These variations are dependent on the criteria chosen to assign a gene to be essential or not. A majority of the genes that were not categorized as essential in one analysis had low average transposon insertions per basepair. In our case and half of the genes that were not found as essential in our experiment were classified as "high fitness" in Christen's work. Moreover, it is known that essential genes can accept transposon insertions raising the question where to put the threshold for the attribution of the essentiality to a certain gene. Similarly, Curtis and Brun performed a Tn-Seq analysis on *Caulobacter* and other alphaproteobacteria to identify the pool of essential genes in alphaproteobacteria (Curtis & Brun, 2014). They classified the genes of those bacteria in three different groups: essential, unresolved and non-essential. The "unresolved" group is similar to the "high fitness" category of Christen where Tn insertions were tolerated but highly underrepresented. In this category, they also found genes considered as essential or non-essential in Christen and colleagues. In conclusion, determining a gene as essential essentially relies on criteria that are uneasy to be

defined. Nevertheless, our Tn-Seq analysis widely overlaps conclusions made in previous studies.

The *pleC* gene shows a very particular transposon insertion profile in the Δ*divJ* strain with a highly increased amount of insertions along the whole gene except in the ATPase domain coding region (**Figure 28**). Several hypotheses could explain this heterogeneous Tn insertions. First, $PleC_K$ participates to the phosphorylation of DivK at the G1-S transition and deletion of the ATPase domain affects the kinase activity of PleC, so that it becomes lethal in a Δ*divJ* background. The DivK-P levels should be decreased to a point that is not viable for the cell. Alternatively, deletion of the ATPase domain increases the phosphatase activity of PleC, leading to the complete dephosphorylation of DivK-P in a Δ*divJ* background. It is also known that PleC, harboring multiple PAS domains, shows a ten-fold increased affinity for DivK-P compared to DivK (Childers et al., 2014). It has been shown for DivL, that the PAS domains are necessary for discrimination between DivK-P and DivK because they induce a certain conformation that gives DivL more affinity to DivK-P compared to DivK (Childers et al., 2014). Truncated versions of PleC for every domain should be created to test their respective activities and interaction with PleD and DivK by in vitro kinase assays and ITC, respectively.

MmpA is a metalloprotease embedded into the membrane and involved in the shedding of the localization factor of PleC, PodJ, at the G1-S transition after the PerP-dependent processing of PodJ (J. C. Chen et al., 2006). A strong decrease of Tn insertions into *mmpA* was found in the Δ*divJ* strain compared to the wild-type (**Table 1**), suggesting that a constitutive polar localization of PleC would interfere with its activities. This effect could be particularly critical in strains sensitive for DivK-P like Δ*divJ*. Indeed, a Δ*perP* mutant, constitutively localizing PodJ, showed similar activity of CtrA-dependent promoters (J. C. Chen et al., 2006).

The PTS^{NTR}, by its stimulatory effect on (p)ppGpp production, and the PST are two regulatory pathways described as having a positive effect on the protein abundance of CtrA. It has been shown that (p)ppGpp accumulation delays G1-S transition (Ronneau et al., 2016). Reducing the import of phosphate into the cell or the production of (p)ppGpp should therefore have a negative impact on CtrA. A Δ*divJ* mutant known for harbor hyperactivated CtrA should therefore benefit from these mutations. These results, together with the results of the genes implicated in the proteolytic degradation of CtrA, strongly suggest that the regulation of the CtrA abundance is critical in a Δ*divJ* mutant. This is not surprising because it is already known for a long time that CtrA regulation by dephosphorylation and proteolytic degradation is critical for the cell. In agreement with this idea, Δ*rcdA* was found to be synthetic with Δ*divJ* (Petit, 2012).
The downregulation of the PST could also be beneficial for Δ*divJ* cells by reducing the phosphate pool in the cell and therefore impact the ATP-dependent processes like CtrA phosphorylation.
The PTS^{NTR} was recently shown to regulate the PST through HPr (Petit, 2017). Indeed, the phosphorylation of HPr on its Histidine 18 by EI^{NTR} likely decreases the PhoB activity. This is counteracted by HprK that phosphorylates HPr on its Serine 49, which inhibits phosphorelay on His (Petit, 2017). HPr^{Ser49}-P might therefore prevent the inhibition of the PST by the PTS^{NTR}.

The Tn-Seq analysis also showed that disruption of the PTS^{NTR} is detrimental for the Δ*divJ* strain suggesting an alternative repressive role of this system on the CtrA pathway independent of (p)ppGpp (**Table 2**). To investigate this hypothesis, CtrA-dependent promoter activity should be tested in mutants for the PTS^{NTR} in $spoT^+$ and Δ*spoT* background.

Finally, the results from the Tn-Seq experiment in Δ*divJ* strain and the transpositional screen in Δ*divJ*Δ*pleC cckA*$_{Y514D}$ suggest the growth defects in this strain is due, at least partially, to a hyper-activation of the TacA regulon rather than a hyper-activation of CtrA-P. Indeed, both *tacA* and *rpoN* accumulated Tn insertions in Δ*divJ* (**Table 1**).

On the other hand, the data obtained for the *cckA*$_{Y514D}$ mutant showed some conflicting results incompatible with a hyper-activation of CtrA-P. This mutation is known to be synthetically lethal with a reduction of DivK-P (Lori et al., 2015) since DivK-P constitutes the only way to inhibit CtrA (**Figure 23**). It is therefore possible that disrupting positive but indirect actors of DivK will not be sufficient to induce a growth defect in the cell resulting in a similar transposition rate as the WT. For example, it was thought that a *spmX* deletion in this background would have been counterselected but it appears that the transposition rate is similar to the wild-type (**Table 1**). Indeed, it has been shown that a Δ*spmX* mutant sustains a greater phosphorylation state of DivK compared to the Δ*divJ* strain (28% ± 4 and 9% ±2, respectively) (Radhakrishnan et al., 2008). This is also supported by the fact that very few genes have a two-fold ratio difference between this strain and the wild-type meaning that these strains are similar (**Supplementary table 2**). Nevertheless, a potentially interesting candidate is the CCNA_03525 gene coding for a hypothetical protein, which showed a 5-fold decrease in Tn insertions compared to the wild-type.

5. Material and Methods

5.1. *Caulobacter crescentus* growth conditions

All the *Caulobacter crescentus* strains used in this study are derived from the wild-type strain NA1000 and were grown at 30°C in Peptone-Yeast Extract (PYE) broth. The *E. coli* strains were grown in Luria Bertani (LB) broth. A list of the strains, plasmids and primers used in this study can be found in the supplementary table 3-4, 5 and 6 respectively. The method of strains and plasmids construction can be found in the supplementary materials and methods.

5.2. Attachment assay

Overnight cultures were diluted in 96-wells microplate and incubated for 18 to 24 h. Absorbance for the optical density (OD) at 630 nm was taken (OD^{630}). The medium containing the unattached cells was then discarded and the microplate was washed with dH_2O. Crystal Violet 0,1% (CV) was then added for 15 with shaking (200 rmp) in order to stain the attaching bacteria. The wells were then washed with dH_2O and the CV was then re-dissolved in a 20% Acetic acid solution by incubation for 15 min with shaking (200 rpm). Finally, the absorbance the OD at 595 nm was taken (OD^{595}). In order to normalize attachment to growth, the ration between OD^{595} and OD^{630} was taken. The average of that value for the 12 replicates per condition was taken and normalized to the WT to express the relative attachment efficiency of each mutant.

5.3. Phage sensitivity assay

A fraction of the overnight cultures (200 µl) was transferred into 4ml of PYE TOP Agar (0,45 %) and plated onto a PYE Agar medium. Different dilutions of the CBK (LHR1) & Cr30 (LHR2) phage solutions were made and spotted (5 µl) onto the petri dish. The plate was then incubated at 30°C for a period of 16 to 18 h to visualize the efficiency of infection of the phages for each strain.

5.4. Motility assay

The motility of each strain was evaluated by picking their respective overnight culture into a PYE Swarmer Agar (0,30 %) plate and incubated at 30°C for 3 to 4 days. The motility of each strain was quantified by measuring the area of the swarm colonies for each strain. The motility of each strain was normalized to the WT to express the relative motility of the mutants.

5.5. ß-galactosidase assay

A fraction of an exponential phase culture at OD^{660} ~0.3 - 0.5 (50 µl) is permeabilized with chloroform (50 µl). Z-buffer is added to get a final volume of 800 µl. The reaction starts when the substrate o-nitrophenyl-ß-D-galactoside (ONPG) is added in excess. After Incubation at 30° C, the reaction is stopped by raising the pH to 11 and inactivating the enzyme with Na2CO3 1M when the solution becomes medium-yellow. The Product of the reaction (o-nitrophenol) is measured by its absorption at 420 nm. The absorption at 660 nm is measured on the cell culture. In order to quantify the promoter activity and normalize the enzymatic activity to the growth, the following formula was used:

t: reaction time (min)

v: volume of culture used in assay (ml)

$$M.U. = \frac{DO^{420} \times 1000}{DO^{*} \times t \times v}$$

DO: OD^{660}

M.U.: Miller Units

The average of that value for the 4 replicates was taken for each condition and normalized to the WT.

5.6. *Caulobacter crescentus* synchronization

Exponential phase culture at OD^{660} ~0.6 – 0.9 was centrifuged and resuspended into a final volume of 40 ml ice-cold PO_4^{3-} buffer. An ice-cold solution of Ludox (Sigma; Ref - 420808) was added afterwards and the solution was centrifuged at 9500 RPM for 35min at 4°C to achieve a density gradient separating the denser swarmer cells from the stalked and predivisional cells. The swarmer fraction (G1 bacteria) was then harvested and different washing steps were performed to remove the Ludox by centrifugation at 8000 rpm for 10 min at 4°C, resuspend the cells into ice-cold PO_4^{3-} buffer and remove the supernatant. Finally, the culture is put at a OD^{660} of 0.3.

5.7. Western Blot

Protein extraction was done by resuspending the bacterial pellet into a SDS-loading buffer solution (The volume, expressed in µl, of resuspension is obtained by measuring the OD^{660} of the cell culture and multiplying it by 100). Afterwards, the samples were heated at 95°C for 10 min and 20 µl of each was loaded into a 12% acrylamide gel for SDS-PAGE. The proteins were the transferred on a nitrocellulose membrane which was then blocked for ~ 12 – 14 h in PBS tween 5% milk. The proteins were probed with the appropriate primary and secondary, HRP-labeled, antibody. The list of primary and secondary antibodies for each protein can be found in the supplementary data. Signals were detected using the Clarity™ Western ECL Blotting Substrates (BIO RAD, ref: 1705061).

5.8. Transposition experiment

Transposition of the desired strain was done biparental mating between the S17 *E. coli* strain harboring a plasmid with the hyperactive transposase Tn5 *PxylX* carrying a kanamycin resistance cassette adapted from (christen et al 2011). Stationary phase cultures from the S17 *E. coli* strain and the candidate *Caulobacter* strain were mixed together (50 and 950 µl of each respectively). The cells were then centrifugated and resuspended in 50 µl of fresh PYE. The resuspension was spotted onto a PYE_{Agar} plate and incubated for 4 hours at 30°C. After that, the spot was resuspended in 5 ml PYE and 100 µl was plated onto PYE_{Agar} plates supplemented with naledixic acid and kanamycin. Preliminary testing for the efficiency of transposition determined the number of matings that had to be done and resuspended in 5 ml of PYE to get an average of 10 000 clones per plate. For the Tn-Seq experiment, an average of 300 000 clones per condition was achieved. The suppressor screen was performed with the same principle on approximately 200 000 clones.

5.9. Tn-Seq analysis

After sequencing, the obtained data was processed in order to analyze the results of the experiment. First, a qualitative analysis of the data was performed using the FasQC software (Andrews, 2010). After that, truncation of the first and last five bases of every read was done since the beginning and end of sequencing data present often quality defaults.
All the reads were then mapped on the genome of the NA1000 Caulobacter crescentus strain using the Burrows-Wheeler Aligner algorithm (Li & Durbin, 2010) and were given the coordinate of the nucleotide where the insertion took place. The reads were then ordered following the coordinate of insertion site and every read inserted at the same coordinate were added together. Finally, for each strain, a sum of all the reads was performed for every gene on its total region and the 80 inner percent of the region. The reason for this is that it is known that essential genes can support transposon insertions at the beginning and end of the coding sequence, therefore by removing the first and last ten percent of the gene, more accurate conclusions can be drawn from this experiment in regard to the essentiality of a gene in a certain condition. Moreover, because of the sensitivity of the analysis a lower threshold for acceptance of a unique insertion site had to be decided to eliminate background noise. This lower threshold was set to a minimum of 5 reads in order to consider this site as a unique insertion site.
Finally, to identify the essentiality of a gene at the scale of a region, the sliding window/R200 approach was used described by (Solaimanpour et al., 2015). Shortly, we measure the number of insertions found in window of a fixed size, here chosen 200, and let this window slide on

the whole genome by making it move forward 5 bases at the time. This will enable us to know where the transposon insertions took place in a certain gene with a resolution equal to the size of the window (here 200bp).
To compare the results obtained for each gene between the wild-type and the Δ*divJ* or $cckA_{Y514D}$ strain, a normalization of the reads per gene was performed by calculating the ratio between the number of reads from the reference and the condition. The number of reads per gene from the condition was then multiplied by this ratio to avoid irrelevant differences simply because the transposition events between the strains were not equal.
The aim is to analyze the ratio for transposon insertion per gene between the condition (Δ*divJ* or $cckA_{Y514D}$) and the reference (WT) to identify varying ratios.
Before that, a subtraction of the number of reads per gene between the condition and the WT was done in order to eliminate extreme ratios caused by a very low amount of transposon insertions in each strain. A Δ of 100 as a threshold was taken.
Finally, the genes with a 1,5-fold enrichment or impoverishment in transposon insertions compared to the WT were analyzed and a list of candidates was created.
To graphically visualize this difference, we plotted every unique insertion site with the amount of transposon insertions along the genome for each condition against the WT. In addition, we also graphically represented the ΔR200 to visualize the enrichment/impoverishment of transposon insertion for a specific region of the gene in every condition compared to the WT.

6. References

Aakre, C. D., Phung, T. N., Huang, D., & Laub, M. T. (2013). A bacterial toxin inhibits DNA replication elongation through a direct interaction with the β sliding clamp. *Molecular cell, 52*(5), 617-628.

Abel, S., Bucher, T., Nicollier, M., Hug, I., Kaever, V., zur Wiesch, P. A., & Jenal, U. (2013). Bi-modal distribution of the second messenger c-di-GMP controls cell fate and asymmetry during the caulobacter cell cycle. *PLoS genetics, 9*(9), e1003744.

Abel, S., Chien, P., Wassmann, P., Schirmer, T., Kaever, V., Laub, M. T., . . . Jenal, U. (2011). Regulatory cohesion of cell cycle and cell differentiation through interlinked phosphorylation and second messenger networks. *Molecular cell, 43*(4), 550-560.

Aldridge, P., Paul, R., Goymer, P., Rainey, P., & Jenal, U. (2003). Role of the GGDEF regulator PleD in polar development of Caulobacter crescentus. *Molecular microbiology, 47*(6), 1695-1708.

Andrews, S. (2010). FastQC: a quality control tool for high throughput sequence data. In.

Ardissone, S., Fumeaux, C., Bergé, M., Beaussart, A., Théraulaz, L., Radhakrishnan, S. K., . . . Viollier, P. H. (2014). Cell cycle constraints on capsulation and bacteriophage susceptibility. *Elife, 3*, e03587.

Beaufay, F., Coppine, J., Mayard, A., Laloux, G., De Bolle, X., & Hallez, R. (2015). A NAD-dependent glutamate dehydrogenase coordinates metabolism with cell division in Caulobacter crescentus. *The EMBO journal, 34*(13), 1786-1800.

Bhat, N. H., Vass, R. H., Stoddard, P. R., Shin, D. K., & Chien, P. (2013). Identification of ClpP substrates in Caulobacter crescentus reveals a role for regulated proteolysis in bacterial development. *Molecular microbiology, 88*(6), 1083-1092.

Biondi, E. G., Reisinger, S. J., Skerker, J. M., Arif, M., Perchuk, B. S., Ryan, K. R., & Laub, M. T. (2006). Regulation of the bacterial cell cycle by an integrated genetic circuit. *Nature, 444*(7121), 899-904.

Biondi, E. G., Skerker, J. M., Arif, M., Prasol, M. S., Perchuk, B. S., & Laub, M. T. (2006). A phosphorelay system controls stalk biogenesis during cell cycle progression in Caulobacter crescentus. *Molecular microbiology, 59*(2), 386-401.

Bodenmiller, D., Toh, E., & Brun, Y. V. (2004). Development of surface adhesion in Caulobacter crescentus. *Journal of bacteriology, 186*(5), 1438-1447.

Bogyo, M., McMaster, J. S., Gaczynska, M., Tortorella, D., Goldberg, A. L., & Ploegh, H. (1997). Covalent modification of the active site threonine of proteasomal β subunits and the Escherichia coli homolog HslV by a new class of inhibitors. *Proceedings of the National Academy of Sciences, 94*(13), 6629-6634.

Brilli, M., Fondi, M., Fani, R., Mengoni, A., Ferri, L., Bazzicalupo, M., & Biondi, E. G. (2010). The diversity and evolution of cell cycle regulation in alpha-proteobacteria: a comparative genomic analysis. *BMC systems biology, 4*(1), 52.

Brun, Y. V., & Shapiro, L. (1992). A temporally controlled sigma-factor is required for polar morphogenesis and normal cell division in Caulobacter. *Genes & development, 6*(12a), 2395-2408.

Chen, J. C., Hottes, A. K., McAdams, H. H., McGrath, P. T., Viollier, P. H., & Shapiro, L. (2006). Cytokinesis signals truncation of the PodJ polarity factor by a cell cycle-regulated protease. *The EMBO journal, 25*(2), 377-386.

Chen, J. C., Viollier, P. H., & Shapiro, L. (2005). A membrane metalloprotease participates in the sequential degradation of a Caulobacter polarity determinant. *Molecular microbiology, 55*(4), 1085-1103.

Chen, Y. E., Tropini, C., Jonas, K., Tsokos, C. G., Huang, K. C., & Laub, M. T. (2011). Spatial gradient of protein phosphorylation underlies replicative asymmetry in a bacterium. *Proceedings of the National Academy of Sciences, 108*(3), 1052-1057.

Chen, Y. E., Tsokos, C. G., Biondi, E. G., Perchuk, B. S., & Laub, M. T. (2009). Dynamics of two Phosphorelays controlling cell cycle progression in Caulobacter crescentus. *Journal of bacteriology, 191*(24), 7417-7429.

Childers, W. S., Xu, Q., Mann, T. H., Mathews, I. I., Blair, J. A., Deacon, A. M., & Shapiro, L. (2014). Cell fate regulation governed by a repurposed bacterial histidine kinase. *PLoS biology, 12*(10), e1001979.

Christen, B., Abeliuk, E., Collier, J. M., Kalogeraki, V. S., Passarelli, B., Coller, J. A., . . . Shapiro, L. (2011). The essential genome of a bacterium. *Molecular systems biology, 7*(1), 528.

Collier, J., McAdams, H. H., & Shapiro, L. (2007). A DNA methylation ratchet governs progression through a bacterial cell cycle. *Proceedings of the National Academy of Sciences, 104*(43), 17111-17116.

Collier, J., Murray, S. R., & Shapiro, L. (2006). DnaA couples DNA replication and the expression of two cell cycle master regulators. *The EMBO journal, 25*(2), 346-356.

Curtis, P. D., & Brun, Y. V. (2014). Identification of essential alphaproteobacterial genes reveals operational variability in conserved developmental and cell cycle systems. *Molecular microbiology, 93*(4), 713-735.

Curtis, P. D., Quardokus, E. M., Lawler, M. L., Guo, X., Klein, D., Chen, J. C., . . . Brun, Y. V. (2012). The scaffolding and signalling functions of a localization factor impact polar development. *Molecular microbiology, 84*(4), 712-735.

Domian, I. J., Quon, K. C., & Shapiro, L. (1997). Cell type-specific phosphorylation and proteolysis of a transcriptional regulator controls the G1-to-S transition in a bacterial cell cycle. *Cell, 90*(3), 415-424.

Duerig, A., Abel, S., Folcher, M., Nicollier, M., Schwede, T., Amiot, N., . . . Jenal, U. (2009). Second messenger-mediated spatiotemporal control of protein degradation regulates bacterial cell cycle progression. *Genes & development, 23*(1), 93-104.

Edwards, P., & Smit, J. (1991). A transducing bacteriophage for Caulobacter crescentus uses the paracrystalline surface layer protein as a receptor. *Journal of bacteriology, 173*(17), 5568-5572.

Fioravanti, A., Fumeaux, C., Mohapatra, S. S., Bompard, C., Brilli, M., Frandi, A., . . . Biondi, E. G. (2013). DNA binding of the cell cycle transcriptional regulator GcrA depends on N6-adenosine methylation in Caulobacter crescentus and other Alphaproteobacteria. *PLoS genetics, 9*(5), e1003541.

Fumeaux, C., Radhakrishnan, S. K., Ardissone, S., Théraulaz, L., Frandi, A., Martins, D., . . . Viollier, P. H. (2014). Cell cycle transition from S-phase to G1 in Caulobacter is mediated by ancestral virulence regulators. *Nature communications, 5*.

Gonin, M., Quardokus, E. M., O'Donnol, D., Maddock, J., & Brun, Y. V. (2000). Regulation of stalk elongation by phosphate inCaulobacter crescentus. *Journal of bacteriology, 182*(2), 337-347.

Guerrero-Ferreira, R. C., Viollier, P. H., Ely, B., Poindexter, J. S., Georgieva, M., Jensen, G. J., & Wright, E. R. (2011). Alternative mechanism for bacteriophage adsorption to the motile bacterium Caulobacter crescentus. *Proceedings of the National Academy of Sciences, 108*(24), 9963-9968.

Hallez, R., Bellefontaine, A.-F., Letesson, J.-J., & De Bolle, X. (2004). Morphological and functional asymmetry in α-proteobacteria. *Trends in microbiology, 12*(8), 361-365.

Hinz, A. J., Larson, D. E., Smith, C. S., & Brun, Y. V. (2003). The Caulobacter crescentus polar organelle development protein PodJ is differentially localized and is required for polar targeting of the PleC development regulator. *Molecular microbiology, 47*(4), 929-941.

Hsing, W., Russo, F. D., Bernd, K. K., & Silhavy, T. J. (1998). Mutations that alter the kinase and phosphatase activities of the two-component sensor EnvZ. *Journal of bacteriology, 180*(17), 4538-4546.

Iniesta, A. A., Hillson, N. J., & Shapiro, L. (2010). Cell pole–specific activation of a critical bacterial cell cycle kinase. *Proceedings of the National Academy of Sciences, 107*(15), 7012-7017.

Iniesta, A. A., McGrath, P. T., Reisenauer, A., McAdams, H. H., & Shapiro, L. (2006). A phospho-signaling pathway controls the localization and activity of a protease complex critical for bacterial cell cycle progression. *Proceedings of the National Academy of Sciences, 103*(29), 10935-10940.

Iniesta, A. A., & Shapiro, L. (2008). A bacterial control circuit integrates polar localization and proteolysis of key regulatory proteins with a phospho-signaling cascade. *Proceedings of the National Academy of Sciences, 105*(43), 16602-16607.

Janakiraman, B., Mignolet, J., Narayanan, S., Viollier, P. H., & Radhakrishnan, S. K. (2016). In-phase oscillation of global regulons is orchestrated by a pole-specific organizer. *Proceedings of the National Academy of Sciences, 113*(44), 12550-12555.

Joshi, K. K., Bergé, M., Radhakrishnan, S. K., Viollier, P. H., & Chien, P. (2015). An adaptor hierarchy regulates proteolysis during a bacterial cell cycle. *Cell, 163*(2), 419-431.

Joshi, K. K., & Chien, P. (2016). Regulated proteolysis in bacteria: caulobacter. *Annual review of genetics, 50*, 423-445.

Lam, H., Matroule, J.-Y., & Jacobs-Wagner, C. (2003). The asymmetric spatial distribution of bacterial signal transduction proteins coordinates cell cycle events. *Developmental cell, 5*(1), 149-159.

Laub, M. T., Chen, S. L., Shapiro, L., & McAdams, H. H. (2002). Genes directly controlled by CtrA, a master regulator of the Caulobacter cell cycle. *Proceedings of the National Academy of Sciences, 99*(7), 4632-4637.

Levi, A., & Jenal, U. (2006). Holdfast formation in motile swarmer cells optimizes surface attachment during Caulobacter crescentus development. *Journal of bacteriology, 188*(14), 5315-5318.

Li, H., & Durbin, R. (2010). Fast and accurate long-read alignment with Burrows–Wheeler transform. *Bioinformatics, 26*(5), 589-595.

Lori, C., Ozaki, S., Steiner, S., Böhm, R., Abel, S., Dubey, B. N., . . . Jenal, U. (2015). Cyclic di-GMP acts as a cell cycle oscillator to drive chromosome replication. *Nature, 523*(7559), 236-239.

Lubin, E. A., Henry, J. T., Fiebig, A., Crosson, S., & Laub, M. T. (2016). Identification of the PhoB regulon and role of PhoU in the phosphate starvation response of Caulobacter crescentus. *Journal of bacteriology, 198*(1), 187-200.

Mähönen, A. P. (2005). Cytokinins regulate vascular morphogenesis in the Arabidopsis thaliana root.

Matroule, J.-Y., Lam, H., Burnette, D. T., & Jacobs-Wagner, C. (2004). Cytokinesis monitoring during development: rapid pole-to-pole shuttling of a signaling protein by localized kinase and phosphatase in Caulobacter. *Cell, 118*(5), 579-590.

Meier, E. L., Daitch, A. K., Yao, Q., Bhargava, A., Jensen, G. J., & Goley, E. D. (2017). FtsEX-mediated regulation of the final stages of cell division reveals morphogenetic plasticity in Caulobacter crescentus. *PLoS genetics, 13*(9), e1006999.

Paul, R., Abel, S., Wassmann, P., Beck, A., Heerklotz, H., & Jenal, U. (2007). Activation of the diguanylate cyclase PleD by phosphorylation-mediated dimerization. *Journal of biological chemistry, 282*(40), 29170-29177.

Paul, R., Jaeger, T., Abel, S., Wiederkehr, I., Folcher, M., Biondi, E. G., . . . Jenal, U. (2008). Allosteric regulation of histidine kinases by their cognate response regulator determines cell fate. *Cell, 133*(3), 452-461.

Petit, K. (2012). *Identification d'acteurs du cycle cellulaire de Caulobacter crescentus au moyen d'un crible de létalité synthétique* (Master), Univerity of Namur,

Petit, K. (2017). *Deciphering the PTS_NTR regulatory functions in Caulobacter crescentus: a pathway controlling the cell cycle according to nutrient availability.* University of Namur,

Pierce, D. L., O'Donnol, D. S., Allen, R. C., Javens, J. W., Quardokus, E. M., & Brun, Y. V. (2006). Mutations in DivL and CckA rescue a divJ null mutant of Caulobacter crescentus by reducing the activity of CtrA. *Journal of bacteriology, 188*(7), 2473-2482.

Radhakrishnan, S. K., Thanbichler, M., & Viollier, P. H. (2008). The dynamic interplay between a cell fate determinant and a lysozyme homolog drives the asymmetric division cycle of Caulobacter crescentus. *Genes & development, 22*(2), 212-225.

Reisinger, S. J., Huntwork, S., Viollier, P. H., & Ryan, K. R. (2007). DivL performs critical cell cycle functions in Caulobacter crescentus independent of kinase activity. *Journal of bacteriology, 189*(22), 8308-8320.

Ronneau, S., Petit, K., De Bolle, X., & Hallez, R. (2016). Phosphotransferase-dependent accumulation of (p) ppGpp in response to glutamine deprivation in Caulobacter crescentus. *Nature communications, 7*.

Sanselicio, S., Bergé, M., Théraulaz, L., Radhakrishnan, S. K., & Viollier, P. H. (2015). Topological control of the Caulobacter cell cycle circuitry by a polarized single-domain PAS protein. *Nature communications, 6*.

Sciochetti, S. A., Lane, T., Ohta, N., & Newton, A. (2002). Protein sequences and cellular factors required for polar localization of a histidine kinase in Caulobacter crescentus. *Journal of bacteriology, 184*(21), 6037-6049.

Shi, H., Colavin, A., Bigos, M., Tropini, C., Monds, R. D., & Huang, K. C. (2017). Deep phenotypic mapping of bacterial cytoskeletal mutants reveals physiological robustness to cell size. *Current Biology*.

Smith, C. S., Hinz, A., Bodenmiller, D., Larson, D. E., & Brun, Y. V. (2003). Identification of genes required for synthesis of the adhesive holdfast in Caulobacter crescentus. *Journal of bacteriology, 185*(4), 1432-1442.

Solaimanpour, S., Sarmiento, F., & Mrázek, J. (2015). Tn-seq explorer: a tool for analysis of high-throughput sequencing data of transposon mutant libraries. *PloS one, 10*(5), e0126070.

Sprecher, K. S., Hug, I., Nesper, J., Potthoff, E., Mahi, M.-A., Sangermani, M., . . . Jenal, U. (2017). Cohesive Properties of the Caulobacter crescentus Holdfast Adhesin Are Regulated by a Novel c-di-GMP Effector Protein. *mBio, 8*(2), e00294-00217.

Subramanian, K., Paul, M. R., & Tyson, J. J. (2013). Potential role of a bistable histidine kinase switch in the asymmetric division cycle of Caulobacter crescentus. *PLoS computational biology, 9*(9), e1003221.

Subramanian, K., Paul, M. R., & Tyson, J. J. (2015). Dynamical localization of DivL and PleC in the asymmetric division cycle of caulobacter crescentus: a theoretical investigation of alternative models. *PLoS computational biology, 11*(7), e1004348.

Tsokos, C. G., & Laub, M. T. (2012). Polarity and cell fate asymmetry in Caulobacter crescentus. *Current opinion in microbiology, 15*(6), 744-750.

Tsokos, C. G., Perchuk, B. S., & Laub, M. T. (2011). A dynamic complex of signaling proteins uses polar localization to regulate cell-fate asymmetry in Caulobacter crescentus. *Developmental cell, 20*(3), 329-341.

Viollier, P. H., Sternheim, N., & Shapiro, L. (2002). A dynamically localized histidine kinase controls the asymmetric distribution of polar pili proteins. *The EMBO journal, 21*(17), 4420-4428.

Wheeler, R. T., & Shapiro, L. (1999). Differential localization of two histidine kinases controlling bacterial cell differentiation. *Molecular cell, 4*(5), 683-694.

Wortinger, M., Sackett, M. J., & Brun, Y. V. (2000). CtrA mediates a DNA replication checkpoint that prevents cell division in Caulobacter crescentus. *The EMBO journal, 19*(17), 4503-4512.

Wright, R., Stephens, C., Zweiger, G., Shapiro, L., & Alley, M. (1996). Caulobacter Lon protease has a critical role in cell-cycle control of DNA methylation. *Genes & development, 10*(12), 1532-1542.

Wu, J., Ohta, N., Zhao, J.-L., & Newton, A. (1999). A novel bacterial tyrosine kinase essential for cell division and differentiation. *Proceedings of the National Academy of Sciences, 96*(23), 13068-13073.

Supplementary data

1. Supplementary tables

Table 1: List of potential candidates for the cckA$_{Y514D}$ strain. The data in the "Essential genome" column is extracted from the analysis done by Christen and colleagues on the essential genome of Caulobacter crescentus (Christen et al., 2011).

CCNA	Function	Essential genome	WT	CckA_Y514D	ratio
CCNA_R0093	Minimal medium sRNA	NA	134	0,00	0,00
CCNA_03525	hypothetical protein	High_Fitness_Costs	1177	214,64	0,18
CCNA_02251	methylglutaconyl-CoA hydratase	Nonessential	206	39,79	0,20
CCNA_00240	PTS system, IIA component	Nonessential	404	80,79	0,20
CCNA_03496	cytosolic protein	Nonessential	1504	323,16	0,22
CCNA_03762	hypothetical protein	Nonessential	244	51,85	0,22
CCNA_01456	hypothetical protein	Nonessential	530	122,99	0,23
CCNA_02521	endonuclease involved in recombination	High_Fitness_Costs	201	48,23	0,24
CCNA_01061	type I secretion adaptor protein RsaE	Nonessential	214	51,85	0,25
CCNA_00147	hypothetical protein	Nonessential	920	233,93	0,26
CCNA_02030	hypothetical protein	High_Fitness_Costs	137	34,97	0,26
CCNA_00374	putative ATP synthase protein I	Nonessential	556	153,14	0,28
CCNA_00315	3-polyprenyl-4-hydroxybenzoate decarboxylase	Nonessential	496	145,90	0,30
CCNA_00540	coproporphyrinogen III oxidase	Nonessential	619	201,37	0,33
CCNA_03516	protoheme IX farnesyltransferase coxE	Nonessential	541	183,28	0,34
CCNA_01060	type I protein secretion ATP-binding protein RsaD	High_Fitness_Costs	430	151,93	0,35
CCNA_01280	hypothetical protein	High_Fitness_Costs	2237	800,66	0,36
CCNA_00243	hypothetical protein	Nonessential	1837	672,85	0,37
CCNA_02433	hypothetical protein	Nonessential	1783	729,52	0,41
CCNA_01012	atrazine chlorohydrolase	Nonessential	1116	457,01	0,41
CCNA_00543	methyl-accepting chemotaxis protein	Nonessential	1056	437,71	0,42
CCNA_00888	hypothetical protein	Nonessential	1094	455,80	0,42
CCNA_03775	hypothetical protein	Nonessential	2055	883,87	0,43
CCNA_00127	hypothetical protein	Nonessential	443	190,52	0,43
CCNA_02088	HesB protein family	Nonessential	345	149,52	0,44
CCNA_00257	adenosylhomocysteinase	Nonessential	1041	453,39	0,44
CCNA_00847	leucine-responsive regulatory protein	Nonessential	1328	584,82	0,44
CCNA_03604	hypothetical protein	Nonessential	1581	698,17	0,44
CCNA_02021	hypothetical protein	Nonessential	354	157,96	0,45
CCNA_01178	oxidoreductase	Nonessential	2100	940,54	0,45
CCNA_02335	myo-inositol-1(or 4)-monophosphatase	Nonessential	623	279,75	0,45
CCNA_03357	hypothetical protein	High_Fitness_Costs	428	194,14	0,45
CCNA_01562	4-hydroxy-2-oxoglutarate aldolase/2-dehydro-3-deoxyphosphogluconate aldolase	Nonessential	264	120,58	0,46
CCNA_00217	thiol:disulfide interchange protein DsbD	High_Fitness_Costs	677	315,92	0,47
CCNA_01521	hypothetical protein	Nonessential	1490	705,40	0,47
CCNA_02250	methylcrotonyl-CoA carboxylase biotin-containing subunit	Nonessential	1899	899,54	0,47
CCNA_00498	hypothetical protein	Nonessential	607	288,19	0,48
CCNA_01176	hypothetical protein	Nonessential	643	306,28	0,48
CCNA_R0063	Minimal medium sRNA	NA	554	265,28	0,48
CCNA_01910	thymidylate kinase	Nonessential	1418	684,91	0,48
CCNA_00541	hypothetical protein	Nonessential	958	463,03	0,48
CCNA_00953	flagellar motor switch protein FliN	Nonessential	742	362,95	0,49
CCNA_02517	hypothetical protein	Nonessential	1736	851,31	0,49
CCNA_02272	hypothetical protein	Nonessential	2581	1280,58	0,50
CCNA_00189	cytosolic protein	Nonessential	477	236,34	0,50
CCNA_01421	6,7-dimethyl-8-ribityllumazine synthase	High_Fitness_Costs	270	133,85	0,50
CCNA_02468	hypothetical protein	Nonessential	1001	498,00	0,50

Table 2: List of potential candidates for the ΔdivJ strain. The data in the "Essential genome" column is extracted from the analysis done by Christen and colleagues on the essential genome of Caulobacter crescentus (Christen et al., 2011).

CCNA	Function	Essential genome	WT	ΔdivJ	ratio
CCNA_00748	ferrous iron transport protein A	essential	0	270,479441	271,479441
CCNA_01324	LSU ribosomal protein L30P	Nonessential	0	213,712151	214,712151
CCNA_00749	ferrous iron transport protein B	essential	0	180,319627	181,319627
CCNA_R0082	tRNA Met	NA	0	180,319627	181,319627
CCNA_03007	L-aspartate oxidase	essential	0	124,665421	125,665421
CCNA_R0064	tRNA Met	NA	0	120,213085	121,213085
CCNA_01332	LSU ribosomal protein L17P	essential	0	116,873832	117,873832
CCNA_01325	LSU ribosomal protein L15P	essential	0	102,403739	103,403739
CCNA_02420	TonB accessory protein exbD	High_Fitness_Costs	6	221,50374	31,7862485
CCNA_00042	cytosolic protein/LSU ribosomal protein L7AE	High_Fitness_Costs	7	205,920562	25,8650703
CCNA_01726	GTP-binding protein	essential	27	656,71963	23,4899868
CCNA_00739	hypothetical protein	Nonessential	6	106,856075	15,4080108
CCNA_R0066	23S RNA	NA	570	6785,36079	11,8850452
CCNA_02231	ABC transporter ATP-binding protein	Nonessential	635	6637,3206	10,437611
CCNA_R0084	23S RNA	NA	641	6610,60658	10,2984526
CCNA_02134	phosphogluconate dehydratase	Nonessential	4472	443,007479	0,09926391
CCNA_02026	hypothetical protein	Nonessential	276	25,6009347	0,09603226
CCNA_03744	dTDP-glucose 4,6-dehydratase	Nonessential	3047	290,514955	0,09564139
CCNA_03651	ATP-dependent nuclease subunit B	Nonessential	4460	416,29346	0,09354258
CCNA_02157	transcriptional regulator	Nonessential	1119	97,9514025	0,08834947
CCNA_03681	ABC transporter ATP-binding protein	High_Fitness_Costs	264	22,2616824	0,08777993
CCNA_03115	cobaltochelatase cobS subunit	essential	1228	91,2728978	0,07507966
CCNA_02335	myo-inositol-1(or 4)-monophosphatase	Nonessential	623	44,5233648	0,07295411
CCNA_01596	DNA helicase II	High_Fitness_Costs	2199	148,040188	0,06774554
CCNA_01918	two-component response regulator	Nonessential	2869	184,771964	0,06472891
CCNA_03577	DNA polymerase I	High_Fitness_Costs	7867	493,096265	0,0627982
CCNA_01210	nucleotidyltransferase family protein	High_Fitness_Costs	139	7,79158883	0,06279706
CCNA_00168	putative capsule polysaccharide export protein	Nonessential	1617	95,7252342	0,05978074
CCNA_00240	PTS system, IIA component	Nonessential	404	21,1485983	0,0546879
CCNA_00667	capsular polysaccharide biosynthesis protein	Nonessential	718	37,84486	0,05402623
CCNA_03031	gamma-D-glutamyl-meso-diaminopimelate peptidase	High_Fitness_Costs	1096	57,8803742	0,053674
CCNA_01521	hypothetical protein	Nonessential	1490	76,8028042	0,05218163
CCNA_01061	type I secretion adaptor protein RsaE	Nonessential	214	10,0177571	0,05124538
CCNA_01864	transcriptional regulator, TetR family	essential	151	6,67850471	0,05051648
CCNA_01943	alpha/beta hydrolase	Nonessential	1046	51,2018695	0,04985852
CCNA_00003	shikimate 5-dehydrogenase	essential	1248	58,9934583	0,04803319
CCNA_02721	peptidase, M16 family	High_Fitness_Costs	1991	89,0467295	0,04520418
CCNA_01686	exopolyphosphatase	High_Fitness_Costs	3292	145,81402	0,04458367
CCNA_00742	hydrolase (HAD superfamily)	Nonessential	1116	47,8626171	0,04374451
CCNA_00708	cobaltochelatase cobT subunit	High_Fitness_Costs	3045	125,778505	0,04162131
CCNA_02572	adenylosuccinate lyase	High_Fitness_Costs	1535	52,3149536	0,03471026
CCNA_02866	hypothetical protein	High_Fitness_Costs	265	7,79158883	0,03305109
CCNA_02151	exodeoxyribonuclease VII small subunit	High_Fitness_Costs	406	11,1308412	0,02980551
CCNA_01618	uracil-DNA glycosylase	essential	1024	27,827103	0,028124
CCNA_02085	anhydromuramoyl-peptide exo-beta-N-acetylglucosaminidase	High_Fitness_Costs	1114	30,0532712	0,02785047
CCNA_02386	O-antigen ligase related enzyme	High_Fitness_Costs	1680	43,4102806	0,02641897
CCNA_00001	ATP/GTP-binding protein	Nonessential	2696	61,2196265	0,02306994
CCNA_00669	hypothetical protein	Nonessential	5135	105,742991	0,02078329
CCNA_02390	phosphoglycolate phosphatase	High_Fitness_Costs	418	6,67850471	0,01832579

CCNA	Function	Essential genome	WT	ΔdivJ	ratio
CCNA_01012	atrazine chlorohydrolase	Nonessential	1116	15,5831777	0,01484618
CCNA_01979	LexA repressor	Nonessential	524	6,67850471	0,01462572
CCNA_03103	shikimate kinase	essential	600	6,67850471	0,01277621
CCNA_02553	ATP-dependent clp protease ATP-binding subunit ClpA	Nonessential	4596	54,5411218	0,01208204
CCNA_00527	hypothetical protein	Nonessential	5116	55,6542059	0,01107176
CCNA_00252	multimodular transpeptidase-transglycosylase PBP 1A	High_Fitness_Costs	1915	14,4700935	0,00807416
CCNA_02251	methylglutaconyl-CoA hydratase	Nonessential	206	0	0,00483092
CCNA_01952	N-acetylmuramoyl-L-alanine amidase	essential	230	0	0,004329
CCNA_03547	peptidoglycan-specific endopeptidase, M23 family	High_Fitness_Costs	2481	7,79158883	0,00354214
CCNA_02042	trigger factor, ppiase	High_Fitness_Costs	389	0	0,0025641
CCNA_03104	3-dehydroquinate synthase	essential	393	0	0,00253807
CCNA_03835	3-oxoacyl-(acyl-carrier-protein) synthase	essential	410	0	0,00243309
CCNA_03356	cytosolic protein "zapA binds to FtsZ"	essential	420	0	0,0023753
CCNA_02941	transcription elongation factor greA	Nonessential	425	0	0,00234742
CCNA_01060	type I protein secretion ATP-binding protein RsaD	High_Fitness_Costs	430	0	0,00232019
CCNA_02135	6-phosphogluconolactonase	Nonessential	498	0	0,00200401
CCNA_02650	anhydro-N-acetylmuramyl-tripeptide amidase	High_Fitness_Costs	645	0	0,00154799
CCNA_03748	dTDP-4-dehydrorhamnose 3,5-epimerase	Nonessential	805	0	0,00124069
CCNA_02300	cell division protein ftsX	essential	887	0	0,00112613
CCNA_03496	cytosolic protein	Nonessential	1504	0	0,00066445
CCNA_02329	exodeoxyribonuclease VII large subunit	High_Fitness_Costs	1738	0	0,00057504
CCNA_02299	cell division ATP-binding protein ftsE	essential	1991	0	0,00050201

Table 3: List of the C. crescentus strains used in this study

Name	Genotype	Reference
RH 50	NA1000	(Evinger & Agabian, 1977)
RH 2085	NA1000 *hfsA*$^+$	J. Coppine (unpublished)
RH 2100	NA1000 *hfsA*$^+$ Δ*pleC*	J. Coppine (unpublished)
RH 2314	NA1000 *hfsA*$^+$ *pleC*$_{H610A}$	This study
	NA1000 *hfsA*$^+$ *pleC*$_{T614R}$	This study
RH 2313	NA1000 *hfsA*$^+$ *pleC*$_{F778L}$	This study
	NA1000 *hfsA*$^+$ *pleC*$_{T792K}$	This study
RH 217	NA1000 Δ*pleC*	R. Hallez
RH 2020	NA1000 *pleC*$_{H610A}$	R. Hallez
	NA1000 *pleC*$_{T614R}$	This study
RH 2021	NA1000 *pleC*$_{F778L}$	R. Hallez
	NA1000 *pleC*$_{T792K}$	This study
	NA1000 *hfsA*$^+$ pRKlac290-PpilA	This study
	NA1000 *hfsA*$^+$ *pleC*$_{H610A}$ pRKlac290-PpilA	This study
	NA1000 *hfsA*$^+$ *pleC*$_{F778L}$ pRKlac290-PpilA	This study
	NA1000 *hfsA*$^+$ pRKlac290-PhvyA-*hvyA*	This study
	NA1000 *hfsA*$^+$ *pleC*$_{H610A}$ pRKlac290-PhvyA-*hvyA*	This study
	NA1000 *hfsA*$^+$ *pleC*$_{F778L}$ pRKlac290-PhvyA-*hvyA*	This study
	NA1000 Δ*pleC hfsA*$^+$ *PvanA::pleC*	This study

	NA1000 *pleC*$_{AA::DD}$	This study
	NA1000 *3Flag-pleC* Δ*cpdR*	This study
RH 1671	NA1000 Δ*socAB*	R. Hallez
RH 1674	NA1000 Δ*socAB* Δ*clpP*	J. Coppine (unpublished)
RH 2279	NA1000 Δ*socAB* Δ*clpX*	J. Coppine (unpublished)
RH 864	NA1000 Δ*clpA*	(Grünenfelder et al., 2004)
RH 339	NA1000 Δ*cpdR*	(Skerker, Prasol, Perchuk, Biondi, & Laub, 2005)
RH 323	NA1000 Δ*rcdA*	(McGrath, Iniesta, Ryan, Shapiro, & McAdams, 2006)
RH 315	NA1000 Δ*popA*	(Duerig et al., 2009)
RH 866	NA1000 Δ*lon*	(Wright, Stephens, Zweiger, Shapiro, & Alley, 1996)
	NA1000 Δ*hslV*	This study
RH 865	NA1000 Δ*ftsH*	(Fischer, Rummel, Aldridge, & Jenal, 2002)
RH 347	NA1000 *cpdR*$_{D51A}$	R. Hallez
	NA1000 Δ*socAB* Δ*clpP PxylX::clpP*	This study
	NA1000 Δ*socAB* Δ*clpX PxylX::clpX*	This study
	NA1000 Δ*socAB* Δ*clpP* Δ*hslV*	This study
	NA1000 Δ*divJ* Δ*pleC cckA*$_{Y514D}$	R. Hallez
RH 2053	NA1000 Δ*pleC cckA*$_{Y514D}$	R. Hallez
	NA1000 Δ*divJ* Δ*pleC cckA*$_{Y514D}$ *rpoN::Tn5*	This study
RH 1827	NA1000 *cckA*$_{Y514D}$	R. Hallez
RH 748	NA1000 Δ*divJ*	R. Hallez

Table 4: List of the E. coli strains used in this study

Name	Genotype	Reference
RH140	S17-1 pNPTS138-*hfsA*$^{+}$	R. Hallez
RH 319	MT607 *pro-82 thi-I hsdR17 (r-m+) supE44 recA56 pRK600*	(Casadaban & Cohen, 1980)
	Top10 pVC6-pleC	This study
RH 1670	Top 10 pNPTS138-Δ*socAB*	R. Hallez
RH 1724	Top 10 pNPTS138-*pleC*$_{F778L}$ (pHR618)	R. Hallez
RH 1959	EC100D pRKlac290-*PpilA*	(Skerker & Shapiro, 2000)
RH 2046	EC100D pRKlac290-*PhvyA-hvyA*	(Ardissone et al., 2014)
RH 2315	Top 10 pNPTS138-*pleC*$_{T614R}$ (pHR890)	This study
RH 2319	Top 10 pNPTS138-*3FLAG-pleC* (pHR893)	This study
	Top 10 pNPTS138-*pleC*$_{T792K}$	This study

RH 2404	Top 10 pNPTS138-Δ*hslV*	J. Coppine (unpublished)

Table 5: List of the plasmids used in this study

Name	Description	Reference
pHR 253	pNPTS138	M. R. Alley, Imperial College London (UK), unpublished
pHR31	pNPTS138-*hfsA*$^{+}$	R. Hallez
pHR 606	pNPTS138-Δ*socAB*	R. Hallez
pHR 616	pMCS-1-*3FLAG_5'*	R. Hallez
pHR 617	pNPTS138-*pleC*$_{H610A}$	R. Hallez
pHR 618	pNPTS138-*pleC*$_{F778L}$	R. Hallez
pHR 890	pNPTS138-*pleC*$_{T614R}$	This study
pHR 893	pNPTS138-*3FLAG-pleC*	This study
	pNPTS138-*pleC*$_{T792K}$	This study
	pRKlac290-*PpilA*	(Skerker & Shapiro, 2000)
	pRKlac290-*PhvyA-hvyA*	(Ardissone et al., 2014)
pHR 947	pNPTS138-Δ*hslV*	This study
	pNPTS138-*pleC*$_{AA::DD}$	This study

Table 6: List of the lysates used in this study

Name	Description
LHR 62	NA1000 Δ*ftsH:: Ω*
LHR 65	NA1000 Δ*clpX::Ω PxylX::clpX*
LHR 66	NA1000 Δ*clpP::Ω PxylX::clpP*
LHR 68	NA1000 Δ*cpdR*

Table 7: list of all the primers used in this study

Name	Sequence
100	gttttcccagtcacgacg
138	gatccaatcttgacgtccgt
174	ggaaacagctatgaccatg
196	ctctggtgctggacaagtgg
197	cgcccacggtttcgatgatc
303	tgaccgcgttctgcagcagg
304	ggtcgccgcgctcgaacaac
639	tgaactcgcgatgggcgacc
848	AAGCTTggtgtttaggaggatgggtc
849	GAATTCagtcagcggaggcatgaatcc

850	GAATTCtgggatggtgattgagcagttg
851	GGATCCgcgccatccactgatcatcg
954	tctgcttaacgatgccGaCg
961	gactacaaagaccatgacggtg
962	ttcatggagcagtacgtcgc
966	acatgatcgacgtgtccgag
983	tcAAGcttgctggcgctgatcaacg
1053	accaacgctacaagggctac
1094	cctaagtaactaaCATATGggcagacacgggggcc
1212	tcGGTACCatgaaagccccaaggccgc
1213	tcGGTACCgccgccacgaagtcgcgag
1235	cgctgaacgccatcaatggc
1252	gttggaacggcgatggacgc
1634	cctaagtaactaaAAGCTTagcctctggtgctggacaag
1635	cctaagtaactaaCATATGgcccttgctcaacgcgcc
1636	cctaagtaactaaGAATTCggcagacacgggggccg
1637	cctaagtaactaaGGATCCacgatccaagctcgtcgtgg
1638	cgaagacgacccagggTaAG
1695	cctaagtaactaaAAGCTTacaacgcaagcatcgctcac
1696	cctaagtaactaaGAATTCttgcccttgacgacggttgg
1697	cctaagtaactaaGAATTcgaaagcctgtaatgaccga
1698	cctaagtaactaaGGATCCagcttcttgcggaacgactc
1699	agacatcgatagcagggctg
1700	tcggccagttgcagttcgac
1701	ctcgcgacttcgtggATgAC

Table 8: List of the primary and secondary antibodies used in this study

Name	Description	Reference
Anti-PleC	Polyclonal Anti-PleC immunoglobulin produced in Rabbit	R. Hallez
Anti-CtrA	Polyclonal Anti-CtrA immunoglobulin produced in Rabbit	R. Hallez
Anti-MreB	olyclonal Anti-MreB immunoglobulin produced in Rabbit	R. Hallez
Anti-M2 (3Flag)	Monoclonal ANTI-FLAG® M2 antibody produced in mouse	Firm: Sigma-Aldrich F1804
Anti-Mouse	Polyclonal Rabbit Anti-Mouse Immunoglobulins/HRP	Firm: Dako P0260
Anti-Rabbit	Polyclonal Swine Anti-Rabbit Immunoglobulins/HRP	Firm: Dako P0217

2. Supplementary materials and methods

2.1. Construction of Caulobacter crescentus strains

- NA1000 *hfsA*$^+$ (RH 2085)

Biparental mating between RH50 (NA1000) and RH140 (S17-1-pNPTS138-*hfsA*$^+$) selected on PYE Nal Kan, streaked on PYE Kan, cultivated o/n in PYE and plated on PYE 3% Suc. SucR candidates patched on PYE Kan and PYE. KanS colonies were tested in an attachment assay.

- NA1000 *hfsA*$^+$ Δ*pleC* (RH 2100)

Biparental mating between RH2085 (NA1000 *hfsA*$^+$) and RH574 (S17-1-pNPTS138-Δ*pleC*) selected on PYE Nal Kan, streaked on PYE Kan, cultivated o/n in PYE and plated on PYE 3% Suc. SucR candidates patched on PYE Kan and PYE. KanS colonies were screened by PCR with primers 196/197 (1368 bp for deletion and 3618 bp for wt).

- NA1000 *hfsA*$^+$ *pleC*$_{H610A}$ (RH 2314)

Triparental mating between RH2085 (NA1000 hfsA$^+$), RH319 (MT607-pRK600) and RH1723 (Top10-pNPTS138-pleC$_{H610A}$) selected on PYE Nal Kan, streaked on PYE Kan, cultivated o/n in PYE and plated on PYE 3% Suc. Suc^R candidates patched on PYE Kan and PYE.

- NA1000 *hfsA*$^+$ *pleC*$_{T614R}$

Triparental mating between RH2085 (NA1000 *hfsA*$^+$), RH319 (MT607-pRK600) and RH2315 (Top 10 pNPTS138-*pleC*$_{T614R}$) selected on PYE Nal Kan, streaked on PYE Kan, cultivated o/n in PYE and plated on PYE 3% Suc. Suc^R candidates patched on PYE Kan and PYE.

- NA1000 *hfsA*$^+$ *pleC*$_{F778L}$ (RH 2313)

Triparental mating between RH2085 (NA1000 *hfsA*$^+$), RH319 (MT607-pRK600) and RH1724 (Top10-pNPTS138-*pleC*$_{F778L}$) selected on PYE Nal Kan, streaked on PYE Kan, cultivated o/n in PYE and plated on PYE 3% Suc. Suc^R candidates patched on PYE Kan and PYE. Kan^S colonies were screened by PCR with primers 1235/1252

- NA1000 *hfsA*$^+$ *pleC*$_{T792K}$

Triparental mating between RH2085 (NA1000 *hfsA*$^+$), RH319 (MT607-pRK600) and Top10-pNPTS138-*pleC*$_{T792K}$ selected on PYE Nal Kan, streaked on PYE Kan, cultivated o/n in PYE and plated on PYE 3% Suc. Suc^R candidates patched on PYE Kan and PYE. Kan^S colonies were screened by PCR with primers 1235/1638

- NA1000 Δ*pleC* (RH 217)

Biparental mating between RH50 (NA1000) and RH574 (S17-1-pNPTS138-Δ*pleC*) selected on PYE Nal Kan, streaked on PYE Kan, cultivated o/n in PYE and plated on PYE 3% Suc. SucR candidates patched on PYE Kan and PYE. KanS colonies were screened by PCR with primers 196/197 (1368 bp for deletion and 3618 bp for wt).

- NA1000 $pleC_{H610A}$ (RH 2020)

Triparental mating between RH50 (NA1000), RH319 (MT607-pRK600) and RH1723 (Top10-pNPTS138-$pleC_{H610A}$) selected on PYE Nal Kan, streaked on PYE Kan, cultivated o/n in PYE and plated on PYE 3% Suc. Suc^R candidates patched on PYE Kan and PYE.

- NA1000 $pleC_{T614R}$

Triparental mating between RH50 (NA1000), RH319 (MT607-pRK600) and RH2315 (Top 10 pNPTS138-$pleC_{T614R}$) selected on PYE Nal Kan, streaked on PYE Kan, cultivated o/n in PYE and plated on PYE 3% Suc. Suc^R candidates patched on PYE Kan and PYE.

- NA1000 $pleC_{F778L}$ (RH 2313)

Triparental mating between RH50 (NA1000), RH319 (MT607-pRK600) and RH1724 (Top10-pNPTS138-$pleC_{F778L}$) selected on PYE Nal Kan, streaked on PYE Kan, cultivated o/n in PYE and plated on PYE 3% Suc. Suc^R candidates patched on PYE Kan and PYE. Kan^S colonies were screened by PCR with primers 1235/1252

- NA1000 $pleC_{T792K}$

Triparental mating between RH50 (NA1000), RH319 (MT607-pRK600) and Top10-pNPTS138-$pleC_{T792K}$ selected on PYE Nal Kan, streaked on PYE Kan, cultivated o/n in PYE and plated on PYE 3% Suc. Suc^R candidates patched on PYE Kan and PYE. Kan^S colonies were screened by PCR with primers 1235/1638

- NA1000 $hfsA^+$ *pRKlac290-PpilA*

Triparental mating between RH2085 (NA1000 $hfsA^+$), RH319 (MT607-pRK600) and RH1958 (pRKlac290-*PpilA*) selected on PYE Nal Tet and streaked on PYE Tet.

- NA1000 $hfsA^+$ $pleC_{H610A}$ *pRKlac290-PpilA*

Triparental mating between RH2314 (NA1000 $hfsA^+$ $pleC_{H610A}$), RH319 (MT607-pRK600) and RH1958 (pRKlac290-*PpilA*) selected on PYE Nal Tet and streaked on PYE Tet.

- NA1000 $hfsA^+$ $pleC_{F778L}$ *pRKlac290-PpilA*

Triparental mating between RH2313 (NA1000 $hfsA^+$ $pleC_{F778L}$), RH319 (MT607-pRK600) and RH1958 (pRKlac290-*PpilA*) selected on PYE Nal Tet and streaked on PYE Tet

- NA1000 $hfsA^+$ *pRKlac290-PhvyA-hvyA*

Triparental mating between RH2085 (NA1000 *hfsA*$^+$), RH319 (MT607-pRK600) and RH2046 (pRKlac290-*PhvyA-hvyA*) selected on PYE Nal Tet and streaked on PYE Tet.

- NA1000 *hfsA*$^+$ *pleC*$_{H610A}$ *pRKlac290-PhvyA-hvyA*

Triparental mating RH2314 (NA1000 *hfsA*$^+$ *pleC*$_{H610A}$), RH319 (MT607-pRK600) and RH2046 (pRKlac290-*PhvyA-hvyA*) selected on PYE Nal Tet and streaked on PYE Tet.

- NA1000 *hfsA*$^+$ *pleC*$_{F778L}$ *pRKlac290-PhvyA-hvyA*

Triparental mating between RH2313 (NA1000 *hfsA*$^+$ *pleC*$_{F778L}$), RH319 (MT607-pRK600) and RH2046 (pRKlac290-*PhvyA-hvyA*) selected on PYE Nal Tet and streaked on PYE Tet.

- NA1000 *hfsA*$^+$ Δ*pleC PvanA::pleC*

Triparental mating between RH2100 (NA1000 *hfsA*$^+$Δ*pleC*), RH319 (MT607-pRK600) and Top-10 pVC6-*pleC* selected on PYE Nal Cam and streaked on PYE Cam. Cam^R colonies were screened by PCR with primers 138/639.

- NA1000 *pleC*$_{AA::DD}$

Triparental mating between RH50 (NA1000), RH319 (MT607-pRK600) and Top10-pNPTS-*pleC*$_{AA::DD}$ selected on PYE Nal Kan. Integration of the plasmid at the *pleC* locus was confirmed by PCR with the primers 1701/174. Presence of the AA::DD mutation was verified by sequencing after PCR on with the primers 1053/174.

- NA1000 *3Flag-pleC*

Triparental mating between RH50 (NA1000), RH319 (MT607-pRK600) and RH2319 (Top 10 pNPTS138-*3FLAG-pleC*) selected on PYE Nal Kan, streaked on PYE Kan, cultivated o/n in PYE and plated on PYE 3% Suc. Suc^R candidates patched on PYE Kan and PYE. Kan^S colonies were screened by PCR with primers 639/961.

- NA1000 Δ*socAB* (RH 1671)

Triparental mating between RH50 (NA1000), RH319 (MT607-pRK600) and RH1670 (Top10-pNPTS138-Δ*socAB*) selected on PYE Nal Kan, streaked on PYE Kan, cultivated o/n in PYE and plated on PYE 3% Suc. Suc^R candidates patched on PYE Kan and PYE. Kan^S colonies were screened by PCR with primers 848/851 (1210 bp for deletion and 2430 bp for wt).

- NA1000 Δ*socAB* Δ*clpP* (RH 1674)

A CR30 lysate made on RH975 (LHR66) was transduced into RH1671 (NA1000 Δ*socAB*). Transductants were selected on PYE Spec/Strep.

- NA1000 Δ*socAB* Δ*clpX* (RH 2279)

A CR30 lysate made on RH974 (LHR65) was transduced into RH1671 (NA1000 Δ*socAB*). Transductants were selected on PYE Spec/Strep.

- NA1000 *3Flag-pleC ΔcpdR*

A CR30 lysate made on RH339 (LHR68) was transduced into the NA1000 3Flag-pleC strain. Transductants were selected on PYE Tet.

- NA1000 Δ*hslV*

Triparental mating between RH50 (NA1000), RH319 (MT607-pRK600) and RH2404 (Top 10 pNPTS138-Δ*hslv*) selected on PYE Nal Kan, streaked on PYE Kan, cultivated o/n in PYE and plated on PYE 3% Suc. Suc^R candidates patched on PYE Kan and PYE. Kan^S colonies were screened by PCR with primers 1699/1700.

- NA1000 $cpdR_{D51A}$ (RH 347)

Biparental mating between RH50 (NA1000) and RH140 (S17-1-pNPTS138-$hfsA^+$) selected on PYE Nal Kan, streaked on PYE Kan, cultivated o/n in PYE and plated on PYE 3% Suc. SucR candidates patched on PYE Kan and PYE. KanS colonies were tested in an attachment assay.

- NA1000 Δ*SocAB ΔclpP PxylX::clpP*

A CR30 lysate made on RH974 (LHR66) was transduced into the NA1000 Δ*socAB ΔclpP*. Transductants were selected on PYE Tet.

- NA1000 Δ*SocAB ΔclpX PxylX::clpX*

A CR30 lysate made on RH339 (LHR65) was transduced into the NA1000 Δ*socAB ΔclpX* strain. Transductants were selected on PYE Tet.

- NA1000 Δ*SocAB ΔclpP ΔhslV*

Triparental mating between NA1000 Δ*hslv*, RH319 (MT607-pRK600) and RH1670 (Top10-pNPTS138-Δ*socAB*) selected on PYE Nal Kan, streaked on PYE Kan, cultivated o/n in PYE and plated on PYE 3% Suc. Suc^R candidates patched on PYE Kan and PYE. Kan^S colonies were screened by PCR with primers 848/851 (1210 bp for deletion and 2430 bp for wt). Next, a CR30 lysate made on RH974 (LHR66) was transduced into the NA1000 Δ*socAB ΔhslV* strain. Transductants were selected on PYE Spec Strep.

- NA1000 Δ*divJ ΔpleC* $cckA_{Y514D}$ (RH 2223)

Triparental mating between RH1103 (NA1000 ΔpleC ΔdivJ), RH319 (MT607-pRK600) and RH1796 (Top10-pNPTS138-cckAY514D) selected on PYE Nal Kan, cultivated o/n in PYE and plated on PYE 3% Suc. SucR candidates patched on PYE Kan and PYE. KanS colonies

were screened by PCR with primers 954/966 (694 bp) and sequencing with primers 954 & 966. Clone #2 contains the mutation Y514D.

- NA1000 Δ*pleC* $cckA_{Y514D}$ (RH 2053)

Biparental mating between RH1827 (NA1000 cckAY514D) and RH574 (S17-1-pNPTS138-ΔpleC) selected on PYE Nal Kan, streaked on PYE Kan, cultivated o/n in PYE and plated on PYE 3% Suc. SucR candidates patched on PYE Kan and PYE. KanS colonies were screened by PCR with primers 196/197 (1368 bp for deletion and 3618 bp for wt). Clone #1 had the expected PCR profile.

- NA1000 $cckA_{Y514D}$ (RH 1827)

Triparental mating between RH50 (NA1000), RH319 (MT607-pRK600) and RH1796 (Top10-pNPTS138-cckAY514D) selected on PYE Nal Kan, cultivated o/n in PYE and plated on PYE 3% Suc. SucR candidates patched on PYE Kan and PYE. KanS colonies were screened by PCR with primers 954/966 (694 bp) and sequencing with primers 962 & 966.

- NA1000 Δ*divJ*

Biparental mating between RH50 (NA1000) and RH744 (S17-1-pNPTS138-ΔdivJ) selected on PYE Nal Kan, streaked on PYE Kan, cultivated o/n in PYE and plated on PYE 3% Suc. SucR candidates patched on PYE Kan and PYE. KanS colonies were screened by PCR with primers 303/304 (1437 bp). Clone #1 had the expected PCR profile.

2.2 Construction of E. coli strains

- RH 140 S17-1 pNPTS138-$hfsA^{+}$(pHR231)

pHR224 cut by Eco RI, DNA fragment of 628 bp purified from agarose gel and ligated into pHR253 (pNPTS138) cut by Eco RI. Clone #2 with expected Eco RI restriction profile (5361 bp + 628 bp).

- Top10 pVC6-*pleC*

PCR on NA1000 gDNA with primers 1094/1212 to amplify the *pleC* gene and restricted with NdeI and KpnI. It was then cloned into pHR884 (pVC-6) vector cut in NdeI/KpnI. The plasmid was subsequently restriced with the PacI enzyme to eliminate the empty plasmids. PCR was performed to check the presence of the gene after transformation into the Top10 strain with the primers 100/138, clone number 4 had the expected profile. The plasmid was finally checked by restriction with EcoRI and had the expected restriction profile.

- RH2315 Top 10 pNPTS138-$pleC_{T614R}$ (pHR890)

DNA fragment of C. crescentus pleC (CC2482) encompassing mutations T614R was synthesized by IDT_gBlock (500 bp), cloned into pHR253 (pNPTS138) cut with Eco RV

- RH1724 Top 10 pNPTS138-*pleC*$_{F778L}$ (pHR618)

PCR on NA1000 pleC$_{F778L}$ gDNA with primers 983/1213 and cloned into pHR253 (pNPTS138) vector cut with Eco RV.

- Top 10 pNPTS138-*pleC*$_{T792K}$

DNA fragment of C. crescentus pleC (CC2482) encompassing mutations T792K was synthesized by IDT_gBlock (500 bp), cloned into pHR253 (pNPTS138) cut with Eco RV.

- Top 10 pNPTS138-*pleC*$_{AA::DD}$

DNA fragment of C. crescentus pleC (CC2482) encompassing mutations AA::DD mutation was synthesized by IDT_gBlock (500 bp), cloned into pHR253 (pNPTS138) cut with Eco RV.

- RH 2319 Top 10 pNPTS138-*3FLAG-pleC* (pHR893)

Upstream and 5' regions of C. crescentus pleC was amplified from RH50 gDNA by PCR respectively with primers 1634/1635 and 1636/1637 and cloned into pHR355 (pSK) and pHR616 (pMCS-1-3FLAG_5'), respectively. The pSK-1634/1635 recombinant plasmid were verified by sequencing (PSK-1634-1635_M13-40FOR_4, 30 March 2017). The PCR 1636/1637 was digested with Eco RI/Bam HI, ligated into the pHR616 (pMCS-1-3FLAG_5') cut with the same restriction enzymes and sequenced (PHR616-1636_163_M13-40FOR_1, 30 March 2017). The pSK-1634/1635 and pMCS-1-3FLAG-1636/1637 recombinant plasmids were then digested respectively with Hind III/Nde I and Nde I/Bam HI; and ligated into the pHR253 (pNPTS138) vector cut with Hind III and Bam HI.

- RH 1670 Top 10 pNPTS138-Δ*socAB* (pHR606)

Upstream and downstream regions of C. crescentus socAB (CC3514-CC3515) were amplified from RH50 gDNA by PCR respectively with primers 848/849 (620 bp) and 850/851 (590 bp) and cloned into pHR355 (pSK). The pSK-848/849 and pSK-850/851 recombinant plasmids, verified by sequencing (848-849_4_M13-26REV_3; 850-851_8_M13-26REV_4 & 848-849_4_M13F-20_2, 8 January 2014), were then digested respectively with Hind III/Eco RI and Eco RI/Bam HI; and ligated into the pHR253 (pNPTS138) vector cut with Hind III and Bam HI.

- RH 2404 Top10 pNPTS138-Δ*hslV* (pHR947)

Upstream and downstream regions of C. crescentus hslV (CC3727) were amplified from RH50 gDNA by PCR respectively with primers 1695/1696 and 1697/1698 and cloned into

pHR355 (pSK). The pSK-1660/1661 and pSK-1662/1663 recombinant plasmids, verified by sequencing (PSK1695-1696_M13-40FOR_1 & PSK1697-1698_M13-40FOR_2, 11 July 2017), were then respectively digested with Hind III/Eco RI and Eco RI/Bam HI; and ligated into the pHR253 (pNPTS138) vector cut with Hind III and Bam HI. Clone #1 had the expected restriction profile.

3. Supplementary references

Ardissone, S., Fumeaux, C., Bergé, M., Beaussart, A., Théraulaz, L., Radhakrishnan, S. K., … Viollier, P. H. (2014). Cell cycle constraints on capsulation and bacteriophage susceptibility. Elife, 3, e03587.

Casadaban, M. J., & Cohen, S. N. (1980). Analysis of gene control signals by DNA fusion and cloning in Escherichia coli. Journal of Molecular Biology, 138(2), 179–207.

Curtis, P. D., & Brun, Y. V. (2010). Getting in the Loop: Regulation of Development in Caulobacter crescentus. Microbiology and Molecular Biology Reviews, 74(1), 13–41. https://doi.org/10.1128/MMBR.00040-09

Duerig, A., Abel, S., Folcher, M., Nicollier, M., Schwede, T., Amiot, N., … Jenal, U. (2009). Second messenger-mediated spatiotemporal control of protein degradation regulates bacterial cell cycle progression. Genes & Development, 23(1), 93–104.

Evinger, M., & Agabian, N. (1977). Envelope-associated nucleoid from Caulobacter crescentus stalked and swarmer cells. Journal of Bacteriology, 132(1), 294–301.

Grünenfelder, B., Tawfilis, S., Gehrig, S., Østerås, M., Eglin, D., & Jenal, U. (2004). Identification of the protease and the turnover signal responsible for cell cycle-dependent degradation of the Caulobacter FliF motor protein. Journal of Bacteriology, 186(15), 4960–4971.

Jenal, U., & Fuchs, T. (1998). An essential protease involved in bacterial cell-cycle control. The EMBO Journal, 17(19), 5658–5669.

Joshi, K. K., Bergé, M., Radhakrishnan, S. K., Viollier, P. H., & Chien, P. (2015). An Adaptor Hierarchy Regulates Proteolysis during a Bacterial Cell Cycle. Cell, 163(2), 419–431. https://doi.org/10.1016/j.cell.2015.09.030

McGrath, P. T., Iniesta, A. A., Ryan, K. R., Shapiro, L., & McAdams, H. H. (2006). A dynamically localized protease complex and a polar specificity factor control a cell cycle master regulator. Cell, 124(3), 535–547.

Skerker, J. M., Prasol, M. S., Perchuk, B. S., Biondi, E. G., & Laub, M. T. (2005). Two-component signal transduction pathways regulating growth and cell cycle progression in a bacterium: a system-level analysis. PLoS Biol, 3(10), e334.

Skerker, J. M., & Shapiro, L. (2000). Identification and cell cycle control of a novel pilus system in Caulobacter crescentus. The EMBO Journal, 19(13), 3223–3234.

Wright, R., Stephens, C., Zweiger, G., Shapiro, L., & Alley, M. R. (1996). Caulobacter Lon protease has a critical role in cell-cycle control of DNA methylation. Genes & Development, 10(12), 1532–1542.

Christen, B., Abeliuk, E., Collier, J. M., Kalogeraki, V. S., Passarelli, B., Coller, J. A., . . . Shapiro, L. (2011). The essential genome of a bacterium. *Molecular systems biology, 7*(1), 528.

Fischer, B., Rummel, G., Aldridge, P., & Jenal, U. (2002). The FtsH protease is involved in development, stress response and heat shock control in Caulobacter crescentus. *Molecular microbiology, 44*(2), 461-478.